

Oil Sands Process-Affected Water Characterization and Application of Adsorption Process for
the Removal of Naphthenic Acids

by

Mohamed Darwish Ibrahim

A thesis submitted in partial fulfillment of the requirements for the degree of

Doctor of Philosophy

in

Environmental Engineering

Department of Civil and Environmental Engineering

University of Alberta

© Mohamed Darwish Ibrahim, 2018

Abstract

Many techniques have been used to identify and quantify the naphthenic acids (NAs) in the oil sands process-affected water (OSPW) such as gas chromatography mass spectrometry (GC-MS), high performance liquid chromatography mass spectrometry (HPLC-MS), ultra-performance liquid chromatography time-of-flight mass spectrometry (UPLC-TOFMS), and Fourier transformation infrared (FTIR) spectroscopy. Extraction methods widely used in NAs quantification are liquid-liquid extraction (LLE), and solid phase extraction (SPE) methods. In his research, as a step forward to the establishment of standard method for quantifying NAs, the effects of extraction methods on quantifying NAs using FTIR and UPLC-TOFMS methods by implementing two standards (Fluka NAs and OSPW extract) were studied. Our results showed higher recovery of both the O_x-NAs (i.e., total NAs or sum of classical (O₂) and oxidized species) and naphthenic acid fractions compounds (NAFCs) in SPE compared to LLE, regardless the water source. However, for O₂ species, LLE and SPE acquired significant similar concentrations with higher abundance values in LLE (e.g., OSPW samples: (63.1 %) than SPE (58.5%). The high hydrophobicity of O₂ species governed the extraction efficiency and increased their transport (i.e., from water to solvent) thus increasing their recovery in LLE.

To improve our understanding of FTIR method, which is suggested as a standard method for routine monitoring of OSPW, a statistical analysis was implemented to assess the effect of sample type, preparation methods and standard type on quantifying the acid extractable fraction (AEF) using FTIR method. For samples preparation, LLE and SPE methods were used in this study while Fluka and OSPW extract were used as standard chemicals for calibration and quantification. It was found that SPE AEF was 1.37 times the AEF yielded using the LLE method. The AEF quantified using the OSPW extract standard method was 2.5 times higher than that

quantified using the Fluka NA standard. SPE method, which is based on the adsorption process, was found to be effective in separating the NAs from the OSPW samples. Therefore, among different OSPW treatment techniques, adsorption process was selected to study the removal the NAs from the OSPW samples.

Carbon xerogel (CX) is a material that can be synthesized to provide textural characteristics that adhere to specific contaminants present in all forms. Therefore, mesoporous carbon CX was synthesized in the laboratory and used as an adsorbent to study its performance in removing model NAs. The adsorption capacity and kinetics were compared to those obtained using granular activated carbon (GAC).

The effects of solution pH, temperature, and ion strength on the adsorption of a Trans-4-Pentylcyclohexanecarboxylic acid (TPCA), A NA model compound, on the CX and GAC surface were investigated herein. Moreover, the kinetics and thermodynamics of the process were included in this study. Results confirmed that the adsorption was a physical process (activation energy $E_a = 9.75$ and 1.2 KJ.mol^{-1} for CX and GAC, respectively) and best described by Langmuir isotherm ($R^2 = 0.97$ and 0.96 for CX and GAC, respectively). The maximum adsorption capacity of the CX and GAC based on Langmuir isotherm was calculated as 69.9 and 102 mg g^{-1} , respectively. The adsorption kinetics followed the pseudo first order and intra-particle diffusion kinetics models were both appropriate in defining the adsorption of TPCA to CX and GAC ($R^2 \geq 0.90$). Pore diffusion was the rate limiting step, but film diffusion still maintained a significant role in the rate of diffusion of NAs. The effect of initial solution pH on the adsorption process was significant, while temperature and ion strength effect were minimal.

The findings of this work are important for standardizing the NA identification and quantification method for monitoring industrial process water including the OSPW. Moreover, the

deep understanding of the effect of the sample pre-treatment, chemical standards and the sample type on the FTIR method results, opens a new venue for comparing the results from different studies that were generated using different techniques. The generated comparative database will be usefull for the monitoring and remediation of OSPW. The removal of NA model compounds from alkaline water using new adsorbent will help in developing a treatment approach designed to remove the contaminant from OSPW as first step towards safely releasing it into the environment.

Preface

All research completed on this thesis is an original work in which I, Mohamed D. Ibrahim, planned, designed and conducted all these experiments as well as the interpretation, the analysis of the data and the preparation of the manuscripts, under the supervision of Dr. Mohamed Gamal El-Din. Other colleagues also contributed to manuscript edits, sample analysis, or chemical preparation, and some of them were co-authors of the manuscripts submitted for publication. Other analyses were done in other departments of the University of Alberta, as specified below.

Chapter 2: A version of this chapter will be submitted to Talanta journal as Meshref, M.N.A., Ibrahim M.D., Huang, R., Chen, Y., Klammerth, N., Chelme-Ayala, P., Hughes, S.A., Brown, C., Mahaffey, A., and Gamal El-Din, M.: “Quantification of Oil Sands Organic Acids Using Fourier Transform Infrared Spectroscopy and Ultra-performance Liquid Chromatography Time-of-Flight Mass Spectrometry: Impacts of the Extraction and Calibration Methods” (2017). Mr. M. N. A. Meshref is co-first author and helped in the liquid-liquid extraction of the OSPW samples. Naphthenic acids (NAs) quantification using FTIR was conducted by me and Dr. M. N. A. Meshref with the help of developing the experimental procedure of FTIR quantification method by Dr. Brandon Weber as well as minor help of students, group members and technicians in the laboratory. NA quantification by UPLC-TOFMS was conducted by Dr. Rongfu Huang in Dr. Gamal El-Din’s research group. Mr. Yuan Chen helped in the UPLC-TOFMS data processing and solid phase extraction of the samples with minor help from Ms. Shimiao Dong. From Dr. Gamal El-Din’s research group, Dr. R. Huang and Dr. P. Chelme-Ayala contributed to the manuscript edits. Dr. Sarah A. Hughes, Mrs. Christine Brown and Dr. Ashley Mahaffey all from Shell Canada Company, also contributed to the manuscript edits.

Chapter 3: A version of this chapter will be submitted to the Candian Journal of Civil Engineering as “Ibrahim M. D., Meshref, M.N.A., Hughes, S. A., and Gamal El-Din, M. “Differentiating Among Oil Sands Process-Affected Water and Groundwater Samples Determined By Fourier Transform Infrared Spectroscopy via Non-Parametric Statistical Analysis” (2017). Mr. M. N. A. Meshref helped in the liquid-liquid extraction of the OSPW samples. Naphthenic acids (NAs) quantification using FTIR was conducted by me and Mr. M. N. A. Meshref with the help of developing the experimental procedure of FTIR quantification method by Dr. Brandon Weber as well as minor help of students, group members and technicians in the laboratory.

Chapter 4: A version of this chapter will be submitted to Chemosphere journal as “Ibrahim M. D., Messele, S., and Gamal El-Din, M.: “Adsorption Isotherm, Kinetic Modeling and Thermodynamics of Trans-4-Pentylcyclohexanecarboxylic acid on Mesoporous Carbon Xerogel” (2017). Dr. S.A. Messele prepared the caron xerogel and contributed to manuscript edits and TPCA quantification using liquid chromatogram mass spectrometer (LC-MS) along with Dr. Mingyu of Dr. Gamal El-Din research group.

Dedication

“And mankind has not been given of knowledge except a little.” Quran 17:85

I would like to dedicate this work to:

My Father and my mother for their encouragement, patience and everything they gave me,

My precious wife Doaa for her endless support and patience,

My beautiful daughter Jumana, and lovely son Omar. You have made me stronger, better and more fulfilled than I could have ever imagined. I love you to the moon and back.

Also, this work is dedicated to the soul of my mother-in-law and my father-in-law.

My brothers Ahmed and Abdullah, and my sister Heba.

All my uncles (including Wagih, Khalid, Mousad, Arabi, Nabil and Mohamed) and all my aunts (including Nadia, Salwa, and Sahar), souls of my grandparents, and my sisters-in-law for their support and prayers.

Finally, for all extended family, all my friends and all my country, Egypt.

Acknowledgment

In the name of Allah, the most Gracious, the most Merciful. First, I would like to thank Allah Almighty for guiding me to my accomplishments.

Then first and foremost, I would like to extend my most gratitude to my supervisor Dr. Mohamed Gamal El-Din for his support and his motivating guidance during my program. I benefited from his broad knowledge and professional manner through the research experience under his supervision.

I also would like to thank Dr. Pamela Chelme-Ayala and Dr. Selamawit A. Messele in Dr. Gamal El-Din's research group for their sincere efforts and support. I appreciate all their generous help and their proofreading of my dissertation.

My sincere gratitude also goes to the project managers and postdoctoral fellows in Dr. Gamal El-Din's research group, who helped me revise research proposals, conference posters and presentations, as well as paper manuscripts. They are Dr. Nikolaus Klammerth, Dr. Kerry N. McPhedran, Dr. Alla Alpatova, Dr. Vanessa Incani, and Dr. Rongfu Huang.

I also thank the technicians in Dr. Gamal El-Din's research group and Civil and Environmental Department: Mrs. Maria Demeter, Dr. Brandon Weber, Ms. Nian Sun, and Mrs. Chen Liang. I would like to extend my appreciation to my friends and colleagues, and staff in the Department of Civil and Environmental Engineering and former and current group members including Dr. Ahmed Moustafa, Dr. Mohamed Meshref, Mr. Haitham Elnakar, Dr. Md. Shahinoor Islam, Dr. Yanyan Zhang, Mr. Yuan Chen, Dr. Chengjin Wang, Ms. Shimiao Dong, Dr. Jinkai Xue, Mr. Zenguan Shu, Mr. Mohamed Khan, Mrs. Chelsea Benally, Ms. Somaye Nasr, Dr. Shu Zhu, Dr. Ying Zhang, Mrs. Chao Li and all my other colleagues.

I would like to thank my best friends Mr. Ehab Hamzah, Dr. Ahmed Taha, Dr. Mohamed El Arabi, and Mr. Mostafa Mohamed for all the great support during my Ph.D. journey.

This research was supported by Shell Canada Ltd. and by Natural Sciences and Engineering Research Council of Canada (NSERC) Senior Industrial Research Chair (IRC) in Oil Sands Tailings Water Treatment. Special thanks also go to Dr. Gamal El-Din's research group in the Department of Civil and Environmental Engineering at the University of Alberta for the technical and management support.

Table of Contents

| | |
|---|-------------|
| Abstract..... | ii |
| Preface..... | v |
| Dedication | vii |
| Acknowledgment..... | viii |
| Table of Contents | x |
| List of Figures..... | xvi |
| List of Abbreviations | xxiv |
| Chapter 1 : General Introduction and Research Objectives | 1 |
| 1.1. Naphthenic Acids (NAs)..... | 2 |
| 1.2. Emerging treatment technologies for the OSPW | 4 |
| 1.2.1. Advanced Oxidation Processes (AOPs)..... | 4 |
| 1.2.2. Membrane | 4 |
| 1.2.3. Biological Treatment..... | 5 |
| 1.2.4. Adsorption..... | 6 |
| 1.3. Research Scope | 13 |
| 1.4. Objectives | 14 |
| 1.5. Thesis Outline | 15 |

Chapter 2 : Quantification of oil sands organic acids using Fourier transform infrared spectroscopy and ultra-performance liquid chromatography time-of-flight mass spectrometry: Impacts of the extraction and calibration methods. 17

2.1. Introduction 17

2.2. Materials and methods..... 20

2.2.1. Sources of water..... 20

2.2.2. Chemical and reagents 20

2.2.3. Sample preparation 21

2.2.3.1. Liquid-liquid extraction (LLE) 21

2.2.3.2. Solid-phase extraction (SPE) 21

2.2.4. Analytical methods 22

2.4.1. Ultra-performance liquid chromatography time-of-flight mass spectrometry (UPLC-TOFMS) analysis22

2.4.2. Fourier transform infrared (FTIR) spectroscopy analysis 23

2.2.5. Statistical analysis..... 24

2.3. Results and discussion 24

2.3.2.3. Calibration methods and appropriate standard..... 40

2.3.2.4. UPLC-TOFMS versus FTIR..... 45

2.4. Conclusions..... 49

Chapter 3 : Differentiating Among Oil Sands Process-Affected Water and Groundwater Samples Determined by Fourier Transform Infrared Spectroscopy via Non-Parametric Statistical Analysis 51

3.1. Introduction 51

3.2. Material and methods 54

| | |
|---|-----------|
| 3.3.1. Water samples collection | 54 |
| 3.3.2. Liquid-Liquid extraction (LLE) | 55 |
| 3.3.3. Solid-phase extraction (SPE) | 55 |
| 3.3.4. FTIR analysis | 55 |
| 3.3.5. Statistical analysis | 56 |
| 3.3. Results and discussion | 57 |
| 3.4.1. Differences between sampling locations | 57 |
| 3.4.2. Differences between measurement methods | 63 |
| 3.4.3. Differences between calibration methods | 64 |
| 3.4.4. Differences between separation methods | 66 |
| 3.4.5. Differences between replicates | 67 |
| 3.4. Conclusion and Recommendations | 68 |
| | |
| Chapter 4 : Adsorption Isotherm, Kinetic Modeling and Thermodynamics of Trans-4-Pentylcyclohexanecarboxylic Acid on Mesoporous Carbon Xerogel..... | 71 |
| 4.1. Introduction | 71 |
| 4.2. Materials and methods..... | 74 |
| 4.2.1. Material | 74 |
| 4.2.2. Carbon xerogel preparation..... | 75 |
| 4.2.3. TPCA preparation and analysis..... | 75 |
| 4.2.4. Adsorbents characterization | 75 |
| 4.2.5. Equilibrium time experiment | 77 |
| 4.2.6. Isotherm experiments | 77 |
| 4.2.7. Kinetic experiments | 78 |
| 4.2.8. Effect of solution pH, temperature and ion strength | 79 |

| | |
|--|------------|
| 4.2.9. Statistical analysis | 80 |
| 4.3. Results and discussion | 80 |
| 4.3.1. Textural property characterization | 80 |
| 4.3.2. Surface morphology and functional groups (SEM, FT-IR and XPS) | 81 |
| 4.3.3. Thermal gravimetric analysis (TGA) | 84 |
| 4.3.4. pH_{PZC} | 85 |
| 4.3.5. Equilibrium time experiments | 86 |
| 4.3.6. Adsorption isotherm modeling | 88 |
| 4.3.7. Adsorption Kinetics | 92 |
| 4.3.8. Intra-particle diffusion model | 97 |
| 4.3.9. Temperature effect | 100 |
| 4.3.10. Ionic strength effect | 101 |
| 4.3.11. pH effect | 102 |
| 4.3.12. Activation energy | 103 |
| 4.3.13. Thermodynamic calculations | 105 |
| 4.3.14. Adsorption mechanism | 107 |
| 4.4. Conclusion | 108 |
| Chapter 5 : Final Conclusions and Recommendations | 111 |
| 5.1. Thesis summary | 111 |
| 5.2. Conclusions Summary | 112 |
| 5.3. Recommendations and future work | 114 |
| References | 116 |

List of Tables

| | |
|---|----|
| Table 2-1 Classical NAs (O_2 -NAs) as well as sum of classical NAs and oxidized NAs (O_x -NAs). NA concentrations in ($mg L^{-1}$) were estimated by UPLC-TOFMS while naphthenic acid fractions compounds (NAFCs) concentrations in ($mg L^{-1}$) were estimated by FTIR for all groundwater and OSPW samples..... | 26 |
| Table 2-2 Summary of Kruskal-Wallis test results for the sub group of OSPW samples, sub group of groundwater samples and the entire group of samples..... | 28 |
| Table 2-3. Calculated SPE/LLE ratio for all samples using UPLC-TOFMS and FTIR analyses. | 31 |
| Table 2-4 Comparison between the determination of naphthenic acid fractions compounds (NAFCs) by FTIR and determination of O_x -NAs by UPLC-TOFMS using OSPW extract and Fluka standards after samples pre-treatment with LLE and SPE. | 39 |
| Table 3-1 AEF results quantified by FTIR using FLuka and OSPW extract standards calibration methods with SPE and LLE separation methods. All results are in $mg L^{-1}$. GW stands for groundwater sample OSPW stands from OSPW samples. Errors are standard error with sample size =3..... | 58 |
| Table 3-2 Samples pairwise test p-value matrix. P-values more than 0.05 are highlighted..... | 59 |
| Table 3-3 pairwise test result p-value matrix | 64 |
| Table 4-1 Physico-chemical properties of TPCA model NA compounds used..... | 74 |
| Table 4-2 BET surface area, micro, meso porous area for CX, and GAC..... | 81 |
| Table 4-3 Concentration of oxygen-containing functional groups as determined by XPS analysis | 84 |

| | |
|---|-----|
| Table 4-4 Langmuir, Freundlich, and D-R isotherms parameters | 89 |
| Table 4-5 Kinteric parametrs from first, second, bagham, and Weber-Morris models that describes the TPCA adsorption on CX and GAC..... | 95 |
| Table 4-6 Thermodynamic parameters results..... | 106 |

List of Figures

| | |
|---|----|
| Figure 1-1 Sample naphthenic acid structures where R is an alkyl chain, Z describes the hydrogen deficiency, and m is the number of CH ₂ units (source: Clemente and Fedorak, 2005)..... | 3 |
| Figure 1-2 Adsorbent particle illustrating associated resistances | 7 |
| Figure 1-3 Pore size distribution, adapted from (Menéndez and Martín-Gullón, 2006) | 8 |
| Figure 1-4 Typical adsorption isotherm between amounts of adsorbed per mass unit of adsorbent and the equilibrium concentration | 9 |
| Figure 2-1 Schematic diagram showing the different pre-treatment methods and analyses performed in the present study, including the different water samples. Abbreviations are listed as follows: groundwater, GW; oil sand process-affected water, OSPW; solid-phase extraction, SPE; liquid-liquid extraction, LLE; ultra-performance liquid chromatography time-of-flight mass spectrometry, UPLC-TOFMS; Fourier transform infrared spectroscopy, FTIR; and naphthenic acids, NAs..... | 25 |
| Figure 2-2 Change of O _x -NAs [sum of NAs at (2≤x≤6) or sum of classical (O ₂) NAs and oxidized NAs; as measured by UPLC-TOFMS analyses] and naphthenic acid fractions compounds (NAFCs as measured by FTIR analyses) concentrations in the three sample batches or replicates (1 = June, 2 = August, and 3 = October 2015) using the different pre-treatment methods and all analyses. Top of the figure: OSPW samples: 1, 2 and 3; Groundwater (GW) samples: 4, 5, 6, 7, 8, 9 and 10. Horizontal lines represent first quartile, medians, and third quartiles define the boxes, while the bottom and top tails represent the 10 th and 90 th percentiles. Data points for each boxplot are randomly placed to minimize points overlapping. Notes: Data points are presented as Instrument-Sample Preparation-Calibration standard. | |

TOF = UPLC-TOFMS, SPE = Solid-phase extraction, LLE = liquid-liquid extraction, Fluka = Fluka commercial NA extract, and OSPW = oil sands process-affected water NA extract.

..... 27

Figure 2-3 Differences between solid-phase extraction (SPE) and liquid-liquid extraction (LLE) pre-treatment using box plot of O_x -NAs [sum of NAs at $(2 \leq x \leq 6)$ or sum of classical (O_2) NAs and oxidized NAs as measured by UPLC-TOFMS analyses] and naphthenic acid fractions compounds (NAFCs; as measured by FTIR analyses) for the different water samples; OSPW samples: 1, 2 and 3, groundwater (GW) samples: 4, 5, 6, 7, 8, 9 and 10. Horizontal lines represent first quartile, medians, and third quartiles define the boxes, while the bottom and top tails represent the 10th and 90th percentiles. Data points for each boxplot are randomly placed to minimize points overlapping. Notes: Data points are presented as Instrument-Sample Preparation-Calibration standard. TOF = UPLC-TOFMS, Fluka = Fluka commercial NA extract, and OSPW = oil sands process-affected water NA extract. 30

Figure 2-4 Comparison between the determination of naphthenic acid fractions compounds (NAFCs) after SPE and LLE pre-treatment using FTIR and Fluka as standard. Note: Groundwater (GW) and oil sand process-affected water (OSPW); solid-phase extraction (SPE); and liquid-liquid extraction (LLE). The grey zone represents the 95% confidence level for the regression. FTIR-LLE-Fluka and FTIR-SPE-Fluka refer to the analysis of sample by FTIR pretreated by LLE and SPE, respectively, and using Fluka as standard. 33

Figure 2-5 Comparison between the determination of naphthenic acid fractions compounds (NAFCs) using FTIR after SPE and LLE pretreatment and using OSPW extract as standard. Note: solid-phase extraction is denoted as SPE; and liquid-liquid extraction is denoted as LLE. 34

Figure 2-6 Relative abundance of classical NAs (O_2 -NAs), for all samples using UPLC-TOFMS with different pretreating conditions liquid-liquid extraction (LLE) and solid-phase extraction (SPE). OSPW samples: 1, 2 and 3; groundwater (GW) samples: 4, 5, 6, 7, 8, 9 and 10..... 35

Figure 2-7 Box plot comparing the quantification of O_x -NAs [sum of NAs at ($2 \leq x \leq 6$) or sum of classical NAs and oxidized NAs as measure by UPLC-TOFMS] using solid-phase extraction (SPE) pretreated samples; and liquid-liquid extraction (LLE) pretreated samples as well as quantification of naphthenic acid fractions compounds (NAFCs; as measured by FTIR) using Fluka standard and OSPW extract with the two pre-treatment methods (SPE and LLE). OSPW samples: 1, 2 and 3; Groundwater (GW) samples: 4, 5, 6, 7, 8, 9 and 10. The mean is denoted as circled plus \oplus . Horizontal lines represent first quartile, medians, and third quartiles define the boxes, while the bottom and top tails represent the 10th and 90th percentiles. Data points for each boxplot are randomly placed to minimize points overlapping. Notes: X-axis categories are presented as Instrument-Sample Preparation-Calibration standard. TOF = UPLC-TOFMS, Fluka = Fluka commercial NA extract, and OSPW = oil sands process-affected water NA extract..... 37

Figure 2-8 Comparison between UPLC-TOFMS determination of O_x -NAs after SPE and LLE pretreatment using OSPW extract as standard. Note: Solid-phase extraction (SPE); and liquid-liquid extraction (LLE); the confidence level is 95% for the regression. TOF-LLE-OSPW and TOF-SPE-OSPW refer to the analysis of sample by UPLC-TOFMS pretreated by LLE and SPE, respectively and using OSPW extract as standard. 38

Figure 2-9. Percent abundance (%) of carbon number (n) and Z distribution for OSPW NA extract and Fluka NA standard. NA general formula: $C_nH_{2n+Z}O_x$ where the number of carbons, the

number of hydrogen lost, the number of oxygen are represented by n, Z and x respectively.
 $(7 \leq n \leq 26)$, $(0 \leq Z \leq 18)$, and $(2 \leq x \leq 6)$. OSPW Ext. refers to OSPW extract..... 41

Figure 2-10 Profiles of O_x -NAs and classical (O_2 -NAs) species of OSPW extract (left panels a,c) and Fluka standard (right panels b,d)..... 43

Figure 2-11. Profiles of oxidized NA or NA species ($3 \leq x \leq 6$) of OSPW extract (left panels a,c,e,g) and Fluka standard (right panels b,d,f,h). 44

Figure 2-12 Comparison between Fluka and OSPW extract standards using FTIR results (naphthenic acid fractions compounds (NAFCs)) in SPE. Note: Groundwater (GW), oil sand process-affected water (OSPW); and solid-phase extraction (SPE). 45

Figure 2-13 Comparison between the determination of naphthenic acid fractions compounds (NAFCs) by FTIR-OSPW extract and determination of UPLC-TOFMS (O_x -NAs) using OSPW extract after samples LLE pre-treatment. Notes: Groundwater (GW) and oil sand process-affected water (OSPW); and liquid-liquid extraction (LLE). The grey zone represents the 95% confidence level. O_x -NAs refer to the sum of classical NAs (i.e., O_2) and oxidized NAs (i.e., O_3 , O_4 , O_5 , and O_6 , etc.). TOF-LLE-OSPW refers to the analysis of sample by UPLC-TOFMS pretreated by LLE and using OSPW extract as standard while FTIR-LLE-OSPW refers to the analysis of sample by FTIR pretreated by LLE and using OSPW extract as standard..... 46

Figure 2-14 Comparison between the determination of UPLC-TOFMS (O_x -NAs) and (naphthenic acid fractions compounds (NAFCs)) by FTIR using OSPW extract after samples pre-treatment with solid-phase extraction (SPE). Notes: Groundwater (GW) and oil sand process-affected water (OSPW). The grey zone represents the 95% confidence level. O_x -NAs refer to the sum of classical NAs (i.e., O_2) and oxidized NAs (i.e., O_3 , O_4 , O_5 , and O_6 , etc.). TOF-

SPE-OSPW and FTIR-SPE-OSPW refer to the analysis of sample by UPLC-TOFMS and FTIR, respectively, after pretreated by SPE using OSPW extract as standard..... 47

Figure 2-15 Comparison between the determination of naphthenic acid fractions compounds (NAFCs) by FTIR-Fluka and determination of O_x-NAs (sum of classical NAs (i.e., O₂) and oxidized NAs (i.e., O₃, O₄, O₅, and O₆, etc.)) by UPLC-TOFMS using OSPW extract after samples pre-treatment: a) LLE and b) SPE. Notes: Groundwater (GW) and oil sand process-affected water (OSPW); solid-phase extraction (SPE); and liquid-liquid extraction (LLE). The grey zone represents the 95% confidence level. FTIR-LLE-Fluka and FTIR-SPE-Fluka refer to the analysis of sample by FTIR pretreated by LLE and SPE, respectively, and using Fluka as standard; TOF-LLE-OSPW and TOF-SPE-OSPW refer to the analysis of sample by UPLC-TOFMS pretreated by either LLE or SPE, respectively, and using OSPW extract as standard. 48

Figure 3-1 Boxplot illustrating the FTIR analysis results based on the samples ID. Horizontal lines represent first quartile, median, and third quartiles define the boxes, while the bottom and top tails represent the 5th and 95th percentiles. 58

Figure 3-2 Box plot represents AEF analysis grouped by Pairwise Kruskal-Wallis test groups: Group1 (samples 1, 2, and 3) group2 (samples 6,7, and 8) group3 (samples 4,5,and 6) group4 (sample 9)..... 59

Figure 3-3 Cluster analysis results with two and four level clustering first number refers to the replicate while the second and third number refer to the sample number for example 204 represents the second replicate for sample number 4. 60

Figure 3-4 Boxplot of AEF results of the OSPW and groundwater (GW) samples. Horizontal lines represent first quartile, median, and third quartiles define the boxes, while the bottom and top tails represent the 5th and 95th percentiles. 61

Figure 3-5 Boxplot shows the FTIR results grouped by the sampling location Horizontal lines represent first quartile, median, and third quartiles define the boxes, while the bottom and top tails represent the 5th and 95th percentiles. 62

Figure 3-6 Boxplot elucidating the analysis results for the samples (1 to 10) using FTIR Fluka and OSPW standards as well as the two extraction methods LLE and SPE. Horizontal lines represent first quartile, median, and third quartiles define the boxes, while the bottom and top tails represent the 5th and 95th percentiles. 63

Figure 3-7 Boxplot of the samples AEF concentrations grouped by the calibration method. Horizontal lines represent first quartile, median, and third quartiles define the boxes, while the bottom and top tails represent the 5th and 95th percentiles. 65

Figure 3-8 boxplot illustrating the AEF results grouped by the separation method (LLE and SPE). Horizontal lines represent first quartile, median, and third quartiles define the boxes, while the bottom and top tails represent the 5th and 95th percentiles. 67

Figure 3-9 Boxplot illustrating the AEF results grouped by the batch number. Horizontal lines represent first quartile, median, and third quartiles define the boxes, while the bottom and top tails represent the 5th and 95th percentiles. 68

Figure 4-1 SEM imaging for CX, and GAC at 50 k times 81

Figure 4-2 FT-IR spectrum of CX and GAC. 82

Figure 4-3 CX XPS C1s peak deconvolution 83

Figure 4-4 GAC XPS C1s peak deconvolution 83

| | |
|--|----|
| Figure 4-5 TGA analysis for raw and saturated adsorbents..... | 85 |
| Figure 4-6 pH_{pzc} experiment result. Horizontal line represents the $\Delta pH=0$ | 86 |
| Figure 4-7 TPCA removal percentage using Xerogel 5.5 and GAC. Experiment conditions- total solution volume: 50 mL, shaking Speed: 210 rpm, initial concentration: 50 mg L ⁻¹ , adsorbents concentration: 0.5 g.L ⁻¹ | 88 |
| Figure 4-8 TPCA Langmuir isotherm for CX and GAC Experiment conditions- total solution volume: 50 mL, shaking Speed: 210 rpm, initial concentration: 60 mg L ⁻¹ , adsorbents concentration: 0.5 g.L ⁻¹ | 90 |
| Figure 4-9 TPCA Freundlich isotherm for CX and AC. Experiment conditions- total solution volume: 50 mL, shaking Speed: 210 rpm, initial concentration: 60 mg L ⁻¹ , adsorbents concentration: 0.5 g.L ⁻¹ | 90 |
| Figure 4-10 TPCA D-R isotherm for CX and GAC. Experiment conditions- total solution volume: 50 mL, shaking Speed: 210 rpm, initial concentration: 60 mg L ⁻¹ , adsorbents concentration: 0.5 g.L ⁻¹ | 91 |
| Figure 4-11 Pseudo-first-order modeles for CX and GAC..... | 93 |
| Figure 4-12 Pseudo second order model for TPCA removal using GAC and CX. Experiment conditions- total solution volume: 50 mL, shaking Speed: 210 rpm, initial concentration: 60 mg L ⁻¹ , adsorbents concentration: 0.5 g.L ⁻¹ | 94 |
| Figure 4-13 All kinetic models with the actual data for CX..... | 96 |
| Figure 4-14 All kinetic models with the actual data for GAC..... | 97 |
| Figure 4-15 Bangham model for TPCA removal using GAC and CX. Experiment conditions- total solution volume: 50 mL, shaking Speed: 210 rpm, initial concentration: 60 mg L ⁻¹ , adsorbents concentration: 0.5 g L ⁻¹ | 98 |

Figure 4-16 Weber-Morris model for TPCA removal using GAC and CX. Experiment conditions- total solution volume: 50 mL, shaking Speed: 210 rpm, initial concentration: 60 mg L⁻¹, adsorbents concentration: 0.5 g.L⁻¹ 99

Figure 4-17 Temperature effect on q (q normalized by the adsorbent surface area) of TPCA using CX and GAC. Experiment conditions- total solution volume: 50 mL, shaking Speed: 210 rpm, initial concentration: 60 mg L⁻¹, adsorbents concentration: 0.5 g.L⁻¹ 100

Figure 4-20 effect of Ion strength on TPCA adsorption after 24 hours using CX, and GAC. Experiment conditions- total solution volume: 50 mL, shaking Speed: 210 rpm, initial concentration: 60 mg L⁻¹, adsorbents concentration: 0.5 g.L⁻¹ 102

Figure 4-21 Effect of pH on TPCA adsorption after 24 hours using CX, and GAC. Experiment conditions- total solution volume: 50 mL, shaking Speed: 210 rpm, initial concentration: 60 mg L⁻¹, adsorbents concentration: 0.5 g.L⁻¹, pH =8.0. 103

Figure 4-18 Linear Arrhenius equation ln K₂ vs 1/T 104

Figure 4-19 Ln K_c vs 1/T..... 106

List of Abbreviations

| | |
|--------------------------------|--|
| ΔG | Gibbs free energy |
| ΔH | Enthalpy |
| ΔS | Entropy |
| AC | Activated carbon |
| AEF | Acid extractable fraction |
| AOPs | Advanced oxidation processes |
| BET | Brunaur-emmett-teler |
| COD | Chemical oxidation demand |
| CX | Carbon xerogel |
| D-R | Dubinin-radushkevitch |
| DCM | Dichloromethane |
| DFT | Density functional theory |
| Ea | Activation energy |
| ETF | External tailings facility |
| FT-IR | Fourier transform infrared |
| FTICR-MS | Fourier transfer ion cyclotron resonance mass spectrometry |
| GAC | Granular activated carbon |
| GC-MS | Gas chromatography mass spectrometry |
| GW | Groundwater |
| H ₂ SO ₄ | Sulfuric acid |

| | |
|---------------------|--|
| HPLC-MS | High performance liquid chromatography mass spectrometry |
| LLE | Liquid–liquid extraction |
| MF | Microfiltration |
| NaCl | Sodium chloride |
| NAFCs | Naphthenic acid fraction compounds |
| NAs | Naphthenic acids |
| OSPW | Oil sands process-affected water |
| O _x -NAs | Naphthenic acids with x Oxygen molecules |
| PAC | Powdered activated carbon |
| PC | Petroleum coke |
| PZC | Point of zero charge |
| RO | Reverse osmosis |
| SAGD | Steam assisted gravity drainage |
| SEM | Scanning electron microscope |
| SPE | Solid-phase extraction |
| TGA | Thermogravimetric analysis |
| TOC | The total organic carbons |
| TPCA | Trans-4-Pentylcyclohexanecarboxylic acid |
| UPLC-TOFMS | Ultra-performance liquid chromatography time-of-flight mass spectrometry |
| VOC | Volatile organic compounds |
| XPS | X-ray photoelectron spectroscopy |

Chapter 1 : General Introduction and Research Objectives

Oil sands in Alberta are the world's largest crude oil deposit covering an area of 142,200 km² (Alberta-Government, 2014). Alberta's bitumen reserves is about 168 billion barrels. In terms of global crude oil reserves, Alberta ranked third after Saudi Arabia and Venezuela. In 2012, Alberta's production of bitumen, from the oil sands and from conventional oil, was about 1.9 million and 557,000 barrels/day respectively (Alberta-Government, 2013). Two methods are currently used in bitumen extractions from the oil sands deposits; surface mining and *in-situ* extraction (Alberta-Government, 2014; Pereira et al., 2013b). Only 3% of the oil sands mines area can be surface mined, the rest (97%) is too deep to be surface mined, therefore, the bitumen is extracted using *in-situ* extraction technique (Alberta-Government, 2014).

In the surface mining process, the oil sands ore is moved from the surface mine to the extraction location. Bitumen upgrading process then takes place after the extraction process. For *in-situ* mining operations, hot steam is blown into the deep mine to liquefy the bitumen then it can be collected and withdrawn using a well and pumps. An 80% of the bitumen reserves will be extracted through the *in-situ* techniques (Alberta-Government, 2013). To extract one barrel of bitumen, a total amount of 9 barrels of water is used (Brown et al., 2013). About 80 % of the total water used in extraction is recycled from the tailing ponds (Alberta-Government, 2014). The rest of the water (3 to 4 barrels) is being imported from the Athabasca river (Alberta-Government, 2014; Allen, 2008a). Only in 2014, 168 million cubic meters of fresh water were used in oil sands operations, about 60% of which were withdrawn from Athabasca River (about 100 million m³).

This amount of fresh water accounts for 0.5% of the annual average of the river flow and 2.2% of the minimum monthly flow in 2014 (CAPP, 2015).

Due to Alberta's zero discharge policy, the oil sands process-affected water (OSPW) are stored in constructed ponds on site for recycling purposes and ultimately for appropriate treatment before releasing to the surrounding environment upon the oil sands mines closure. These commitments are as per the contracts between the oil sands company and government of Alberta (Scott et al., 2005b). As of 2015, the total area of existing tailing ponds was 220 Km². OSPW mainly contains 70 to 80 % water, and 20 to 30 % solids. OSPW is alkaline (pH 8-9), slightly brackish (total dissolved solids = 2000 – 2500 mg L⁻¹) and acutely toxic to aquatic and terrestrial biota (Allen, 2008b). OSPW contains a complex mixture of polar organic compounds (Ross et al., 2012a). The main source of acute toxicity in the OSPW was attributed to the acid extractable fraction (AEF), which includes naphthenic acids (NAs) and other organics (Allen, 2008a; Clemente and Fedorak, 2005; Reinardy et al., 2013b; Ross et al., 2012a).

1.1. Naphthenic Acids (NAs)

NAs are complex mixtures of alicyclic and aliphatic carboxylic acids. NAs are naturally occurring substance in petroleum at deferent concentration levels depending on the source of the petroleum (Clemente and Fedorak, 2005; El-Din et al., 2011). NAs are non-volatile, and chemically stable. NAs follow the general formula of C_nH_{2n+Z}O_x, where n represents the carbon number and (8 to 30), Z identifies the hydrogen deficiency (0 to -12), and X represent the number of oxygen (2 to 6), see Figure 1-1 (Clemente and Fedorak, 2005; Grewer et al., 2010a; Rowland et al., 2011a; West et al., 2013).

Due to the complexity of the NAs, the structure of each individual compound of the NAs has not been accomplished yet. However, some detection methods were developed to identify the NAs concentration based on carbon and Z number (Headley and McMartin, 2004). Methods widely used in quantitative analysis are Fourier Transform Infrared (FT-IR) spectroscopy, Gas

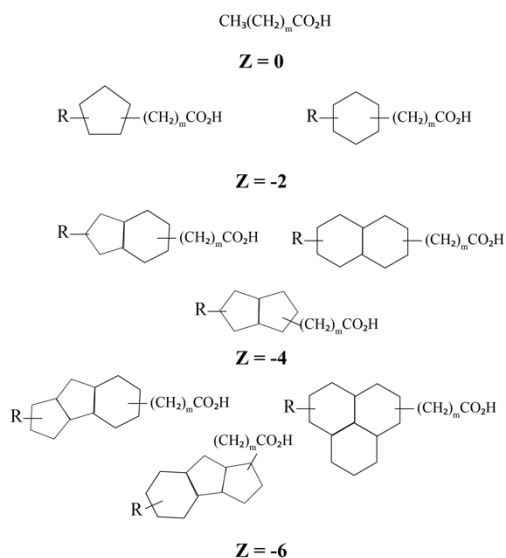


Figure 1-1 Sample naphthenic acid structures where R is an alkyl chain, Z describes the hydrogen deficiency, and m is the number of CH₂ units (adapted from: Clemente and Fedorak, 2005)

Chromatography Mass Spectrometry (GC-MS), and High Performance Liquid Chromatography mass spectrometry (HPLC-MS) (Clemente and Fedorak, 2005). FT-IR method is used in quantifying the total acids extractable fraction (AEF) which contain the NAs and other organic acids (Greuer et al., 2010a), while GC-MS and HPLC-MS are used to quantify the NAs based on their carbon and Z numbers (Clemente and Fedorak, 2005). NA concentrations vary according to OSPW age and ore source. For the aged tailing ponds NA concentrations are ranged from 50 to 70 mg L⁻¹ (Allen, 2008a), while in fresh OSPW it can reach upto 110 mg mgL⁻¹ (Brown and Ulrich,

2015; Headley and McMartin, 2004; Merlin et al., 2007). NAs are also widely known for its corrosive effect that affects the extraction and upgrading equipment in the oil sands industries (Clemente and Fedorak, 2005; Turnbull et al., 1998).

1.2. Emerging treatment technologies for the OSPW

Recently, different studies investigated the potential of different water treatment methods for treating the OSPW such as advanced oxidation processes, membrane processes, biological treatment, wetlands, and adsorption (Allen, 2008b).

1.2.1. Advanced Oxidation Processes (AOPs)

AOPs are oxidation processes designed to produce free hydroxyl radicals ($\cdot\text{OH}$). The $\cdot\text{OH}$ can be produced using the hydrogen peroxide (H_2O_2), ultraviolet light (UV), and ozone (O_3) (Quinlan and Tam, 2015). Using ozone dose 170 mg L^{-1} , the removal percentage of NAs from the OSPW was up to 98.8% (Brown et al., 2013; Islam et al., 2014b; Wang et al., 2014). The ozonated OSPW was reported to be more biodegradable as most of the high molecular weight highly alkyl branched NAs were broken in lower molecules (Kannel and Gan, 2012). However, one of the drawbacks of the AOPs is the complexity of its by-products and the high cost of the process (Kannel and Gan, 2012). Other AOPs used in OSPW treating are UV-illuminated titanium dioxide TiO_2 (UV/ TiO_2), UV-illuminated periodate (UV/ IO_4^-), UV-illuminated persulfate (UV/ $\text{S}_2\text{O}_8^{2-}$), and UV illuminated H_2O_2 (UV/ H_2O_2) (Liang et al., 2011).

1.2.2. Membrane

Membrane processes are used to remove pollutants, solutes or particulates, from water through separation. Membranes are classified based on the size of the removed pollutants to macro

filtration, microfiltration, ultrafiltration, nanofiltration, and reverse osmosis (Sawyer et al., 2003). Membrane applications in removing the NAs from the OSPW were effective. About 98% and 100 % removal of the total organic carbons (TOC) and chemical oxidation demand (COD) of the OSPW were achieved by using microfiltration (MF) and reverse osmosis (RO) (Allen, 2008b). Problems associated with the membrane filtration are the fouling that caused by the oil and solids, the durability of the membrane and the disposal of the retentate (Allen, 2008b). Furthermore, the membrane filtration operating cost is very high as it needs high pressure to force the feed water to go through the filter (Kannel and Gan, 2012). Many studies were conducted to reduce the membrane fouling by coupling the membrane treatment with coagulation-flocculation (CF) processes (Kim et al., 2011; Kim et al., 2012) or modifying the membrane material to reduce the fouling on the membrane surfaces (Alpatova et al., 2013).

1.2.3. Biological Treatment

Biological methods for reclaiming the OSPW, such as bioreactor, was found to be cost-effective methods, however, the biodegradation mechanisms are poorly understood (Kannel and Gan, 2012). Wetland biological treatment shows lower removal percentages of the NAs and other organic contaminants. Because OSPW is in a cold climate area, the biological processes involved in the wetland is slow. Another factor that limits the wetland application in remediation of the OSPW is the leaching of the organic and inorganic contaminants that might take place from the constructed wetland ponds to the near groundwater and/or water streams, which endanger the aquatic biota (Pourrezaei, 2013).

1.2.4. Adsorption

Adsorption is a process, in which, molecules from one phase accumulate on a surface of a material from another phase. For example, contaminants from air (gas) or water (liquid) is removed by accumulation on a surface onto activated carbon (AC) (solid) (Benjamin, 2010; Sawyer et al., 2003).

For the contaminant particles to be removed through adsorption process, it must go through the following four steps (Edzwald, 2010), as illustrated in Figure 1-2.

- 1) Transport through bulk solution,
- 2) External (film) resistance transport,
- 3) Internal (intra-particle) transport, and
- 4) Adsorption

In terms of thermodynamics, there are two types of adsorptions: physical (physisorption) and chemical adsorption (chemisorption) (Bansal and Goyal, 2005d; Lowell, 2006; Sawyer et al., 2003). Physical adsorption results from weak forces such as van der Waals' forces, which are close in magnitude to condensation of vapors into liquids. On the other hand, chemisorption results from much stronger forces and involves exchange or sharing of electrons between the adsorbate and the adsorbents (Sawyer et al., 2003).

The differences between the two types of adsorptions are many; the most important difference is the magnitude of enthalpy of the adsorption. In physical adsorption, the order of enthalpy is of the same order as that of liquefaction which lies in the range of 10 to 20 KJ.mol⁻¹. The order of enthalpy in case of chemisorption is 40 to 100 KJ.mol⁻¹ (Bansal and Goyal, 2005c). Another important difference is that the physical adsorption is nonspecific and the adsorbed molecules can be restored to its original state through desorption process, while in case of the

chemisorption, the adsorption is specific and it is seldom to restore the original state of the adsorbed molecules. Also, the physical adsorption can be multi-layer while chemisorption usually is mono layer process (Bansal and Goyal, 2005b; Sawyer et al., 2003).

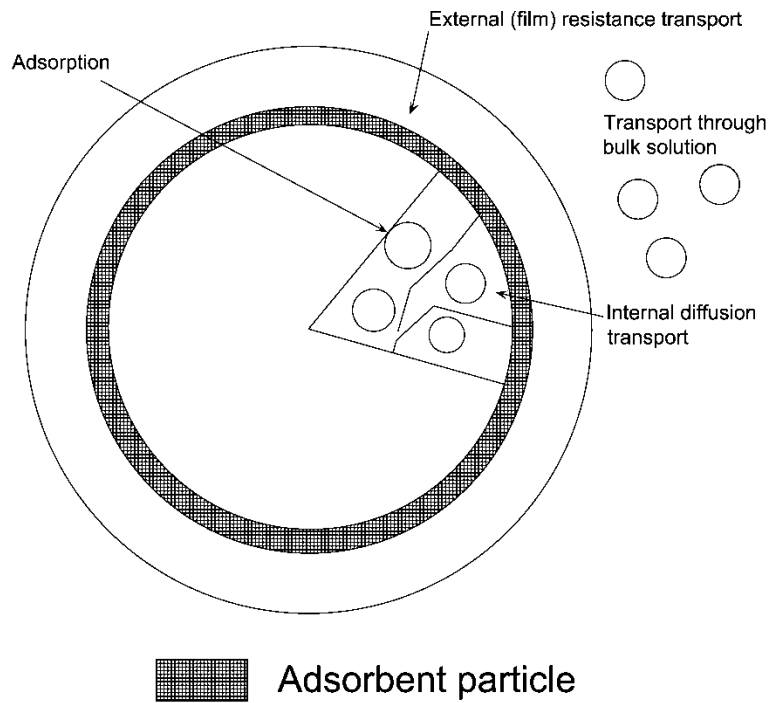


Figure 1-2 Adsorbent particle illustrating associated resistances

Factors affecting the adsorption process are the capacity of the adsorbent, the pore volume and size distribution, temperature, adsorbate concentration in the solution, the affinity of the adsorbent to adsorbate, etc. (Bansal and Goyal, 2005b; Sawyer et al., 2003; Weber, 1974). The adsorbent particles pore sizes are classified, according to the international union of pure and applied chemistry (IUPAC), into three main categories: macro, meso and micropores. Macropores are the pores that have width greater than 50 nm, while the micropores width is less than 2 nm. The mesopores width is ranged in between the micropores and macropores widths (2-50 nm), See Figure 1-3.

Initially, when the adsorbent exposed to the adsorbate, the adsorption takes place in a high rate, as the whole adsorbent surface is available for adsorption. Then, desorption rate from the adsorbent surface increases. After certain time, the equilibrium reached when the rate of adsorption equals the rate of desorption (Sawyer et al., 2003).

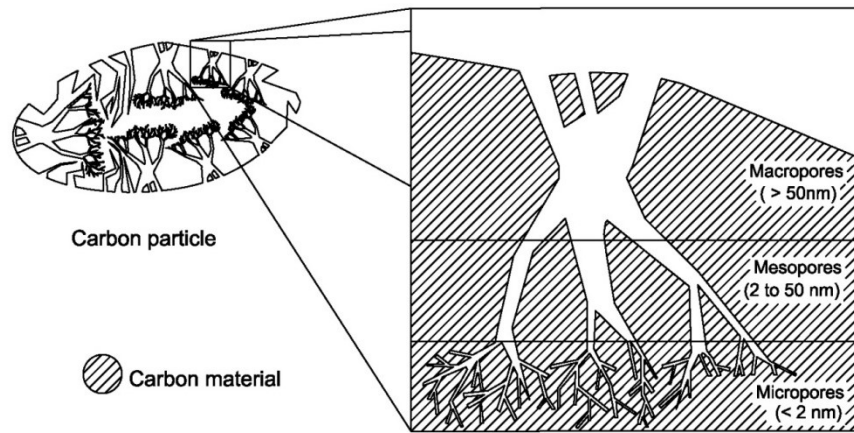


Figure 1-3 Pore size distribution, adapted from (Menéndez and Martín-Gullón, 2006)

A common way of describing the adsorption systems at the equilibrium is the isotherm. Adsorption isotherm is a relationship that relates the amount of the adsorbate by unit mass of solid at the surface of the adsorbent to the concentration in the solution at a known temperature, see Figure 1-4. Different models have been developed to express this relationship mathematically such as Langmuir and Freundlich, Brunaur-Emmett-Teler (BET), and Dubinin isotherms. Each of these models has some assumptions that make it applicable to specific cases only (Benjamin, 2010; Rouquerol, 2014; Sawyer et al., 2003).

Langmuir and Freundlich isotherm are used equally to describe the physisorption and chemisorption. The BET and Dubinin isotherms are mostly used in describing the physical adsorption (Bansal and Goyal, 2005b). Langmuir isotherm was derived theoretically from

thermodynamic and statistical approaches. In Langmuir isotherm, it is assumed that all the adsorbent surface sites are energetically homogeneous and there is no interaction between the sites. Freundlich isotherm is a special case of Langmuir isotherm and it is more applicable to chemisorption, however, it was successfully used to describe physical adsorption as well.

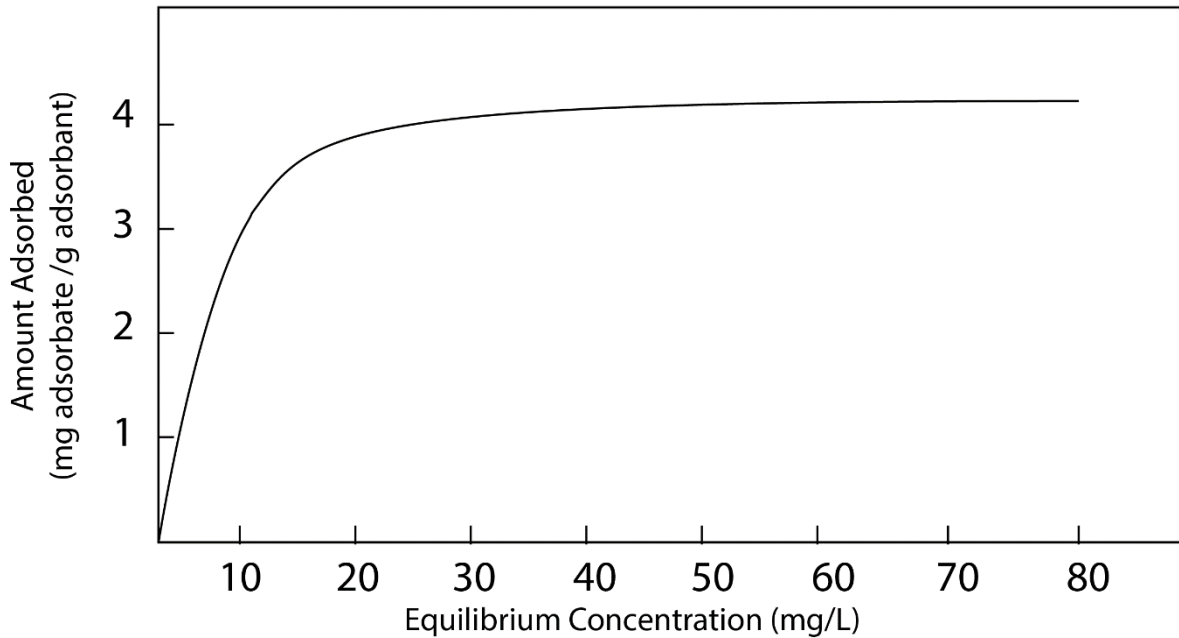


Figure 1-4 Typical adsorption isotherm between amounts of adsorbed per mass unit of adsorbent and the equilibrium concentration

Dubinin isotherm, which is based on potential theory, was developed primarily for microporous adsorbents. Dubinin equation represents the temperature dependence of the adsorption. This allows thermodynamic calculation that leads to calculation of the entropy of the adsorption process (Bansal and Goyal, 2005b).

The most used adsorbent is the activated carbon (AC). AC is produced in two forms granular (GAC) and powdered activated carbon (PAC). AC is widely used in water and wastewater treatment applications such as odor and taste control, removing the organic and heavy metals etc.

AC carbon is also used in removing the volatile organic compounds (VOC), and it is used as a media in filters. Other AC applications are depolarization of oils and fats, decolourization of sugar solutions, removing dyes and organics from leather and textile industries wastes. AC applications in liquid and gas phases are detailed elsewhere (Bansal and Goyal, 2005b; Mattson and Mark, 1971).

There are a variety of raw materials that can be used to produce AC such as coal, petroleum coke, lignite, coconut, and wood. AC production can be through either physical or chemical processes. Both physical and chemical processes start with carbonization, which is converting the raw material to a char. Then, the activation step takes place after the carbonization. For physical process, the carbonization is done in the absence of air at temperature less than 700 °C, while the activation step takes place in the presence of oxidizing gases such as hot steam or carbon dioxide (CO₂) with temperature of 800 to 900 °C. In the chemical activation process, the carbonization and activation processes took place in the same time by adding the activating agent, such as phosphoric acid, to the raw material (Edzwald, 2010; Zubot, 2011). The produced activated characteristics depend on the raw material as well as the activation process.

Another adsorbent is a carbon xerogel (CX). CXs are a class of synthesized porous material that has low density, high porosity, high surface area and tailorable surface chemistry. CX are synthesized by carbonization of resorcinol and formaldehyde organic gels (Mahata et al., 2007; Pekala, 1989; Ramirez-Montoya et al., 2017). The advantage of the CX is the ability of controlling its textural properties, such as pore size distribution and morphology, and chemical characteristics, such as surface chemistry, of the produced material by adjusting number of variables during the synthesis process (Rey-Raap et al., 2014).

Factors that affect the CX characteristics are drying conditions, pH, type and amount of solvent, concentration of reactants, temperature and time of the synthesis process and the carbonization process, whereas the pH and concentration of reagents are the most two important factors that affects the final characteristics of the CX (Bermudez et al., 2015; Job et al., 2005; Rey-Raap et al., 2016).

Given that the final CX properties can be controlled during the synthesis process, the porous structure can be tailored to fit the usage of the material. For example, thermal insulation requires low density, low surface area, pores in the mesoporosity range (Lu et al., 1995; Rey-Raap et al., 2014). Hydrogen storage applications require a high microporosity and appropriate micropore size distribution (Rey-Raap et al., 2014). CX also was used as electrode material as it's microporosity, mesopores are required in order to facilitate a good dynamic charge propagation(Rey-Raap et al., 2014). CX were successfully used as adsorbents in air and water purification applications such as CO₂ capturing, VOC removal and removal of oil and toxic organic compounds from wastewater (Moreno-Castilla and Maldonado-Hodar, 2005; Rey-Raap et al., 2014).

For adsorption application in OSPW remediation, granular activated carbon (GAC), petroleum coke (PC), and organic rich soils were examined as adsorbents to remove NAs (Janfada et al., 2006; Pourrezaei et al., 2014b). GAC with acidification showed a 75% removal of the NAs from the OSPW. Three different organic rich soils were tested to remove the NAs. Results showed higher sorption in higher organic content soil samples and NAs with carbon number 13 to 17 were the most adsorbed (Janfada et al., 2006).

Another study was carried out to investigate the performance of various types of adsorbents (such as silica alumina, zeolite, and activated carbon, among others) in removing NAs from

aqueous solution. Total organic carbon (TOC) was used as the parameter to assess the NAs removal. The number of dissolved solids was taken into consideration. Results show that AC and Ni-based alumina were the best adsorbents in terms of total organic carbon (TOC) removal by achieving 50 and 40 % removal, respectively. According to the results, the addition of the total dissolved solids TDS decreases the performance dramatically (Azad et al., 2013). Iranmanesh et al. (2014) evaluated the NAs adsorption using AC. The AC was prepared by physical and chemical activation processes using sawdust as the precursor material. The AC that produced from chemical activation process shows a higher performance in terms of removal of the NAs than the physically activated AC (Iranmanesh et al., 2014). The difference in the performance is attributed to the higher mesoporosity and surface area of the AC prepared by chemically activation (Iranmanesh et al., 2014).

PC is a carbonaceous solid produced as a by-product of the bitumen upgrading process (Scott and Fedorak, 2004). Raw PC was used in removing NAs from water, resulting in removing about 75% of the NAs from OSPW after 16 hours with adsorbent load of 200 g.L^{-1} (Pourrezaei et al., 2014a). In another study, it has been reported that by mixing 20 and 30 wt% of the raw petroleum coke (PC) with OSPW in the conveying pipes between the production site and the ponds used in storing the OSPW resulted in 82% and 94% removal of the NAs, respectively from OSPW. The PC could remove the more structurally complicated part of the NAs and it was attributed to the mesoporous range of the PC (Kannel and Gan, 2012; Zubot, 2011). Both types of the PC, fluid and delayed cokes, were used as a precursor material to produce AC (Small et al., 2012a). The activation increased the NAs removal capacity from 0.22 mg g^{-1} of raw PC to 588.8 mg g^{-1} of activated PC (Small et al., 2012b; Zubot, 2010). The drawback of the PC activation was the heavy

metals leaching observed during the adsorption process (Small, 2011). The speciation of the heavy metals was studied in detail by Jensen-Fontaine (Jensen-Fontaine, 2012).

1.3. Research Scope

Restoring the oil sands mines to its original state is part of the contract signed between the government of Alberta and all oil sands companies before the companies took the control over of the oil sands mines. The restoration will be for the forests that may be removed from the top of the oil sands mines, and wastes that will be collected during the production time either liquid (OSPW) or/and solid (petroleum coke). Up to now, there are no economically viable treatment methods that can be used in treating the OSPW to be safely disposed to the surrounding environment. Till developing the water treatment technology, the OSPW is stored in tailing ponds that grow as the oil production continues. One of the major tasks that the oil sands companies is doing during the oil production is the regular water quality monitoring of the tailing ponds and its toxic components.

Water quality monitoring programs usually carried out regularly by defining the sampling sites, the time interval between the samples and water parameters that will be monitored. In case of the OSPW, water parameters that should be taken into consideration are many. One of the most important parameters is the NAs. The challenge in monitoring the NAs is the absence of standard method to quantify the NAs from aqueous samples. So far, different methods were used in quantifying the NAs such as FT-IR, GC-MS, and HPLC-TOFMS. FT-IR method is widely used by many oil sands companies in quantifying the AEF that contains the NAs besides other extractable organics.

The FT-IR method is carried out by acidifying the water sample then the AEF is extracted using liquid/liquid (LLE) or solid phase extraction (SPE), and then the extracted fraction is

quantified using the FT-IR based on a standard solution that can be either synthetic (commercial) standard or natural extract from the OSPW. Each of the previous steps affects the result of the FT-IR. This understanding of the effects of each of the steps involved in FT-IR method will help in comparing the results from different studies that carried out differently and to assist in developing a standard method that will be used in quantifying the AEF/NAs from OSPW. Also, it will help in planning the monitoring programs in the oil sands mines area not only in the current stage of regular monitoring, but also in the restoration/treatment stage.

1.4. Objectives

The first objective in this research is to understand the effect of different factors on FT-IR results and how the FT-IR results are compared to a high-resolution quantification method that uses the mass spectrometers in AEF/NAs quantification. The second objective of this research is to assess the performance of CX and GAC adsorbent in removing TPCA from aqueous solution.

The specific objectives of this thesis are listed below:

- To comprehend the difference between non-mass spectrometric quantification method (FT-IR) method and high-resolution/ mass spectrometric (TOF-MS) AEFs quantification methods
- To understand the effect of standards chemical, separation method and the water sample type on the result of the FT-IR
- To study the differences between AEF results through applying non-parametric statistical method
- To prepare and characterize the CX, and GAC
- To explore the potential of using the CX in removing model naphthenic acid (TPCA)
- To develop the isotherm of removing the model NA on CX and compare the results to the commercially available GAC results
- To study the adsorption mechanism of model NA from water using the CX and GAC.

- To investigate the effect of temperature, ion strength, and pH on the removal efficiency of the model NA by adsorption on CX and GAC

1.5. Thesis Outline

This thesis is divided into two main parts. First part deals with the NAs analytical method FT-IR and how it compares to HPLC-TOF-MS, while the second part evaluates the CX and GAC in removing the TPCA from water.

Chapter 1 is a general introduction that provides a background about the oil sands industry and why it is important to Alberta, Canada and the world, then it casts some light on the OSPW's origin, storing and some of the treatment methods that deal with OSPW treatment specially the adsorption process. GAC and CX along with some of their applications were also introduced in the introduction chapter

Chapter 2 compares two NAs quantification methods, FT-IR (low resolution analytical method) and HPLC-TOF-MS (high resolution analytical method). The sample extraction methods (LLE and SPE), standard used in quantification (Fluka vs natural extract) as well as the water type (OSPW vs ground water) were the parameters used in the comparisons.

Chapter 3 focus was on the FT-IR method from statistical point of view. Non-parametric statistical methods were used to understand the effect of the sampling location, the standard chemical, and sample preparation methods on the FT-IR results.

Chapter 4 investigates the potential of using CX as an adsorbent to remove the TPCA model compound from water. In this chapter, CX was synthesized at pH 5.5. The CX was characterized using surface characterization methods such as scanning electron microscope (SEM) surface area quantification, Fourier transformation infrared (FTIR) spectroscopy, and X-ray

photoelectron spectroscopy (XPS). Isotherms were developed for fitting the adsorption of the TPCA on the CX surface. Commercially available GAC was used as a reference to judge the performance of the CX. The effect of temperature, pH, and ionic strength on the adsorption efficiency is studied. Finally, thesis summary and conclusions were stated in Chapter 5.

Chapter 2 : Quantification of oil sands organic acids using Fourier transform infrared spectroscopy and ultra-performance liquid chromatography time-of-flight mass spectrometry: Impacts of the extraction and calibration methods.¹

2.1. Introduction

The oil sands industry in Northern Alberta, Canada produces large amounts of oil sands process-affected water (OSPW) (Shell Canada Limited, (2016; Board, 2012). OSPW is currently stored in tailings ponds to permit the recycling of water, and due to their toxicity to aquatic organisms (Hagen et al., 2014a; Mahaffey and Dubé, 2016; Martin, 2015; Sun et al., 2014a; van den Heuvel, 2015). OSPW is a highly complex mixture of suspended solids, salts, metals, and organic compounds (i.e., naphthenic acids (NAs), oil, grease and other hydrocarbons) (McQueen et al., 2017). The characterization of the organic fraction of OSPW alone is a great challenge because of the thousands of organic compounds present in OSPW (Barrow et al., 2010) which can hardly be characterized by simple methods while mass spectrometric techniques coupled with chromatographic can provide some options (Barrow et al., 2015; Grewer et al., 2010b; Hagen et al., 2014b; Huang et al., 2015a; Pereira et al., 2013d; Ross et al., 2012b; Rowland et al., 2011a; Rowland et al., 2011b; Shang et al., 2013; Woudneh et al., 2013).

NAs are natural constituents of bitumen and have been reported to be the main contributor to the acute and chronic toxicity of OSPW (Morandi et al., 2015b; Verbeek et al., 1994; Yue et al., 2015a). NAs are a complicated mixture of carboxylic acids with the general formula of $C_nH_{2n+Z}O_x$, where n denotes the carbon number, Z the hydrogen deficiency number (zero or a negative even

¹ A version of this chapter will be submitted to Talanta journal as: “Meshref, M.N.A., Ibrahim M.D., Huang, R., Chen, Y., Klammerth, N., Chelme-Ayala, P., Hughes, S.A., Brown, C., Mahaffey, A., and Gamal El-Din, M. “Quantification of Oil Sands Organic Acids Using Fourier Transform Infrared Spectroscopy and Ultra-performance Liquid Chromatography Time-of-Flight Mass Spectrometry: Impacts of the Extraction and Calibration Methods”.

integer), and x the number of oxygen atoms. Recent advances in analytical techniques and methods have revealed that the NAs comprise of not only classical NAs ($x=2$) but also oxidized NAs with $x \geq 3$ (Huang et al., 2015a), as well as some other species such as aromatic NAs (Jones et al., 2012; Reinardy et al., 2013a; Scarlett et al., 2013). Furthermore, it has been reported that NAs may contain heteroatoms such as nitrogen or sulphur atoms in the molecule (Headley et al., 2015; Headley et al., 2013c; Noestheden et al., 2014; Zhang et al., 2015).

To date, there are a couple of methods available for the extraction and pre-treatment of NAs and naphthenic acid fraction compounds (NAFCs) from water samples like OSPW for analysis. The first is a protocol for liquid–liquid extraction (LLE) using dichloromethane (DCM) was developed by Syncrude Canada Ltd (Jivraj MN, 1995; Rogers et al., 2002) and well implemented in a number of studies (Headley et al., 2013b; Huang et al., 2015b; Rogers et al., 2002; Scott et al., 2008a; Young et al., 2007; Young et al., 2008). The second common sample clean-up method used in OSPW sample preparation is the solid-phase extraction (SPE) method (Headley et al., 2013b; Yue et al., 2015a; Yue et al., 2016).

In addition to sample pre-treatment, there are several different instrument methods used for OSPW NA analysis, including ultra-performance liquid chromatography time-of-flight mass spectrometry (UPLC-TOFMS), Fourier transfer ion cyclotron resonance mass spectrometry (FTICR-MS), and Fourier transformation infrared (FTIR) spectroscopy methods. Both UPLC-TOFMS and FTICR-MS are used to identify and categorize the composition and explore the profile of NA species and their relative abundance in the water samples based on Z , n and x numbers. Alternatively, FTIR has been implemented to measure the acid extractable fraction or NAFCs (i.e., organic compounds isolated from OSPW during the LLE and SPE sample clean-up processes). Although the estimates of FTIR method are not specific to individual NAs, and lack

the ability to resolve carbon numbers and Z families, FTIR results are still implemented as surrogate parameters to monitor the efficiency of water treatments, OSPW water quality, and NA degradation (Gamal El-Din et al., 2011a). The correlation between NAs and NAFCs was previously studied (Han et al., 2009; Martin et al., 2008) and observed using treated process water samples, where the determination of the NAFCs encompassed all NA species among other compounds (Islam et al., 2014a). However, there is a lack of knowledge whether the correlation holds true with groundwater (GW) with different concentration levels and sample matrices (Grewer et al., 2010b; Ross et al., 2012b). The classical and oxidized NAs have been found to represent ~64% of the composition of NAFCs (Nyakas et al., 2013). The commercial NAs (e.g., Fluka or Merichem mixtures) have been widely used as NA calibration standard to quantify NAs (Headley et al., 2010b; Hindle et al., 2013; S. Mishra, 2010; Sun et al., 2014a). However, the variations in their composition between production lots might have an impact on the mixture composition and hence the quantification method (Hindle et al., 2013; West et al., 2011).

Therefore, the main objective of this study was understand the difference between two different analytical methods (a non-mass spectrometry (MS) method [FTIR] and high-resolution MS method [UPLC-TOFMS]) with different extraction methods (LLE and SPE) to analyze O_x-NAs (sum of classical NAs and oxidized NAs) and NAFCs using statistical multivariate analysis. The specific objectives were aimed to: i) examine the influence of selectivity between the samples' extraction/pre-treatment method (SPE and LLE); ii) examine the differences in characterization between FTIR and UPLC-TOFMS using different water sources; and iii) explore the similarities and differences between OSPW extract standard and commercial NA extract used as calibration standards. The correlation of these different methods and techniques would help the research community to adopt the best tools available for sample preparation and analysis.

2.2. Materials and methods

2.2.1. Sources of water

Water samples were collected from ten different locations within the Shell Canada Limited's Albian Sands oil sands mining operations located in northeastern Alberta, Canada. Three samples (labeled OSPW-1 to OSPW-3) were collected from oil sands tailings ponds, in addition to seven groundwater samples collected from either different aquifers or locations and/or depths in the same oil sands area and labeled as GW-4 to GW-10. Two of the OSPW samples were the supernatant (i.e., collected from the zone of clear water) of the external tailings facility (ETF) for both the Jackpine Mine (OSPW-1) and Muskeg River Mine (OSPW-2) ETFs while the third OSPW sample (OSPW-3) is recycled water that was directed back into the extraction process. The recycled water collected from a recycle pond was the combination of the two ETFs water as well as other ospw water from site. The groundwater and OSPW samples were stored at 4 °C until use. The same 10 samples were collected from the same locations at different times: June, August, and October of 2015 for a total of 30 samples.

2.2.2. Chemical and reagents

Sulfuric acid (H₂SO₄) and dichloromethane (DCM) Optima grade used in the extraction process were from Fisher Scientific (ON, Canada). Formic acid and Fluka commercial NA standards were purchased from Sigma-Aldrich (ON, Canada). In our study, we used Fluka commercial NAs because they have been implemented in several studies (Headley et al., 2009; McMartin et al., 2004; S. Mishra, 2010) due to its comprehensive characteristics and compositions (Barrow et al., 2004; Headley et al., 2010a; Rudzinski et al., 2002; Scott et al., 2005a). Optima-grade water, methanol, and acetonitrile (Fisher Scientific, ON, Canada) were used for the

instrument analysis. Isolute® layered SPE columns (6 mL ENV+) were purchased from Biotage, (NC, USA).

2.2.3. Sample preparation

2.2.3.1. Liquid-liquid extraction (LLE)

Due to the surfactant properties of NAs and to avoid dissolution of organic contaminants on the surfaces after contacting with DCM, glass laboratory wares and Teflon™ were used in all experiments (Rogers et al., 2002). OSPW and groundwater samples were centrifuged to remove suspended particles (Rogers et al., 2002). Each sample was divided into four working aliquots of 100 mL (sample weight ≈100 g). The pH of each sample was adjusted to pH 2 using H₂SO₄ for further extraction. Each adjusted centrifuged water sample of 100 mL in every beaker was extracted using two times of 50 mL DCM, where the entire dried residues were recorded for calculating the fraction weight. Air flushing/drying unit was used to dry the extract. After shaking and venting the mixture for 3 minutes, the mixture was left for another 3 minutes to assure complete separation. The solvent: sample ratio was 1:2, as stated in the original protocol by Jivraj et al. (1995).

2.2.3.2. Solid-phase extraction (SPE)

Like LLE, water samples were divided into four aliquots of 100 mL after centrifugation. The samples were acidified to pH 1 using formic acid before extraction. An ENV+ (Biotage) cartridge was used as received and conditioned with 5 mL water, followed by 5 mL of methanol and finally with 10 mL of water. The 100 mL sample was loaded into the column and the eluent went to the waste. Then, the sample in the column was rinsed (i.e., eluent to waste) with 5 mL of water. After that, 6 mL of methanol was added to elute the fraction out from the column. The 6

mL methanol was evaporated and dried using air. The fractions were then used for further analysis of UPLC-TOFMS and FTIR.

2.2.4. Analytical methods

2.4.1. Ultra-performance liquid chromatography time-of-flight mass spectrometry (UPLC-TOFMS) analysis

Chromatographic separations were performed using a Waters UPLC Phenyl BEH column (1.7 μm , 150 mm \times 1 mm), with mobile phases of 10 mM ammonium acetate in water (A), 10 mM ammonium acetate in 50/50 methanol/acetonitrile (B), and the injection volume of 10 μL . The elution gradient was 0–2 min, 1% B; 2–3 min, increased from 1% to 60% B; 3–7 min, from 60% to 70% B; 7–13 min, from 70% to 95% B; 13–14 min, from 95% to 1% B, and hold 1% B until 20 min to equilibrate column with a flow rate of 100 $\mu\text{L}\cdot\text{min}^{-1}$. The column temperature was set at 50°C and the sample temperature at 10°C. Samples were analyzed using the UPLC-TOFMS (Synapt G2, Waters) with the TOF analyzer in high-resolution mode (mass resolution is 40000) and the investigated mass range of 100–600 (m/z). The electrospray ionization (ESI) source was operated in negative ion mode to measure NA concentrations in the samples (Pereira et al., 2013a). Data acquisition was controlled using MassLynx (Waters) and data extraction from spectra was performed using TargetLynx (Waters). This method was developed previously for NA semi-quantification based on the signal of a compound versus the signal of spiked internal standard (Huang et al., 2015b; Wang et al., 2013a).

A pre-calibrated OSPW extract (Environment and Climate Change Canada, Saskatoon, SK) was used as standard for preparation of the external standard calibration curve with 5, 10, 25, 50, 75, 100 mg mg L⁻¹ in 50/50 acetonitrile/water (Headley et al., 2013b; Martin et al., 2008). Duplicate pretreated samples were prepared for injection; however, a single injection was used

due to the superior accuracy, constant reliability and precision of the UPLC-TOFMS technique as reported in previous studies (Hwang et al., 2013; Martin et al., 2010; Sun et al., 2014a). Because the SPE or LLE fractions were concentrated for 100 times from 100 mL sample to 1 mL fraction, discrete dilution times were applied to different samples with the solvent 50/50 acetonitrile/water, based on the weight of each fraction, to fit the measured concentrations into the dynamic range of the external curve. The SPE or LLE extractions were necessary to remove the sample matrix and to concentrate the samples in order to estimate the NA concentration using the external calibration curve.

2.4.2. Fourier transform infrared (FTIR) spectroscopy analysis

FTIR quantification of NAFCs was conducted using a Nicolet 8700 FTIR spectrometer. The fixed path length of KBr liquid cell was 3 mm. Purge gas generator from Parker Balston Model 75-52 was used while running the samples. Omnic Software was used to acquire and process the spectrum. The sample spectrum was recorded for 128 scans after a 7-minute purge. The peak height or absorbance was recorded at both wavelengths of 1743 and 1706 cm^{-1} . The concentration of NAFCs in the water samples was calculated based on a prepared calibration curve and the total of recorded peak heights (Scott et al., 2008a). All samples were analyzed in duplicate.

Two calibration curves using two sets of standards were prepared as shown in the Supporting Material (Figs. S1 and S2). The first calibration curve was established from a commercial mixture of NAs (Fluka). The quantification of NAFCs was estimated using both OSPW extract and Fluka standard. The appropriateness of estimating the NAFCs and NAs concentration from the curve of commercial NA mixtures (Merichem) has been previously reported (Martin et al., 2008; Scott et al., 2008a; Young et al., 2007; Young et al., 2008).

2.2.5. Statistical analysis

Statistical analyses were performed using R 3.3 software. R is a language and environment for statistical computing. R Foundation for Statistical Computing, Vienna, Austria, URL <http://www.R-project.org/>. The normality of the data was checked by Shapiro–Wilk test. Kruskal-Wallis and Mann-Whitney-Wilcoxon tests were performed for non-normally distributed data with a significance level of 0.05. Mann-Whitney-Wilcoxon and Kruskal-Wallis tests are the non-parametric alternatives to T-test and ANOVA, respectively. The null hypothesis is that all samples are similar or come from same population while the alternative hypothesis is that not all samples come from same population. Data were grouped with regard to the sampling locations, instrumental methods, standard used in calibration (FTIR-Fluka vs FTIR-OSPW Extract vs UPLC-TOFMS-OSPW Extract), and sample pre-treatments or extraction method (LLE vs SPE). For instance, the terminologies used in this study are as follows: FTIR-SPE-Fluka refers to analysis of sample by FTIR pretreated by SPE and using Fluka as standard; FTIR-LLE-OSPW refers to analysis of sample by FTIR pretreated by LLE and using OSPW extract as standard; TOF-SPE-OSPW and TOF-LLE-OSPW refer to analysis of samples by UPLC-TOFMS pretreated by either SPE or LLE, respectively and using OSPW extract as standard.

2.3. Results and discussion

Efforts have been made to investigate the differences and variations between the profiles of industrial processed water (e.g., OSPW) and natural waters (e.g., groundwater) (Frank et al., 2014a; Ross et al., 2012b). While the studies about the water quality in the oil sands region (Frank et al., 2014a; Ross et al., 2012b) aimed to deduce chemical indicators or surrogate parameters to monitor the variations of the water characteristics as well as to investigate suspected seepage or

natural biodegradation, our study focused on comparing different analytical tools to measure the concentrations of NAs and NAFCs (Figure 2-1). Different water samples (i.e., OSPW samples: 1, 2 and 3; groundwater samples (GW): 4, 5, 6, 7, 8, 9 and 10) were collected in three replicates. The variations of O₂-NA, O_x-NAs and NAFCs concentrations for each batch with time are illustrated in Table 2-1. Figure 2-2 also shows the concentrations of O_x-NAs and NAFCs for all samples (i.e., OSPW samples: 1, 2 and 3; GW: 4, 5, 6, 7, 8, 9 and 10) in each replicate. Overall, the Kruskal-Wallis test was implemented to assess the differences between all samples as one group and based on their source (OSPW or GW). The results showed that there was no significant difference between samples 1, 2, and 3 (OSPW samples; $p > 0.05$), but statistical differences existed between groundwater samples ($p < 0.05$; Table 2-2).

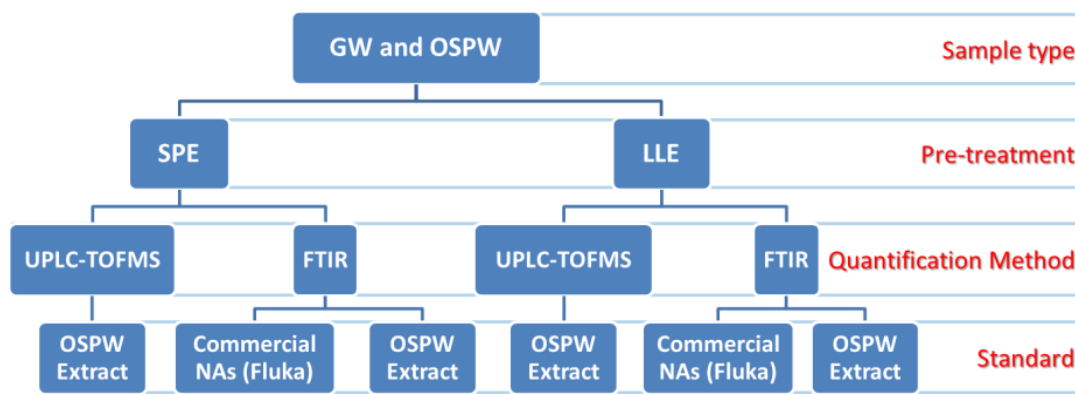


Figure 2-1 Schematic diagram showing the different pre-treatment methods and analyses performed in the present study, including the different water samples. Abbreviations are listed as follows: groundwater, GW; oil sand process-affected water, OSPW; solid-phase extraction, SPE; liquid-liquid extraction, LLE; ultra-performance liquid chromatography time-of-flight mass spectrometry, UPLC-TOFMS; Fourier transform infrared spectroscopy, FTIR; and naphthenic acids, NAs.

Table 2-1 Classical NAs (O_2 -NAs) as well as sum of classical NAs and oxidized NAs (O_x -NAs). NA concentrations in ($mg\ mg\ L^{-1}$) were estimated by UPLC-TOFMS while naphthenic acid fractions compounds (NAFCs) concentrations in ($mg\ mg\ L^{-1}$) were estimated by FTIR for all groundwater and OSPW samples.

| Sample # | UPLC-TOFMS | | | | FTIR | | | |
|----------|-----------------------------|--------------|-----------------------------|--------------|------------------------|-------------|-----------------------|---------------|
| | OSPW Extract standard | | | | Fluka standard | | OSPW Extract standard | |
| | TOF-LLE | TOF-SPE | TOF-LLE | TOF-SPE | FTIR-LLE | FTIR-SPE | FTIR-LLE | FTIR-SPE |
| | O_2 -NAs ($mg\ L^{-1}$) | | O_x -NAs ($mg\ L^{-1}$) | | NAFCs ($mg\ L^{-1}$) | | | |
| OSPW-1 | 20.07 ± 1.26 | 20.08 ± 2.51 | 32.93 ± 3.12 | 36.11 ± 2.80 | 33.6 ± 2.4 | 40.8 ± 18 | 87.1 ± 5.80 | 102.5 ± 28.10 |
| OSPW-2 | 28.35 ± 1.88 | 28.56 ± 3.74 | 43.51 ± 2.80 | 46.44 ± 3.88 | 40.7 ± 2.7 | 60.3 ± 3.20 | 105.5 ± 7.20 | 149.1 ± 18.40 |
| OSPW-3 | 22.29 ± 1.24 | 21.73 ± 2.49 | 34.99 ± 1.78 | 36.24 ± 2.77 | 34.1 ± 1.7 | 50 ± 6.20 | 88.3 ± 5.20 | 119.4 ± 11.60 |
| GW-4 | 4.29 ± 0.42 | 4.99 ± 0.18 | 6.08 ± 0.64 | 7.477 ± 0.45 | 4.9 ± 0.60 | 4.4 ± 1.30 | 13.7 ± 1.70 | 9.9 ± 5.60 |
| GW-5 | 6.33 ± 1.39 | 7.25 ± 0.85 | 8.95 ± 1.81 | 10.87 ± 1.23 | 7.3 ± 0.60 | 6.5 ± 2.90 | 19.9 ± 1.60 | 15.5 ± 7.50 |
| GW-6 | 10.23 ± 0.54 | 9.34 ± 0.84 | 14.91 ± 0.67 | 14.43 ± 1.40 | 12.3 ± 0.5 | 11.1 ± 0.90 | 32.5 ± 1.30 | 27.2 ± 3.10 |
| GW-7 | 7.72 ± 1.26 | 9.57 ± 0.30 | 12.46 ± 2.12 | 15.94 ± 1.89 | 12.6 ± 1.00 | 15.5 ± 3.60 | 33.2 ± 2.70 | 38.7 ± 11.10 |
| GW-8 | 7.95 ± 0.6 | 8.98 ± 1.21 | 11.35 ± 0.70 | 12.62 ± 1.14 | 11 ± 1.40 | 10.7 ± 1.40 | 29.3 ± 3.60 | 26.4 ± 3.50 |
| GW-9 | 0.64 ± 0.07 | 0.63 ± 0.67 | 1.08 ± 0.13 | 1.547 ± 1.44 | 1 ± 0.20 | 0.7 ± 1.70 | 3.5 ± 0.80 | 1.1 ± 1.20 |
| GW-10 | 0.93 ± 0.03 | 1.03 ± 0.20 | 1.65 ± 0.08 | 2.443 ± 0.59 | 2.1 ± 0.20 | 3.5 ± 2.30 | 6.3 ± 0.90 | 7.7 ± 8.90 |

Notes:

- Solid-phase extraction is denoted as SPE; and liquid-liquid extraction is denoted as LLE. OSPW samples: OSPW-1, OSPW-2 and OSPW-3; Groundwater samples are denoted as GW-4, GW-5, GW-6, GW-7, GW-8, GW-9, and GW-10.
- FTIR-LLE and FTIR-SPE refer to the analysis of a sample by FTIR and pretreated by LLE and SPE, respectively; TOF-LLE and TOF-SPE refer to the analysis of a sample by UPLC-TOFMS and pretreated either by LLE or SPE, respectively.
- Error bars are standard errors based on the sample size (n) = 3 or triplicate samples collected over three months (June, August and October 2015).
- Sources of OSPW: OSPW-1 and 2 are collected from external tailings facility from different mine locations while OSPW-3 is recycled water.
- Sources of GW: Groundwater samples are collected from different Basal and channel aquifers from different mine locations.

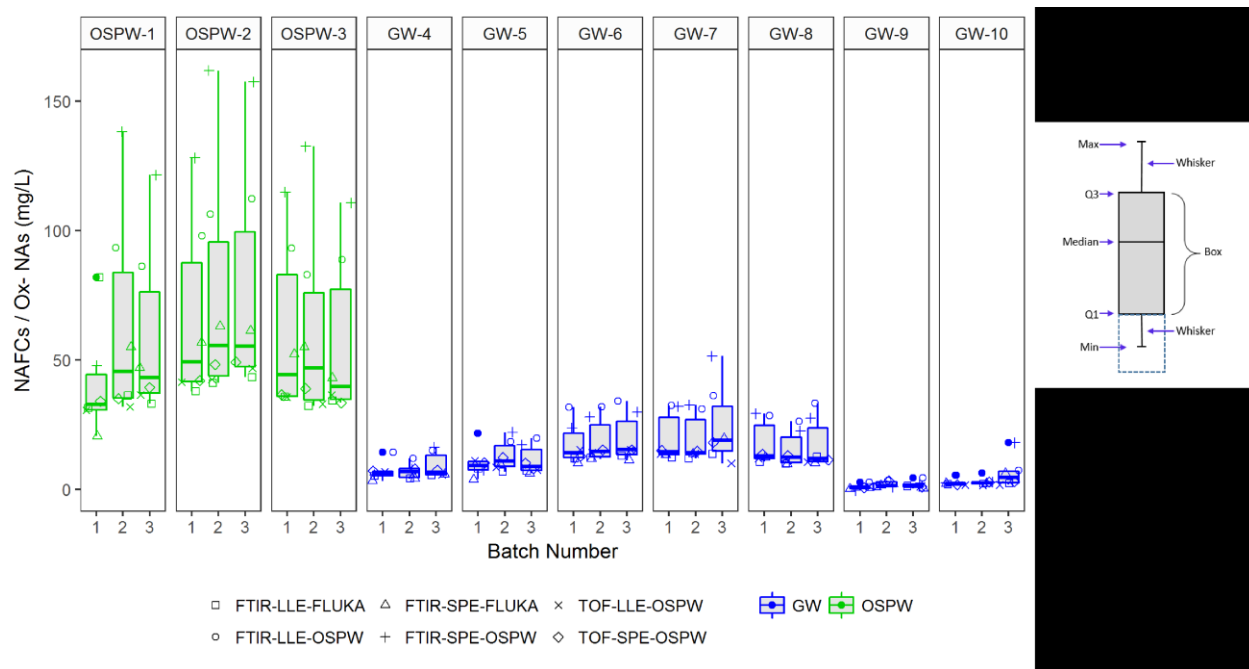


Figure 2-2 Change of Ox-NAs [sum of NAs at ($2 \leq x \leq 6$) or sum of classical (O_2) NAs and oxidized NAs; as measured by UPLC-TOFMS analyses] and naphthenic acid fractions compounds (NAFCs as measured by FTIR analyses) concentrations in the three sample batches or replicates (1 = June, 2 = August, and 3 = October 2015) using the different pre-treatment methods and all analyses. Top of the figure: OSPW samples: 1, 2 and 3; Groundwater (GW) samples: 4, 5, 6, 7, 8, 9 and 10. As illustrated in the right legend sketch, Horizontal lines represent first quartile, medians, and third quartiles define the boxes, while the bottom and top tails represent the 10th and 90th percentiles. Data points for each boxplot are randomly placed to minimize points overlapping. Notes: Data points are presented as Instrument-Sample Preparation-Calibration standard. TOF = UPLC-TOFMS, SPE = Solid-phase extraction, LLE = liquid-liquid extraction, Fluka = Fluka commercial NA extract, and OSPW = oil sands process-affected water NA extract.

Table 2-2 Summary of Kruskal-Wallis test results for the sub group of OSPW samples, sub group of groundwater samples and the entire group of samples.

| Test | Sample locations | Kruskal-Wallis result | | Comment |
|----------------|------------------|-----------------------|---------|-------------|
| | | Chi-squared | P-Value | |
| TOF-SPE-OSPW | All | 28.0 | <0.05 | Not similar |
| | Groundwater | 18.6 | <0.05 | Not similar |
| | OSPW | 5.42 | =0.07 | Similar |
| TOF-LLE-OSPW | All | 27.8 | <0.05 | Not similar |
| | Groundwater | 18.6 | <0.05 | Not similar |
| | OSPW | 2.76 | =0.06 | Similar |
| FTIR-SPE-Fluka | All | 27.9 | <0.05 | Not similar |
| | Groundwater | 18.4 | <0.05 | Not similar |
| | OSPW | 5.4 | 0.07 | Similar |
| FTIR-LLE-Fluka | All | 28.2 | <0.05 | Not similar |
| | Groundwater | 18.9 | <0.05 | Not similar |
| | OSPW | 5.6 | =0.07 | Similar |
| FTIR-SPE-OSPW | All | 27.5 | <0.05 | Not similar |
| | Groundwater | 18.2 | <0.05 | Not similar |
| | OSPW | 3.3 | =0.19 | Similar |
| FTIR-LLE-OSPW | All | 28.0 | <0.05 | Not similar |
| | Groundwater | 18.6 | <0.05 | Not similar |
| | OSPW | 5.42 | =0.07 | Similar |

Notes:

- Solid-phase extraction is denoted as SPE; and liquid-liquid extraction is denoted as LLE.
- FTIR- LLE-Fluka and FTIR-SPE-Fluka refer to the analysis of sample by FTIR pretreated by LLE and SPE, respectively, and using Fluka as standard; FTIR-LLE-OSPW and FTIR-SPE-OSPW refer to the analysis of sample by FTIR pretreated by LLE and SPE, respectively, and using OSPW extract as standard; TOF-LLE-OSPW and TOF-SPE-OSPW refer to the analysis of sample by UPLC-TOFMS pretreated by either LLE or SPE, respectively, and using OSPW extract as standard.

2.3.1. Differences between LLE and SPE

The O_x-NAs as well as NAFCs concentrations in mg L⁻¹ detected with the SPE and LLE sample pre-treatment are displayed for the different water samples in Figure 2-3. With respect to O_x-NAs and NAFCs concentration, it can be observed that the recovery of the SPE was similar to

LLE in lower values or GW samples. However, higher values could be observed using SPE compared to LLE for values higher than 30 mg L^{-1} (e.g., OSPW samples 1, 2 and 3). As shown in Table 2-3, the SPE/LLE ratio exceeded 1 in most of samples, especially at high concentrations. For instance, the ratio for OSPW-1 in replicate 1 was 1.02 and 1.50 in UPLC-TOFMS (denoted as TOF in Figures) and FTIR, respectively, while the ratio for same sample in replicate 2 was 1.14 and 1.53 in UPLC-TOFMS, and FTIR, respectively. This high ratio in most of samples suggested the higher recovery in SPE compared to LLE. These findings agree with Headley et al. (2013b), who reported the low selectivity of (ENV+) SPE, allowing more species and components to be extracted. Similar findings were reported by Juhascik and Jenkins (2009), who reported high recoveries by SPE compared to LLE. The authors attributed the discrepancy between the extraction methods (i.e., SPE vs LLE) due to the possibility of partial/or minor loss for some components in the pretreated analyte based on the differences in selectivity of each component for instance the efficient extraction of weakly acids and other compounds by SPE compared to LLE.

Additional to the extraction performance of SPE vs LLE there are operational and logistical differences to consider between the two methods. It has been found that SPE is relatively fast and convenient compared to LLE (Bonnetfous and Boulieu, 1990; Juhascik and Jenkins, 2009; Mohamed et al., 2015b; Wells, 2003) and it is useful as an analytical tool in monitoring compounds of interest /or full characterization of emerging contaminants in the environmental samples (Headley et al., 2013b).

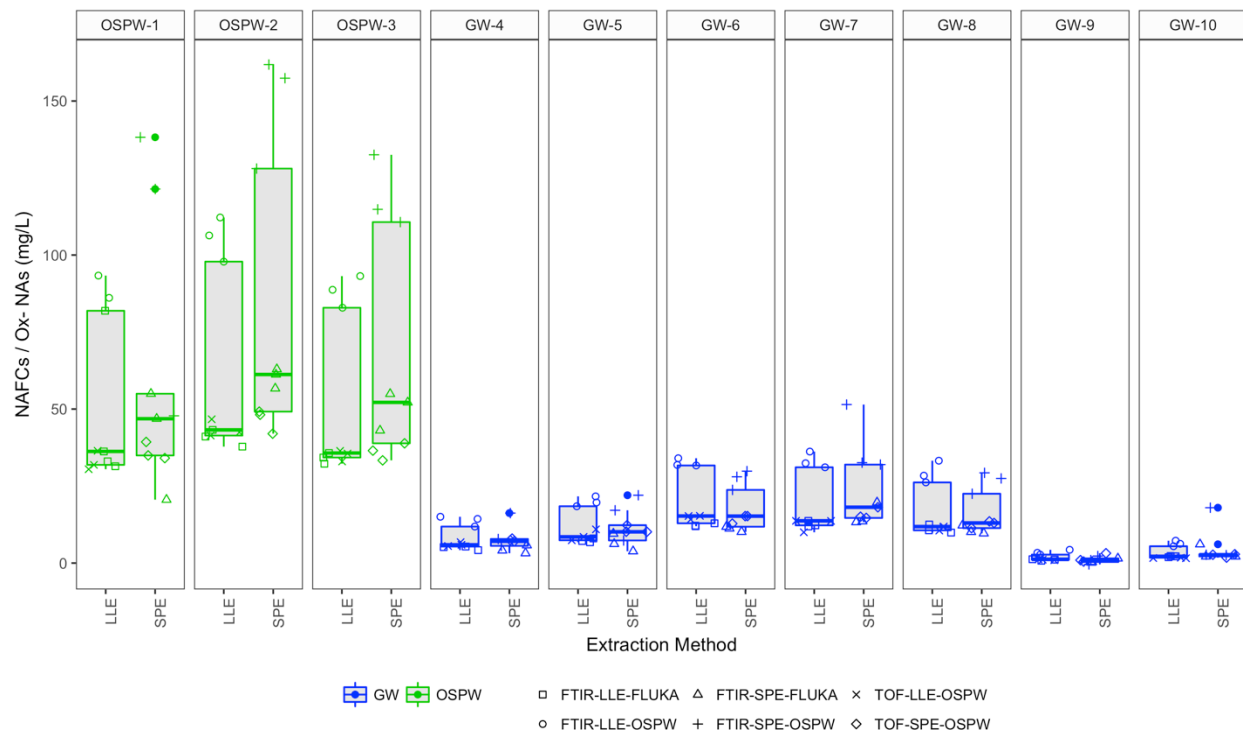


Figure 2-3 Differences between solid-phase extraction (SPE) and liquid-liquid extraction (LLE) pre-treatment using box plot of O_x -NAs [sum of NAs at $(2 \leq x \leq 6)$ or sum of classical (O_2) NAs and oxidized NAs as measured by UPLC-TOFMS analyses] and naphthenic acid fractions compounds (NAFCs; as measured by FTIR analyses) for the different water samples; OSPW samples: 1, 2 and 3, groundwater (GW) samples: 4, 5, 6, 7, 8, 9 and 10. Horizontal lines represent first quartile, medians, and third quartiles define the boxes, while the bottom and top tails represent the 10th and 90th percentiles. Data points for each boxplot are randomly placed to minimize points overlapping. Notes: Data points are presented as Instrument-Sample Preparation-Calibration standard. TOF = UPLC-TOFMS, Fluka = Fluka commercial NA extract, and OSPW = oil sands process-affected water NA extract.

Table 2-3. Calculated SPE/LLE ratio for all samples using UPLC-TOFMS and FTIR analyses.

| Replicate # | Sample # | TOF-OSPW | FTIR-Fluka |
|-------------|----------|---------------|------------|
| | | SPE/LLE Ratio | |
| Replicate 1 | OSPW-1 | 1.02 | 1.50 |
| | OSPW-2 | 1.03 | 1.46 |
| | OSPW-3 | 1.14 | 1.15 |
| | GW-4 | 1.04 | 0.62 |
| | GW-5 | 0.41 | 0.21 |
| | GW-6 | 1.12 | 0.65 |
| | GW-7 | 0.93 | 0.48 |
| | GW-8 | 1.10 | 1.09 |
| | GW-9 | 0.84 | 0.85 |
| | GW-10 | 1.08 | 1.13 |
| Replicate 2 | OSPW-1 | 1.14 | 1.53 |
| | OSPW-2 | 1.18 | 1.70 |
| | OSPW-3 | 1.12 | 0.96 |
| | GW-4 | 1.35 | 0.98 |
| | GW-5 | 2.93 | 1.37 |
| | GW-6 | 1.09 | 1.52 |
| | GW-7 | 1.45 | 1.41 |
| | GW-8 | 1.07 | 1.14 |
| | GW-9 | 1.08 | 0.97 |
| | GW-10 | 1.7 | 0.98 |
| Replicate 3 | OSPW-1 | 1.05 | 1.42 |
| | OSPW-2 | 0.92 | 1.26 |
| | OSPW-3 | 1.08 | 0.81 |
| | GW-4 | 1.34 | 1.08 |
| | GW-5 | 1.02 | 0.29 |
| | GW-6 | 1.08 | 1.42 |
| | GW-7 | 1.37 | 0.87 |
| | GW-8 | 1.81 | 1.44 |
| | GW-9 | 0.99 | 0.87 |
| | GW-10 | 1.65 | 2.65 |

Notes:

- Solid-phase extraction is denoted as SPE; and liquid-liquid extraction is denoted as LLE. OSPW samples: OSPW-1, OSPW-2 and OSPW-3; Groundwater samples are denoted as GW-4, GW-5, GW-6, GW-7, GW-8, GW-9, and GW-10. FTIR-Fluka refers to the analysis of a sample by FTIR and using Fluka as a standard; TOF-OSPW refers to the analysis of a sample by UPLC-TOFMS and using OSPW Extract as a standard.

Additionally, the upsides of SPE over LLE are the lack of operator errors as well as the significant efforts applied during the sample preparation using LLE while the fractionation using SPE is based on the resins in the separation column, sorbents type and flow rate of the water sample. Other disadvantages of LLE include errors and losses that can arise during the separation of the organic phase and the consumption of large volumes of solvents (Juhascik and Jenkins, 2009). Our findings indicated that there was no statistical difference between SPE and LLE results for individual samples and for all samples as one group for a given quantification method, i.e. there was no difference between the LLE and SPE samples which were quantified by FTIR technique using Fluka standard (Mann-Whitney-Wilcoxon P-value >0.05) Figure 2-4 and Figure 2-5). Although there was no a statistical significant difference between the SPE and LLE on quantifying either the NAFCs or Ox-NA, it can be noticed that SPE method usually produced higher recoveries than the LLE method (Table 2-1).

With regards to the of O₂ species, significant similarity in concentrations of both LLE and SPE can be observed as depicted in Table 2-1. For instance, OSPW-1 in TOF-LLE-OSPW and TOF-SPE-OSPW yielded 20.067±1.263 mg L⁻¹ and 20.077±2.512 mg L⁻¹, respectively, while GW-10 yielded 0.927±0.029 mg L⁻¹ and 1.030±0.203 mg L⁻¹ in TOF-LLE-OSPW and TOF-SPE-OSPW, respectively.

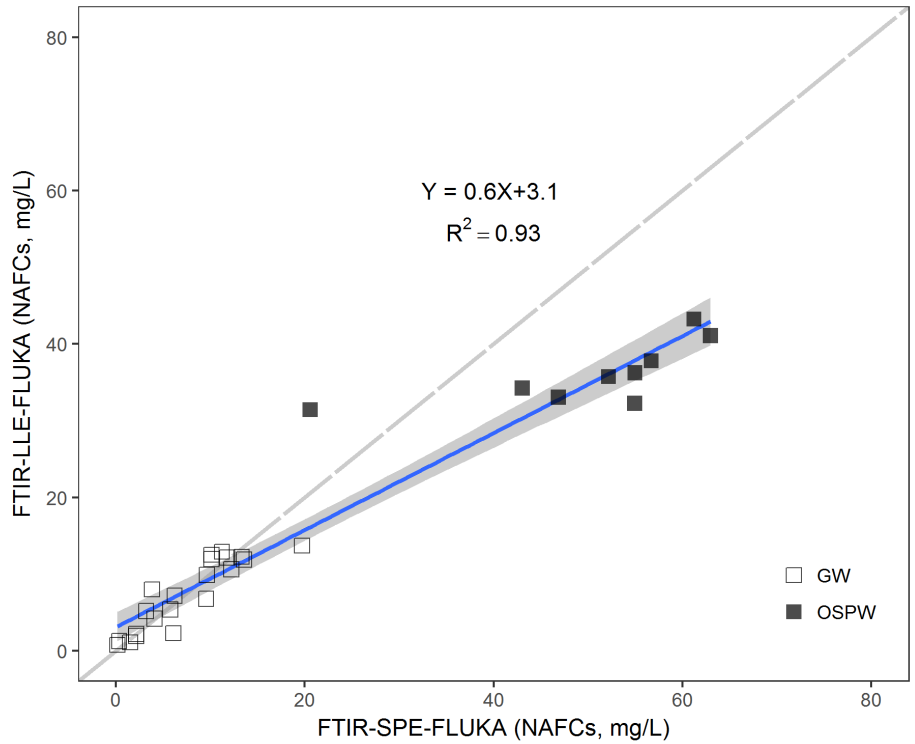


Figure 2-4 Comparison between the determination of naphthenic acid fractions compounds (NAFCs) after SPE and LLE pre-treatment using FTIR and Fluka as standard. Note: Groundwater (GW) and oil sand process-affected water (OSPW); solid-phase extraction (SPE); and liquid-liquid extraction (LLE). The grey zone represents the 95% confidence level for the regression. FTIR-LLE-Fluka and FTIR-SPE-Fluka refer to the analysis of sample by FTIR pretreated by LLE and SPE, respectively, and using Fluka as standard.

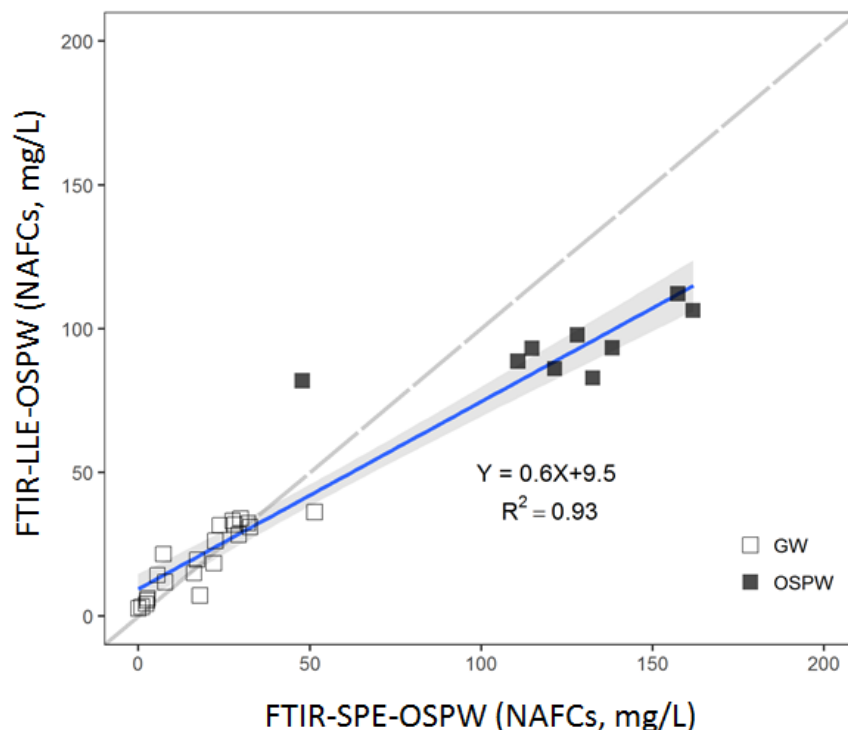


Figure 2-5 Comparison between the determination of naphthenic acid fractions compounds (NAFCs) using FTIR after SPE and LLE pre-treatment and using OSPW extract as standard. Note: solid-phase extraction is denoted as SPE; and liquid-liquid extraction is denoted as LLE.

On the other hand, the differences in most oxidized species (i.e., O₃-NAs and O₄-NAs) between the SPE and LLE using UPLC-TOFMS could be considered minimal due to their low portions (for instance: the sum of the abundance of the O₃-NAs and O₄-NAs in LLE versus SPE respectively; OSPW-1: 26% vs 27% and GW-6: 36% vs 34%); furthermore acute toxicity towards the bacteria *Vibrio fischeri* was previously associated with O₂ species (Morandi et al., 2016; Yue et al., 2015a) rather than oxidized species (Yue et al., 2015a). Therefore, we focused our discussion on O₂ species as the primary component of interest in O_x-NAs. Figure 2-6 illustrates the percentage of the relative abundance of O₂-NAs for all samples using UPLC-TOFMS after the different pre-treatment conditions. With respect to the GW samples, the O₂ species contributed to 63.4±7.3%

and $55.8 \pm 15.3\%$ of the O_x -NAs in the LLE and SPE, respectively, while for the OSPW samples, the contribution was $63.1 \pm 2.1\%$ and $58.5 \pm 3.0\%$ in the LLE and SPE respectively (Figure 2-6). The two current observations relevant to the O_2 species either by the significant similarity of concentrations in both LLE and SPE as well as high recovery in the abundance of O_2 species in LLE may be due to the hydrophobicity influence of these species.

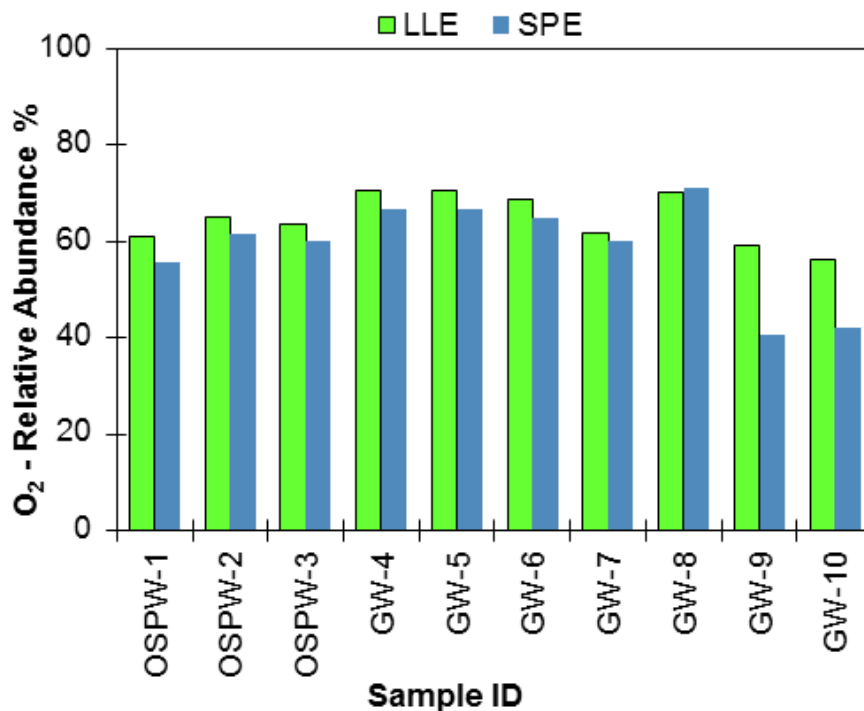


Figure 2-6 Relative abundance of classical NAs (O_2 -NAs), for all samples using UPLC-TOFMS with different pre-treating conditions liquid-liquid extraction (LLE) and solid-phase extraction (SPE). OSPW samples: 1, 2 and 3; groundwater (GW) samples: 4, 5, 6, 7, 8, 9 and 10.

Few aspects can be highlighted to clarify these observations: (1) In the liquid chromatography, the separation mechanism depends on two principal factors the Van der Waals force and hydrophobicity (Bataneh et al., 2006), while Yue et al. (2015a) reported that the most hydrophobic fraction of OSPW did encompass relatively higher amount of O_2 species. (2) The transport between water and hydrophobic extractants such as DCM counts on the hydrophobic

impact or solvophobic impact (Wells, 2003). The hydrophobic impact can be considered as a selectivity parameter which can influence the appearance and disappearance of specific species. The absence of some species after polydimethylsiloxane extractions was reported because of their low hydrophobicity (Zhang et al., 2015). Overall using the three replicates of samples, we determined the non-significance in the differences between SPE and LLE at 95% confidence level (p-value of 0.67). However, deep and comparative insights are warranted in the coming sections to show the differences/similarities in the limits of detection/quantitation and the detection reliability using different standards and different quantification methods.

2.3.2. Quantification analysis

2.3.2.1. Fourier transform infrared (FTIR) spectroscopy

Figure 2-7 displays the concentrations of NAFCs measured by FTIR using both standards Fluka and OSPW extract. The SPE revealed higher concentrations compared to LLE using both standards. All OSPW samples and most of GW samples had higher concentration in SPE versus LLE while the SPE concentration was 0.97 - 1.48 folds higher than LLE. The NAFCs for OSPW samples ranged from 33.6 to 60.3 mg L⁻¹ while the GW was between 0.7 and 15.5 mg L⁻¹. Using different standards to measure NAFCs concentrations, the OSPW extract always produced higher NAFCs compared to Fluka. This could be attributed to the difference in composition of the OSPW extract and the Fluka mixture. The OSPW extract might contain more fractions or structural isomers. For instance, the OSPW extract has more cyclic isomers (Martin et al., 2008) and less branched (Han et al., 2008a) than the commercial NAs. Therefore, we can hypothesize and anticipate the particularity of OSPW extract as a standard in fully characterizing and reflecting wide distributions and compositions of the samples compared to commercial standards (i.e., higher

concentration values due to thorough detection and characterization of more isomers). The statistical analysis of NAFCs for all samples showed similarity between SPE and LLE based on Fluka and OSPW extract calibration curve ($p\text{-value} > 0.05$) as depicted in Figure 2-7 and Figure 2-5, respectively. However, in regard to GW only, the LLE as well as SPE methods had very close values unlike the OSPW samples; SPE tended to produce higher value than LLE.

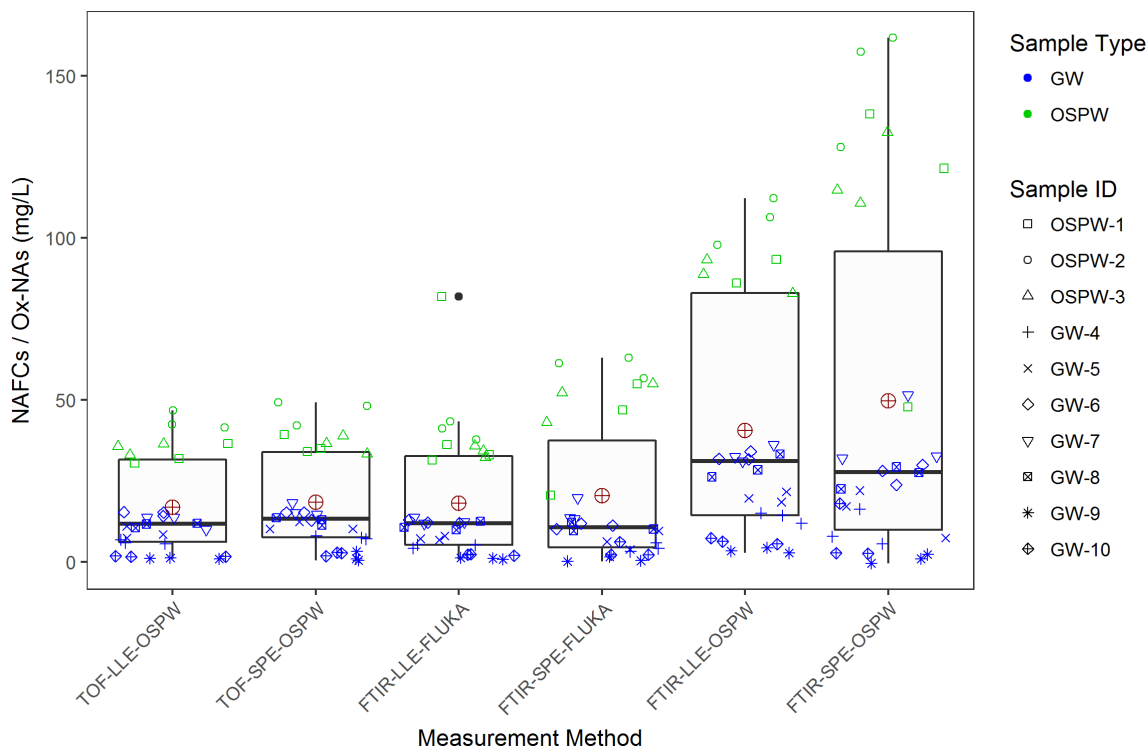


Figure 2-7 Box plot comparing the quantification of O_x -NAs [sum of NAs at ($2 \leq x \leq 6$) or sum of classical NAs and oxidized NAs as measure by UPLC-TOFMS] using solid-phase extraction (SPE) pretreated samples; and liquid-liquid extraction (LLE) pretreated samples as well as quantification of naphthenic acid fractions compounds (NAFCs; as measured by FTIR) using Fluka standard and OSPW extract with the two pre-treatment methods (SPE and LLE). OSPW samples: 1, 2 and 3; Groundwater (GW) samples: 4, 5, 6, 7, 8, 9 and 10. The mean is denoted as circled plus \oplus . Horizontal lines represent first quartile, medians, and third quartiles define the boxes, while the bottom and top tails represent the 10th and 90th percentiles. Data points for each boxplot are randomly placed to minimize points overlapping. Notes: X-axis categories are presented as Instrument-Sample Preparation-Calibration standard. TOF = UPLC-TOFMS, Fluka = Fluka commercial NA extract, and OSPW = oil sands process-affected water NA extract.

2.3.2.2. Ultra-performance liquid chromatography time-of-flight mass spectrometry (UPLC-TOFMS)

As shown in Figure 2-7, consistent O_x -NAs concentrations detected by UPLC-TOFMS can be observed for both LLE and SPE pre-treatment using different water sources. Statistically, the results showed that the O_x -NAs obtained from the UPLC-TOFMS method using the SPE and LLE, were not significantly different as indicated by the Mann-Whitney-Wilcoxon p -value > 0.05 (Figure 2-8 and Table 2-4). OSPW is a very complex mixture (Rowland et al., 2011a) with thousands of individual structures (Anderson et al., 2012b). Thus, no optimum technique has been reported so far to completely characterize (Noestheden et al., 2014; West et al., 2013) or to separate all compounds in OSPW (Headley et al., 2013c; Huang et al., 2015a; Scott et al., 2008a).

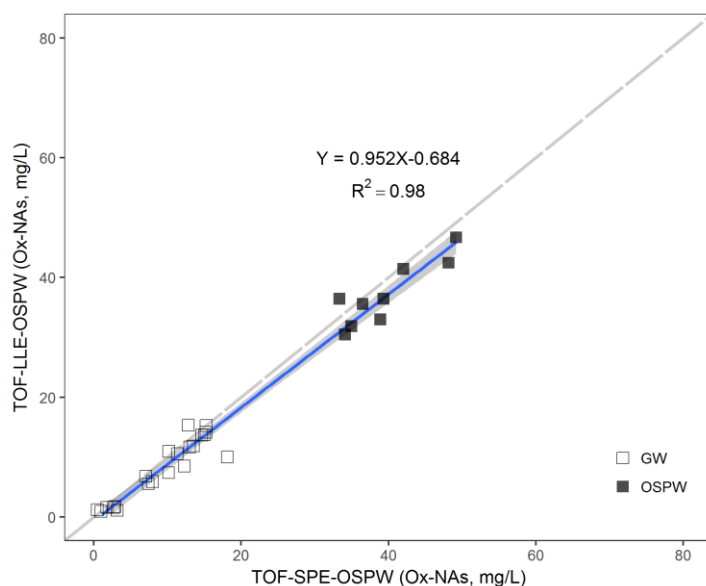


Figure 2-8 Comparison between UPLC-TOFMS determination of O_x -NAs after SPE and LLE pre-treatment using OSPW extract as standard. Note: Solid-phase extraction (SPE); and liquid-liquid extraction (LLE); the confidence level is 95% for the regression. TOF-LLE-OSPW and TOF-SPE-OSPW refer to the analysis of sample by UPLC-TOFMS pretreated by LLE and SPE, respectively and using OSPW extract as standard.

Table 2-4 Comparison between the determination of naphthenic acid fractions compounds (NAFCs) by FTIR and determination of O_x-NAs by UPLC-TOFMS using OSPW extract and Fluka standards after samples pre-treatment with LLE and SPE.

| Correlation | Conditions | Determination method (x) | Determination method (y) | Equation | Determination coefficient (R ²) |
|------------------------|--|--------------------------|--------------------------|-----------------|---|
| SPE vs LLE | UPLC-TOFMS (O _x -NAs) (OSPW extract) | TOF-LLE-OSPW | TOF-SPE-OSPW | Y=1.033X+1.066 | 0.98 |
| SPE vs LLE | FTIR (NAFCs), (OSPW extract) | FTIR-SPE-OSPW | FTIR-LLE-OSPW | Y=0.6X+9.5 | 0.93 |
| SPE vs LLE | FTIR (NAFCs), (Fluka) | FTIR-SPE-Fluka | FTIR-LLE-Fluka | Y=0.6X+3.1 | 0.93 |
| Fluka vs OSPW extract) | FTIR (NAFCs), LLE | FTIR- LLE-Fluka | FTIR-LLE-OSPW | Y=2.6X+0.9 | 0.99 |
| Fluka vs OSPW extract | FTIR (NAFCs), SPE | FTIR- SPE-Fluka | FTIR-SPE-OSPW | Y=2.5X-0.6 | 0.99 |
| UPLC-TOFMS vs FTIR | (O _x -NAs) vs (NAFCs), & (OSPW extract), LLE | TOF-LLE-OSPW | FTIR-LLE-OSPW | Y=2.476X+0.346 | 0.98 |
| UPLC-TOFMS vs FTIR | (O _x -NAs) vs (NAFCs), & (OSPW extract), SPE | TOF-SPE-OSPW | FTIR-SPE-OSPW | Y=3.397X-12.829 | 0.93 |
| UPLC-TOFMS vs FTIR | (O _x -NAs) vs (NAFCs), & (OSPW extract) vs (Fluka), LLE | TOF-LLE-OSPW | FTIR-LLE-Fluka | Y=1.017X+0.535 | 0.98 |
| UPLC-TOFMS vs FTIR | (O _x -NAs) vs (NAFCs), & (OSPW extract) vs (Fluka), SPE | TOF-SPE-OSPW | FTIR-SPE-Fluka | Y=1.371X-4.911 | 0.93 |

Notes:

- Solid-phase extraction is denoted as SPE; and liquid-liquid extraction is denoted as LLE. OSPW samples: OSPW-1, OSPW-2 and OSPW-3; Groundwater samples are denoted as GW-4, GW-5, GW-6, GW-7 GW-8, GW-9, and GW-10.
- FTIR-LLE and FTIR-SPE refer to the analysis of a sample by FTIR and pretreated by LLE and SPE, respectively; TOF-LLE and TOF-SPE refer to the analysis of a sample by UPLC-TOFMS and pretreated either by LLE or SPE, respectively.

Misclassification of some minor acidic components was previously reported due to differences in selectivity between the direct injection electrospray ionization mass spectrometry and high-pressure liquid chromatography/high-resolution mass spectrometry (HPLC/HRMS) (Martin et al., 2008). The authors of the study suggested that the selectivity differences had a significant role on the characterization compared to other parameters and sensitivity of the mass spectrometry. With respect to standard, our decision to use OSPW extract only in calibration curve of UPLC-TOFMS was due to several reasons: 1) the acyclic O₂ species are more dominant in commercial mixture NAs compared to dominance of tricyclic and bicyclic species in OSPW fractions (Marentette et al., 2015a). In addition, there is a lack of oxidized species in Fluka (i.e., further details in Section 3.2.3.); therefore, OSPW extract will provide more convenient composition with a considerable similarity to the real samples in terms of all species than commercial NA standard. 2) It is widely reported to use internal standards in UPLC-TOFMS (Bowman et al., 2014; Sun et al., 2014a; Woudneh et al., 2013) rather than commercial NAs as external standards.

2.3.2.3. Calibration methods and appropriate standard

The differences between OSPW NA and the commercial Merichem NA extract has been investigated by Martin et al. (2008) and Sun et al. (2014a) while analyzing water samples. Their findings suggested that the calibration plots generated from the Merichem preparation are likely suitable for estimating the concentrations of NAs from oil sands sources. However, others still claim that further research is warranted to develop authentic/universal standards for calibration rather than commercial NAs (Scott et al., 2008a; Scott et al., 2008b; Zhao et al., 2012; Zhao, 2012). The authentic standard can better represent the entire composition of OSPW and reflect all species. Thus, in this section, we highlighted the differences between the two calibration curves (prepared with two different NA standards) with regards to two aspects; 1) the composition of standard itself

using UPLC-TOFMS; and 2) the correlation between the results of FTIR using the two standards separately in either LLE or SPE.

To understand the differences in the composition of two standards, samples of Fluka and OSPW NA extract were analyzed using the UPLC-TOFMS. Figure 2-9 presents the percent distributions of carbon number (n) and hydrogen deficiency number (Z), in both standards. In Fluka mixture, the range of n was from 7 to 20 while Z numbers from 0 to -12. However, in OSPW extract, the n was observed from 7 to 22 and Z numbers from 0 to -18. In addition, 93% of the Fluka standard compounds had Z values between 0 and 4 while 37% of the OSPW extract compounds were in the same region (Figure 2-9).

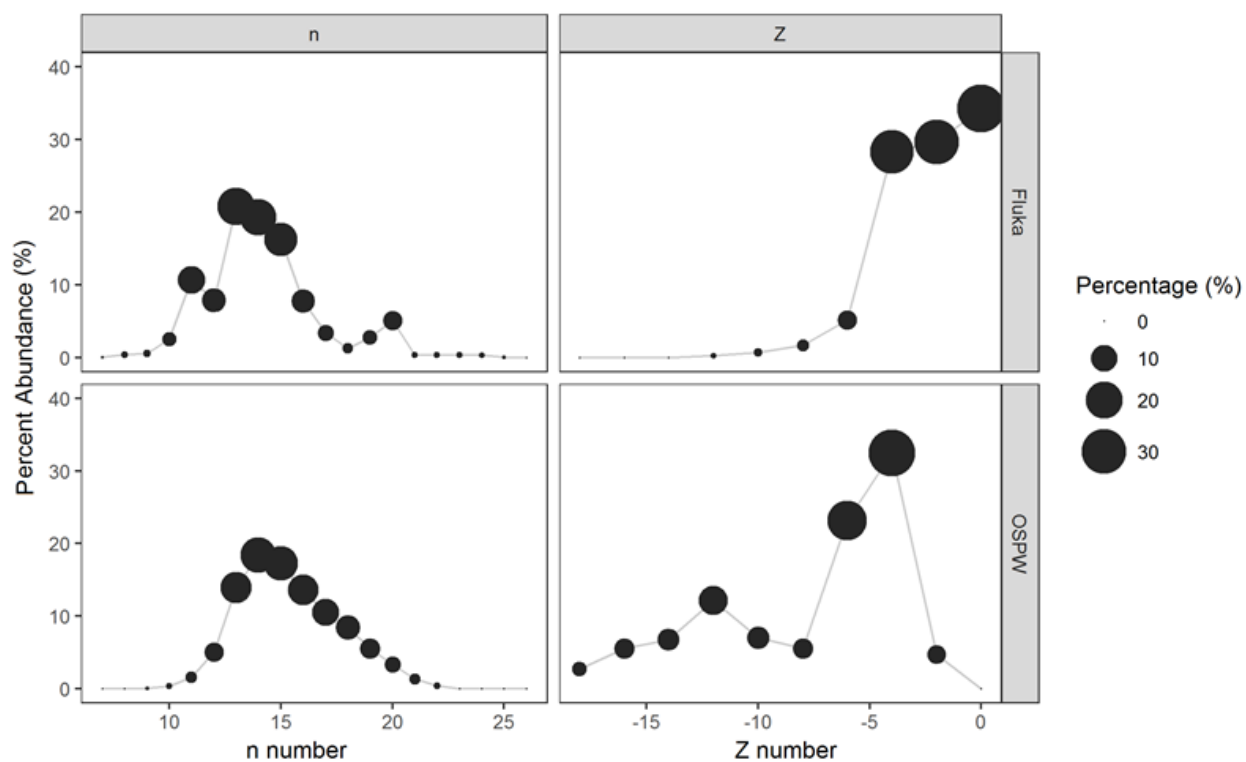


Figure 2-9. Percent abundance (%) of carbon number (n) and Z distribution for OSPW NA extract and Fluka NA standard. NA general formula: $C_nH_{2n+Z}O_x$ where the number of carbons, the number of hydrogen lost, the number of oxygen are represented by n, Z and x respectively. ($7 \leq n \leq 26$), ($0 \leq -Z \leq 18$), and ($2 \leq x \leq 6$). OSPW Ext. refers to OSPW extract.

The statistical Kruskal-Wallis test showed the dissimilarity between OSPW extract and Fluka (p-value < 0.05). To determine the extent of difference between the composition of the OSPW extract and commercial Fluka NAs, the speciation of both standards is illustrated in Figure 2-10 and Figure 2-11, respectively. For the O₂ species, the Fluka showed higher abundance in the lower Z and lower carbon (Figure 2-10-d). Conversely, the O₂ species in the OSPW extract had higher abundance with smaller Z and higher carbon Figure 2-10-c). Carbon (13-22) at Z (-12, -14, -16 and -18) was significant in OSPW extract compared to Fluka. These findings are consistent with what was formerly observed by Headley et al. (2010a) about the higher molecular weights of OSPW NAs compared to Fluka (Armstrong et al., 2008; Headley et al., 2010c). With respect to oxidized NAs (i.e., species (3≤x≤6)) low abundance of these species could be observed in Fluka (Figure 2-11b,d). Similarly, a negligible abundance of oxidized species has been reported for Merichem commercial NA extract (Sun et al., 2014a).

The Mann-Whitney-Wilcoxon test showed that there was a significant difference between the NAFCs values produced from FTIR-OSPW and FTIR-Fluka (Mann-Whitney-Wilcoxon p-value <0.05). However, by comparing the two sets of data, it suggested a linear relationship between the two data sets. A linear regression between the two standards suggest the FTIR-OSPW extract results were 2.56 and 2.47 old higher than FTIR-Fluka for the LLE and SPE, respectively, regardless of the type of the water. Although these results were significantly different, similar coefficient of determination (R²=0.99) was observed in both in LLE and SPE as shown in Figure 2-11 and Figure 2-12 and tabulated in Table 2-4.

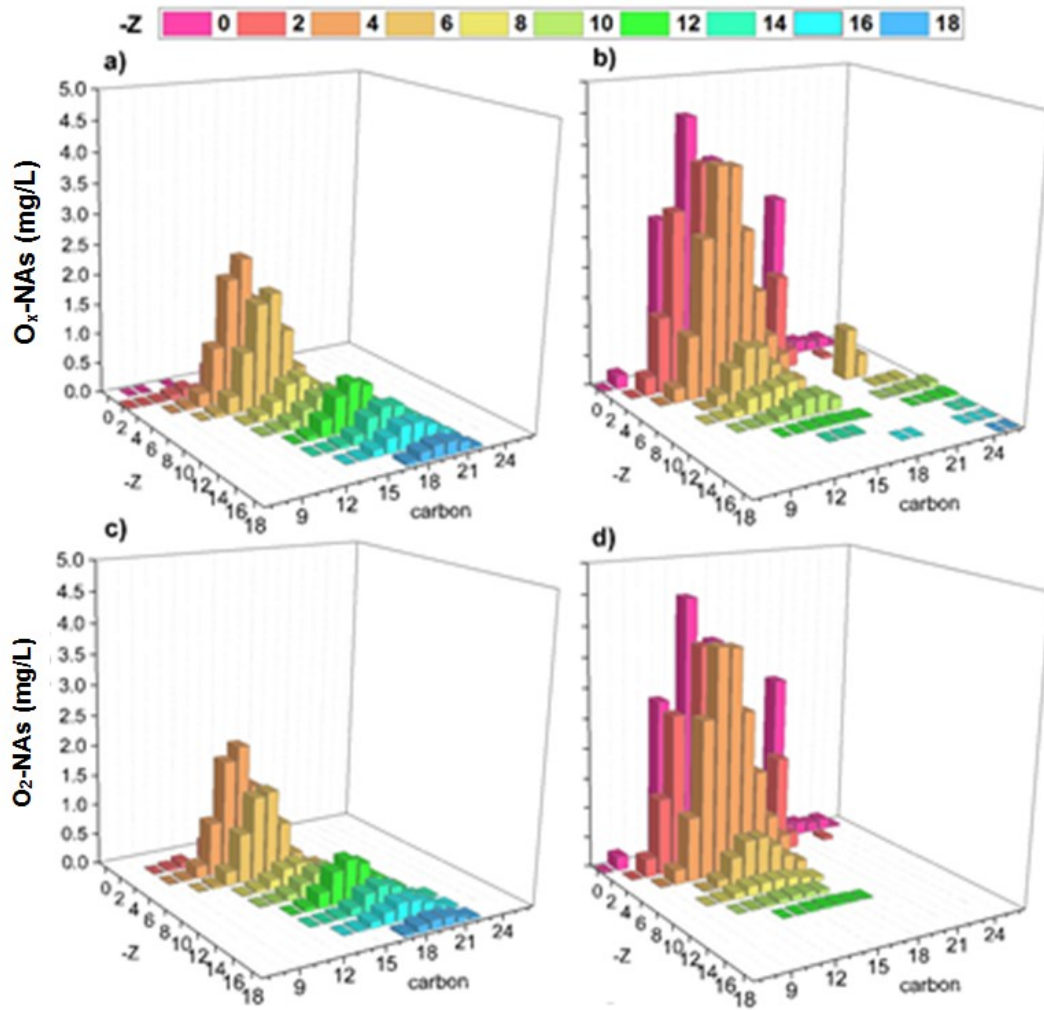


Figure 2-10 Profiles of O_x-NAs and classical (O₂-NAs) species of OSPW extract (left panels a,c) and Fluka standard (right panels b,d).

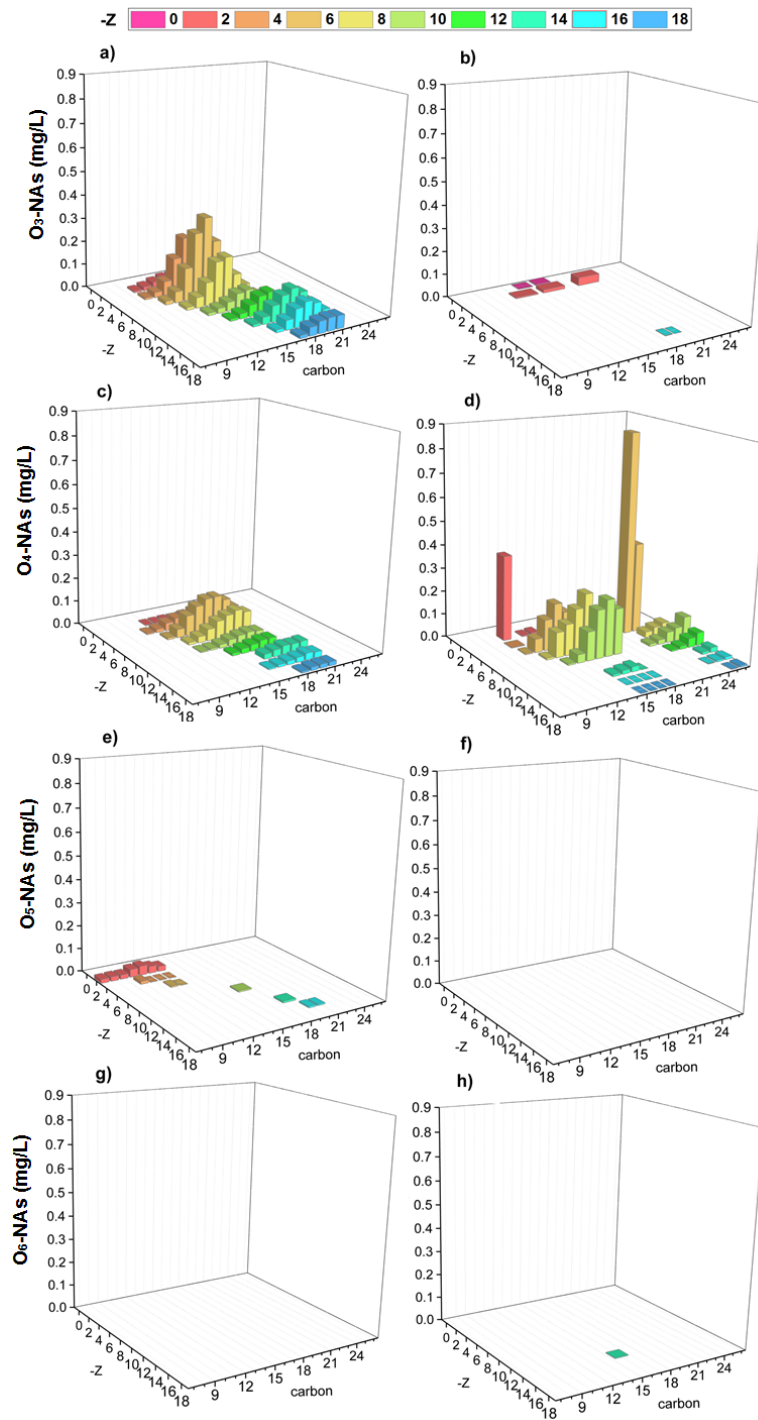


Figure 2-11. Profiles of oxidized NA or NA species ($3 \leq x \leq 6$) of OSPW extract (left panels a,c,e,g) and Fluka standard (right panels b,d,f,h).

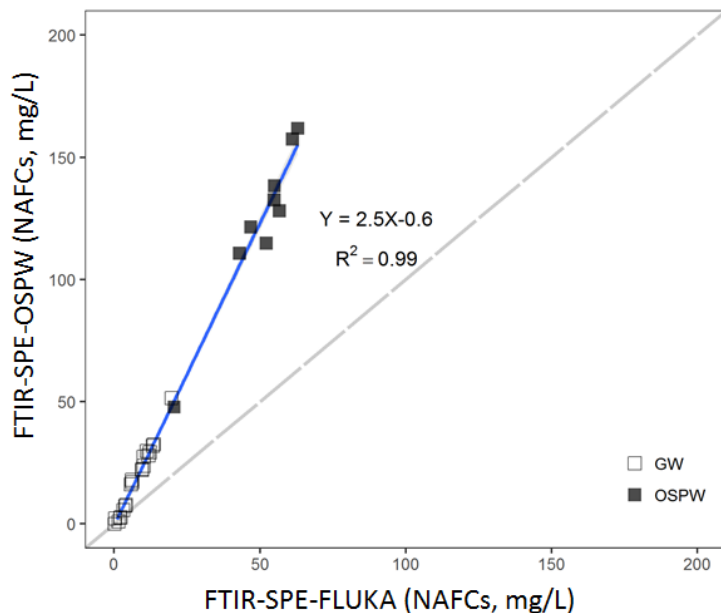


Figure 2-12 Comparison between Fluka and OSPW extract standards using FTIR results (naphthenic acid fractions compounds (NAFCs)) in SPE. Note: Groundwater (GW), oil sand process-affected water (OSPW); and solid-phase extraction (SPE).

2.3.2.4. UPLC-TOFMS versus FTIR

Figure 2-13 and Figure 2-14 show the relationship between results of UPLC-TOFMS (O_x -NA) and FTIR (NAFCs) based on OSPW extract after LLE and SPE respectively while all correlations are shown in SM, Table 2-4. The linear regression in most of the in addition to the former plots (Figure 2-13 and Figure 2-14) showed a good range for the determination coefficient with $R^2=0.92-0.98$. Based on OSPW extract standard, the FTIR results were about 2.47 and 3.4 fold higher than UPLC-TOFMS results in both the LLE and SPE, respectively, regardless of the type of the water. Distinct from the OSPW extract and estimating the NAFCs by FTIR using Fluka standard, the FTIR-Fluka results were about 1.01-1.37 times UPLC-TOFMS (O_x -NA) for LLE and SPE as exhibited in (Figure 2-15(a, b)). The key point in these results is the evidence of the strong correlation and close similarity between the FTIR-Fluka and UPLC-TOFMS especially in LLE.

The findings agreed with previous studies that used the FTIR measurement in terms of NAFCs as surrogate parameter for NAs as an indicator for treatment effectiveness (Gamal El-Din et al., 2011a; Islam et al., 2014a; Zubot et al., 2012a).

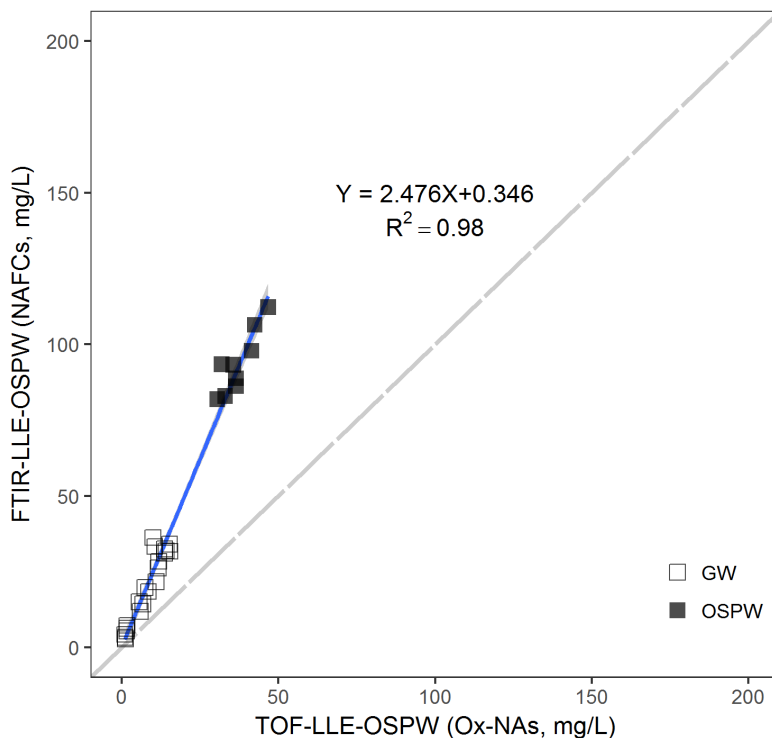


Figure 2-13 Comparison between the determination of naphthenic acid fractions compounds (NAFCs) by FTIR-OSPW extract and determination of UPLC-TOFMS (O_x -NAs) using OSPW extract after samples LLE pretreatment. Notes: Groundwater (GW) and oil sand process-affected water (OSPW); and liquid-liquid extraction (LLE). The grey zone represents the 95% confidence level. O_x -NAs refer to the sum of classical NAs (i.e., O_2) and oxidized NAs (i.e., O_3 , O_4 , O_5 , and O_6 , etc.). TOF-LLE-OSPW refers to the analysis of sample by UPLC-TOFMS pretreated by LLE and using OSPW extract as standard while FTIR-LLE-OSPW refers to the analysis of sample by FTIR pretreated by LLE and using OSPW extract as standard.

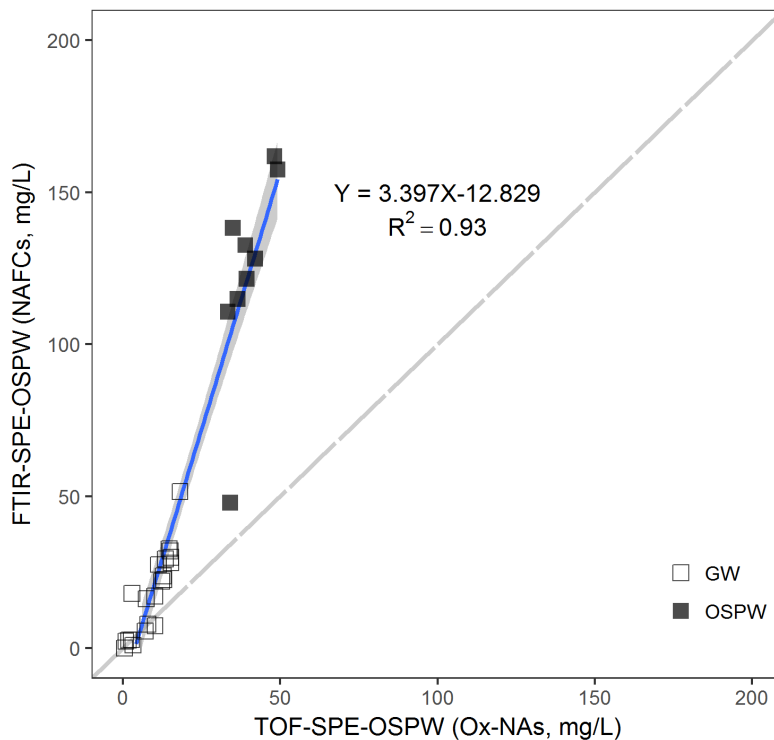


Figure 2-14 Comparison between the determination of UPLC-TOFMS (O_x -NAs) and (naphthenic acid fractions compounds (NAFCs)) by FTIR using OSPW extract after samples pre-treatment with solid-phase extraction (SPE). Notes: Groundwater (GW) and oil sand process-affected water (OSPW). The grey zone represents the 95% confidence level. O_x -NAs refer to the sum of classical NAs (i.e., O_2) and oxidized NAs (i.e., O_3 , O_4 , O_5 , and O_6 , etc.). TOF-SPE-OSPW and FTIR-SPE-OSPW refer to the analysis of sample by UPLC-TOFMS and FTIR, respectively, after pretreated by SPE using OSPW extract as standard.

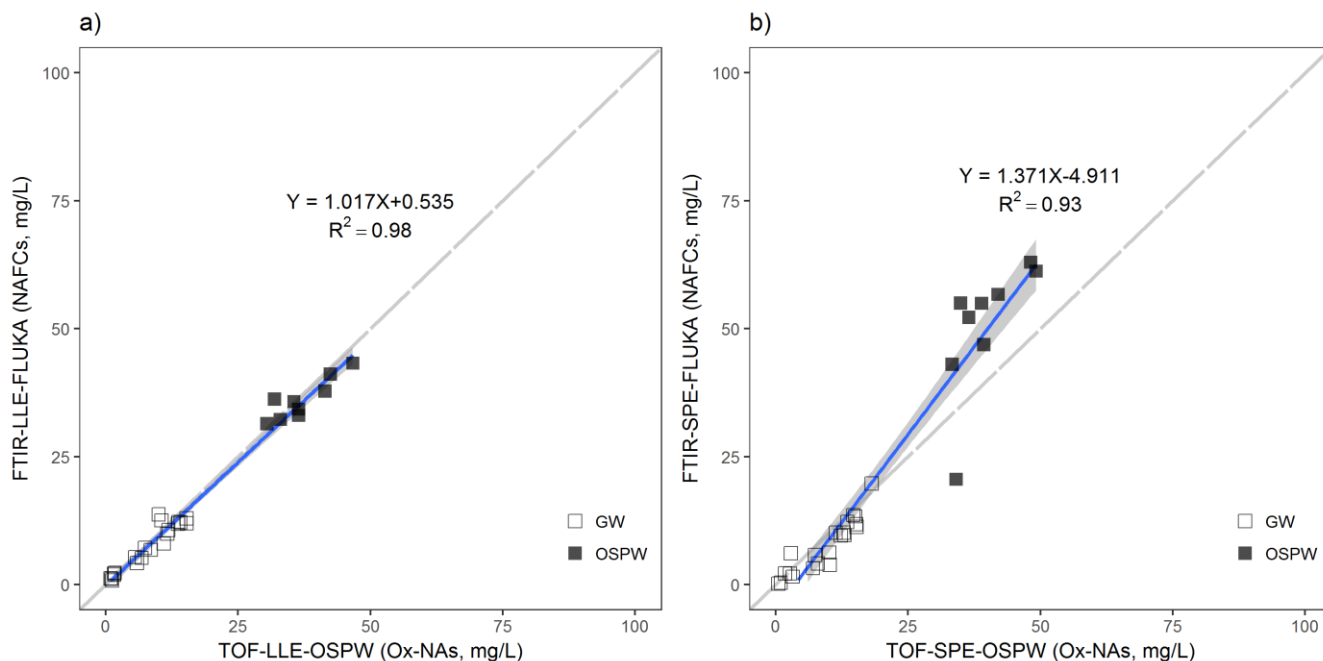


Figure 2-15 Comparison between the determination of naphthenic acid fractions compounds (NAFCs) by FTIR-Fluka and determination of O_x -NAs (sum of classical NAs (i.e., O_2) and oxidized NAs (i.e., O_3 , O_4 , O_5 , and O_6 , etc.)) by UPLC-TOFMS using OSPW extract after samples pre-treatment: a) LLE and b) SPE. Notes: Groundwater (GW) and oil sand process-affected water (OSPW); solid-phase extraction (SPE); and liquid-liquid extraction (LLE). The grey zone represents the 95% confidence level. FTIR-LLE-Fluka and FTIR-SPE-Fluka refer to the analysis of sample by FTIR pretreated by LLE and SPE, respectively, and using Fluka as standard; TOF-LLE-OSPW and TOF-SPE-OSPW refer to the analysis of sample by UPLC-TOFMS pretreated by either LLE or SPE, respectively, and using OSPW extract as standard.

Additionally, the FTIR-Fluka after LLE could be a better alternative to high cost UPLC-TOFMS analysis and greatest representative to measure the NAs in water samples. Although slight differences in concentrations could be observed, there was a significant linear relationship between FTIR and UPLC-TOFMS in our study as reported by Zhao et al. (2012) and confirmed our decision to use only OSPW extract calibration curve in UPLC-TOFMS detection. In summary, the commercially-accessible FTIR method could be used as an affordable substitute for analysis of water samples for NAs.

2.4. Conclusions

This study presented insights about the analysis of OSPW and groundwater samples with FTIR and UPLC-TOFMS measurements using two standards after SPE or LLE pre-treatments. We elucidated the similarities as well as the differences between these techniques to have a better understanding about the impact of pre-treatment and quantification standards on the reliability of the results.

For most of the samples, regardless the water source (OSPW or GW) and quantification methods (UPLC-TOFMS, FTIR), higher recovery of both O_x-NA and NAFCs in SPE was achieved compared to LLE (i.e., 1.0 to 1.4 fold high in SPE based on its less selectivity).

Similar concentrations of O₂ species were observed in both LLE and SPE with higher abundance of O₂ species in LLE (e.g., in the three OSPW samples, (63.1±2.1%) in LLE compared to (58.5±3.0%) in SPE). The increase of O₂ species abundance using LLE was due to the high impact of the hydrophobicity in which the conveyance of acids from water to DCM increased.

Comparing two calibration standards, relative dissimilarity in the compositions of commercial Fluka NA mixture versus OSPW extract as well as abundance of some classes were perceived. However, a very strong correlation was observed in concentrations of the LLE pretreated samples measured by both the FTIR analysis with Fluka standard and UPLC-TOFMS using OSPW extract standard.

Based on this study, SPE is recommended based on efficiency, repeatable detection and maximum recovery of abundant species. Moreover, the SPE process incorporate less hazard material and hazards wastes (such as the DCM in case of LLE). In addition, the findings of this study highlight the possibility of using the results of FTIR-Fluka as surrogate parameters and preliminary tools: (i) to monitor the total NA concentrations in different water matrices at different

concentration levels (i.e. low levels such as groundwater and high levels such as OSPW); (ii) to assess the environmental pollution loading by monitoring the water quality of point and non-point sources; and (iii) to assess the efficiency of different water treatment and reclamation approaches for process waters.

The continuous development of low cost and standardization of analytical techniques (i.e., detection methods, samples preparation and authentic standards) is warranted to characterize complicated matrices such as OSPW and total NAs.

Chapter 3 : Differentiating Among Oil Sands Process-Affected Water and Groundwater Samples Determined by Fourier Transform Infrared Spectroscopy via Non-Parametric Statistical Analysis²

3.1. Introduction

Alberta oil sands is one of the world's largest unconventional oil deposits (Alberta-Government, 2013). Bitumen is extracted from the surface mined Athabasca oil sands deposit using a caustic hot water extraction process. Extraction tailings consist of slurry of water, sand, silt, clay, and residual bitumen referred to as oil sands process-affected water (OSPW). As part of a “zero discharge” approach, OSPW is detained in large tailings ponds for water recycle and further treatment before it can be released to the receiving water (Alberta-Government, 2014; Allen, 2008a; Grewer et al., 2010a). OSPW contains toxic organics, such as naphthenic acids (NAs), and inorganic contaminants, such as heavy metals. OSPW is toxic towards aquatic and terrestrial organisms (Anderson et al., 2012c; Garcia-Garcia et al., 2011; He et al., 2012a; Martin, 2015; Sun et al., 2014b). NAs are a complex mixture of alicyclic and aliphatic carboxylic acids with general formulae of $C_nH_{2n+Z}O_x$, where “n” is the carbon number ($7 \leq n \leq 26$), “Z” is zero or an even negative integer ($0 \leq -Z \leq 18$) that specifies the hydrogen deficiency resulting from rings or unsaturated bonding formation, and x represents the number of oxygen atoms ($2 \leq x \leq 6$) in the NA molecules (Morandi et al., 2015a; Pereira et al., 2013c). Classical NAs follow the general formula $C_nH_{2n+Z}O_2$,

² A version of this chapter will be submitted to Candian Journal of Civil Engineering as “Ibrahim M. D., Meshref, M.N.A., Hughes, S. A., and Gamal El-Din, M. “Differentiating Among Oil Sands Process-Affected Water and Groundwater Samples Determined By Fourier Transform Infrared Spectroscopy via Non-Parametric Statistical Analysis”.

(Clemente and Fedorak, 2005; El-Din et al., 2011; Grewer et al., 2010a; Huang et al., 2015c), and were found to be the most toxic fraction of the NAs (Hughes et al., 2017; Morandi et al., 2015a; Yue et al., 2015b). Many recent studies have discussed OSPW remediation using chemical (Afzal et al., 2012; Meshref et al., 2017; Pérez-Estrada et al., 2011; Wang et al., 2013b), biological (Islam et al., 2014c; Xue et al., 2016b; Zhang et al., 2016), physical (Gamal El-Din et al., 2011b; Moustafa et al., 2015; Moustafa et al., 2014c; Zubot et al., 2012b), and a combination of two or more of these methods (Xue et al., 2016a; Xue et al., 2016c; Zhang et al., 2016).

NA quantification is a challenging task because of its complexity. NAs consist of complex mixtures of organic chemicals. The exact chemical composition of the NAs has not been yet identified because of the inability to separate and identify each of these organic chemicals (Frank et al., 2016; Scott et al., 2005b). Therefore, the NAs are estimated either as a total concentration of the acid extractable fraction (AEF) or as a function of double bond equivalent (DBE) and carbon numbers. An example of methods that estimates the AEF, which includes the NAs along with other extractable fractions such as fatty acids, is Fourier transform infrared (FTIR) spectroscopy method (Jivraj et al., 1995). Methods used to estimate NA concentration based on the Z and n numbers include gas chromatography (GC) and liquid chromatography (LC) (Han et al., 2008b; Martin et al., 2008). GC and LC methods are usually coupled with various detection techniques, such as mass spectrometry. For example, HPLC coupled with time-of-flight (TOF) MS, GCxGC/MS, LCxLC/MS, LC/MS/MS, and Orbitrap MS have been used for qualitative, semi-quantitative, and quantitative estimation of the OSPW AEF (Brown et al., 2013; Headley et al., 2013c; Martin et al., 2008).

FTIR is used as the oil sands industry's standard method in the routine monitoring due to its simplicity, and low cost, (Grewer et al., 2010a; Scott et al., 2008a; Zhao and Mian, 2012).

Before FTIR analysis, a water sample needs to be extracted by dichloromethane (DCM) after it was acidified to \sim pH 2.0 using H_2SO_4 . The organic fraction is then separated and dried then re-dissolved using known amount of DCM. Consequently, the diluted fraction is injected into a UV-Vis spectrometer and the heights that detect the carbonyl single and double bonds (1704 and 1743 cm^{-1}) are collected and compared with the calibration that has been developed using a standard NA mixture (Jivraj et al., 1995).

The calibration method used in the FTIR analysis is usually developed using Fluka or Merichem standard commercial NA mixture (Garcia-Garcia et al., 2012; Islam et al., 2014b). The commercial NA mixtures are similar to natural AEF in terms of n number; however, the commercial NA abundance of peaks with $x > 2$ are almost negligible (Grewer et al., 2010a). This indicates that the AEF found in the natural oil sands water samples are more complex than commercial NA mixtures (Headley and McMartin, 2004),

The FTIR method for NAs in OSPW was developed by Syncrude Canada limited for estimating the single and double bonds in the carbonyl functional group. Not all NAs in the AEF follow this chemical structure. Therefore, not the detected compounds that are not strictly adhering to the preceding NA formula (Brown et al., 2013; Jivraj et al., 1995; Scott et al., 2008a).

Grewer et al. (2010) reported that the total abundance of the compounds that follow the classical and oxidized NAs, $\text{C}_n\text{H}_{2n+z}\text{O}_x$, $x=2$ to 5, account for 30 to 49 % of the total AEF organics. Furthermore, after performing an elemental analysis to commercial standards as well as OSPW water samples collected from OSPW ponds, SAGD and river locations, Grewer et al. (2010) found that the OSPW samples contain N and S organic species while some of the commercial standards do not contain these compounds (Grewer et al., 2010a). It is worthy to note that the organic compounds that can be detected in the IR frequency 1704 and 1743 cm^{-1} could be organic acids,

such as carboxylic and fatty acids, acyclic and cyclic ketones in addition to aldehydes and amides (Dean, 1995). Consequently, it can be concluded that reporting the AEF as NAs (represented by the general formula $C_nH_{2n+z}O_2$) is inaccurate and oversimplification (Brown et al., 2013; Grewer et al., 2010a).

Although the FTIR method is considered as a non-mass spectrometric (non-MS) method in estimating the AEFs in water samples, it can be used as a screening method for regular monitoring programs either in the environment or in the reclamation efforts prior to the oil sands mines closure. Furthermore its low cost, availability, and ease of use make it a preferred method for online monitoring of AEF in water samples on site.

The aim of this study is to use the statistical approaches to further explore the effects of samples types, calibration standards, and separation methods on the FTIR results. Eventually, this study can help in deciding which calibration standard, and separation method should be used. Moreover, by understanding the differences between separation methods and calibration standards, an informed comparison between different results in the literature can be accomplished.

3.2. Material and methods

3.3.1. Water samples collection

Ten different samples were collected from Shell's Albian Sands oil sands mining operation in northern Alberta (Muskeg River Mine and Jackpine Mine). Three of the ten samples were OSPW collected from the Muskeg River Mine external tailings facility (MRM-ETF), Jackpine Mine external tailings facility (JPM-ETF), and the recycle water (RCW) line which is water combined from both ETFs directed back into the process. Rest of the ten samples were collected from 4 groundwater aquifers in the same area. The 4 aquifers were Mid McMurray Aquifer (MMA), Muskeg River Mine Basal Aquifer (MRM-BA), Jackpine Mine Basal Aquifer (JPM-BA), and

Pleistocene Channel Aquifer (PA). Three sampling events took place in June, August and October 2015 to collect samples from these 10 locations. All samples were transported and stored in 4 °C prior the analysis. All water samples were centrifuged (400 rpm, 10 minutes) to remove all suspended solids.

3.3.2. Liquid-Liquid extraction (LLE)

The centrifuged samples were acidified to pH ~ 2. 100 mL of the centrifuged acidified samples were extracted using DCM with 1:1 ratio i.e. 100 mL water sample to be extracted with 2 × 50 mL of the DCM. The solution was then dried using an air flushing/drying unit and the extract weight was measured.

3.3.3. Solid-phase extraction (SPE)

The centrifuged samples were acidified to pH ~1. An ENV+ (Biotage, NC, USA) cartridge was used as received and conditioned with 5 mL water, followed by 5 mL of methanol (MeOH) and finally with 10 mL of water. Then, 100 mL sample passed through the column and rinsed with 5 mL of water. The fraction then extracted using 6 mL of MeOH. The fraction was collected in a test tube which was initially weighed prior to use and recorded its initial weight. The 6 mL eluent was evaporated and dried using air and the final weight of test tubes was recorded on a precise balance after complete dryness.

3.3.4. FTIR analysis

FTIR analysis as carried out using a Nicolet 8700 FTIR spectrometer (Fisher Scientific, Ottawa, ON, Canada). Samples were loaded in a KBr cell with fixed width of 3 mm and purged using purge gas generator from Parker Balston Model 75-52. Peak highest were collected, in duplicates, using Omnic software (that was provided with the device) at wave lengths 1743 and 1706 cm⁻¹ after 7 minutes of purging and 128 scans. Then, AEF concentration was calculated

based on calibration curves prepared in accordance with the Syncrude method. More details are elsewhere (Jivraj et al., 1995; Scott et al., 2008a)

Two calibration methods were prepared using two sets of standards. The first calibration method was established based on a commercial mixture of NAs (Fluka). While the second method was produced using a OSPW-extract that was prepared from ~ 200 L of Shell OSPW collected in 2014 and extracted using LLE with DCM as standard (Headley et al., 2013a; Rogers et al., 2002). The quantification of AEF was conducted using both OSPW extract and Fluka standards. The AEF concentration was previously estimated using the method of commercial NA mixtures (Martin et al., 2008; Young et al., 2007). To date, many standards are used in all laboratories for OSPW analysis due to the limitations to fully characterize the entire composition of OSPW. The stock solution of Fluka NAs was prepared by dissolving the acids in DCM. Aliquots of the stock solution were then diluted with DCM to yield calibration standards with concentrations ranging from 5, 25, 75, 100, 200, and 300 mg L⁻¹.

3.3.5. Statistical analysis

Statistical analyses were performed using R software version 3.3. Shapiro–Wilk test was used to check the normality of the data. Kruskal-Wallis and Mann-Whitney-Wilcoxon tests were performed for non-normally distributed data with a significance level of 0.05. Mann-Whitney-Wilcoxon and Kruskal-Wallis test are the non-parametric that replace T-test and ANOVA, respectively. The null hypothesis assumes that all samples belong to same population and the alternative hypothesis is that at least one of the samples does not belong to the population that other samples belong to. Samples were grouped according to the sample type, calibration method, and extraction method. For instance, the terminologies used in this paper are as: FTIR.Fluka.SPE refers to analysis of sample by FTIR using Fluka as standard and SPE as method of extraction;

FTIR.OSPW.Ext. LLE refers to analysis of sample by FTIR using the OSPW extract as standard and LLE as method of extraction.

3.3. Results and discussion

3.4.1. Differences between sampling locations

Figure 3-1 shows the boxplots of the FTIR results grouped by sample number OSPW-1 to GW-10. It is notable that samples OSPW-1 to OSPW-3 yielded higher medians (50 to 100 mg L⁻¹) and higher variances. Samples GW-4 through GW-10 produced lower medians and smaller variances (Table 3-1 denotes the numerical). The variance among one sample results can be attributed to the measurement procedure (separation and calibration methods), while the differences among the samples medians can be explained by the sample type (OSPW water vs groundwater) and the sampling locations, within the same sample type.

Statistically, according to Kruskal–Wallis tests among all 10 samples, there is a significant difference between all 10 samples (chi-square = 99.8, and p-value < 0.05). To have detailed results about the differences between each of the samples, Pairwise Wilcoxon rank sum test was performed (see Table 3-2). Pairwise test results suggest that there are 4 distinct groups of samples; first group consists of water samples OSPW-1, OSPW- 2, and OSPW-3. Second group consists of samples GW- 6, GW-7 and GW-8. Third group consists of samples GW-4, GW-5, and GW-10. While the sample GW-9 is the only sample in group number 4, this is maybe because the GW-9 AEF value is the lowest among the 10 sample. Figure 3-2 depicts box plot of the AEF results grouped by the Kruskal-Wallis test result groups.

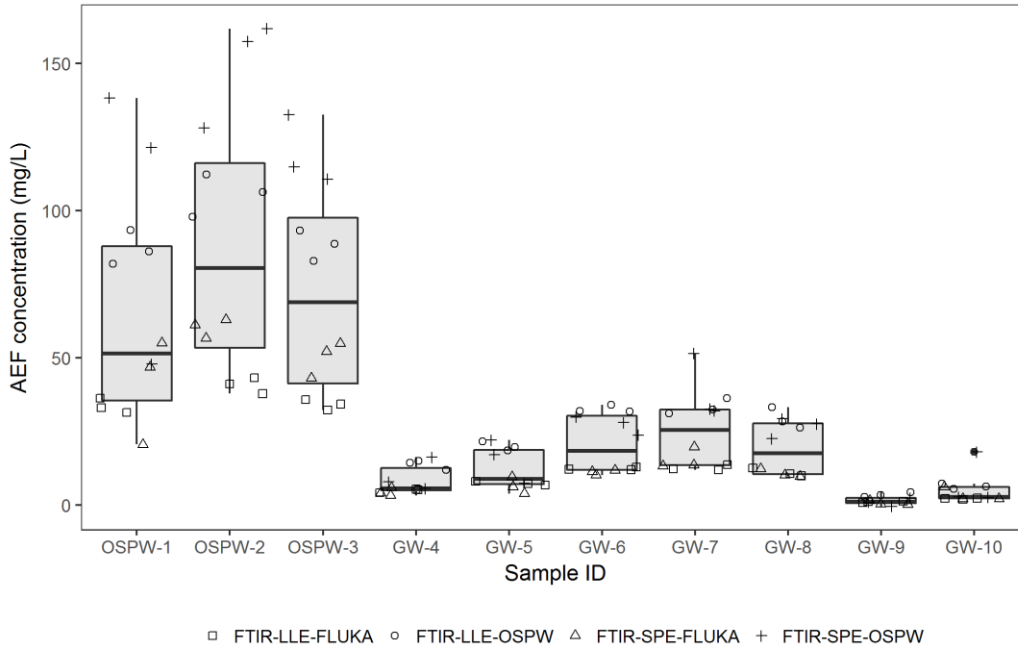


Figure 3-1 Boxplot illustrating the FTIR analysis results based on the samples ID. Horizontal lines represent first quartile, median, and third quartiles define the boxes, while the bottom and top tails represent the 5th and 95th percentiles.

Table 3-1 AEF results quantified by FTIR using FLuka and OSPW extract standards calibration methods with SPE and LLE separation methods. All results are in mg L^{-1} . GW stands for groundwater sample OSPW stands from OSPW samples. Errors are standard error with sample size =3.

| Sample-ID | Fluka | | OSPW | | Sampling location code |
|-----------|-------------|------------|--------------|-------------|------------------------|
| | SPE | LLE | SPE | LLE | |
| OSPW-1 | 40.8 ± 10.4 | 33.6 ± 1.5 | 102.5 ± 27.8 | 87.2 ± 3.4 | OSPW |
| OSPW-2 | 60.3 ± 1.9 | 40.8 ± 1.6 | 149.2 ± 10.6 | 105.5 ± 4.2 | OSPW |
| OSPW-3 | 50.1 ± 3.6 | 34.1 ± 1.1 | 119.4 ± 6.8 | 88.3 ± 3 | OSPW |
| GW-4 | 4.4 ± 0.8 | 5 ± 0.4 | 9.9 ± 3.3 | 13.8 ± 1.00 | Mid_McMurry |
| GW-5 | 6.6 ± 1.7 | 7.4 ± 0.4 | 15.5 ± 4.4 | 20 ± 1.00 | JPM Basal |
| GW-6 | 11.1 ± 0.5 | 12.4 ± 0.3 | 27.2 ± 1.9 | 32.6 ± 0.8 | JPM Basal |
| GW-7 | 15.6 ± 2.1 | 12.7 ± 0.6 | 38.7 ± 6.4 | 33.3 ± 1.6 | JPM Basal |
| GW-8 | 10.7 ± 0.8 | 11.1 ± 0.8 | 26.5 ± 2.1 | 29.3 ± 2.1 | MRM_basal |
| GW-9 | 0.7 ± 0.5 | 1.1 ± 0.2 | 1 ± 0.8 | 3.5 ± 0.5 | JPM PC |
| GW-10 | 3.5 ± 1.4 | 2.2 ± 0.2 | 7.8 ± 5.2 | 6.4 ± 0.6 | JPM PC |

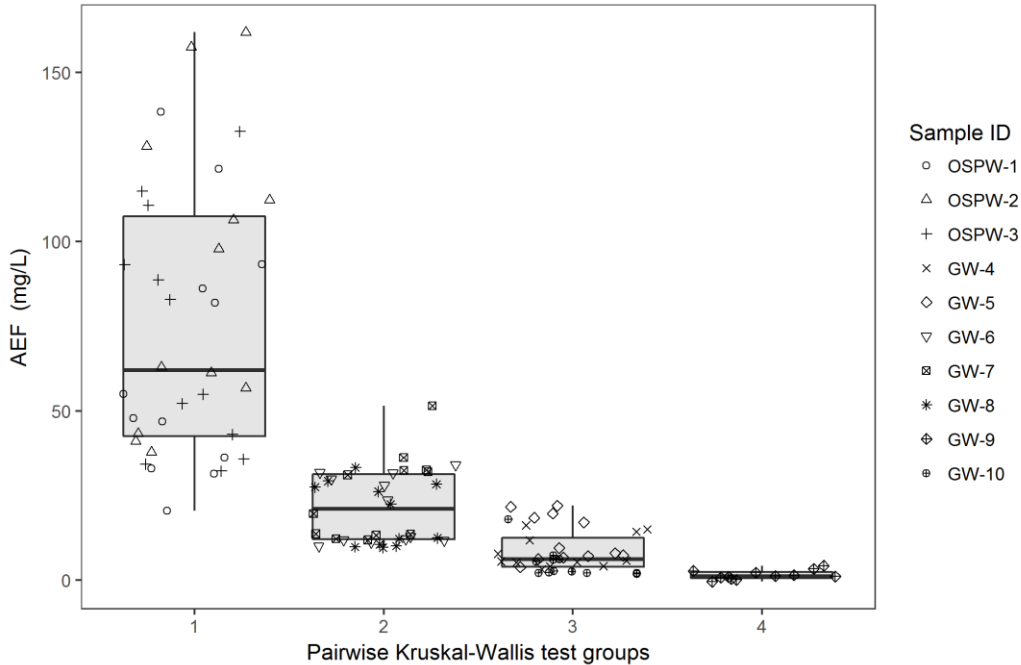


Figure 3-2 Box plot represents AEF analysis grouped by Pairwise Kruskal-Wallis test groups: Group1 (samples 1, 2, and 3) group2 (samples 6,7, and 8) group3 (samples 4,5,and 6) group4 (sample 9).

Table 3-2 Samples pairwise test p-value matrix. P-values more than 0.05 are highlighted

| Sample ID | 1 | 2 | 3 | 4 | 5 | 6 | 7 | 8 | 9 |
|-----------|----------|----------|----------|----------|----------|----------|----------|----------|---------|
| 2 | 0.14317 | - | - | - | - | - | - | - | - |
| 3 | 0.62973 | 0.29134 | - | - | - | - | - | - | - |
| 4 | 7.40E-07 | 7.40E-07 | 7.40E-07 | - | - | - | - | - | - |
| 5 | 3.00E-06 | 7.40E-07 | 7.40E-07 | 0.05966 | - | - | - | - | - |
| 6 | 0.0001 | 7.40E-07 | 1.50E-06 | 0.00232 | 0.01449 | - | - | - | - |
| 7 | 0.00066 | 5.20E-06 | 7.20E-05 | 0.0005 | 0.00829 | 0.14317 | - | - | - |
| 8 | 5.00E-05 | 7.40E-07 | 1.50E-06 | 0.00291 | 0.01449 | 0.44283 | 0.10053 | - | - |
| 9 | 7.40E-07 | 7.40E-07 | 7.40E-07 | 8.90E-06 | 1.50E-06 | 7.40E-07 | 7.40E-07 | 7.40E-07 | - |
| 10 | 7.40E-07 | 7.40E-07 | 7.40E-07 | 0.05186 | 0.00066 | 2.20E-05 | 1.40E-05 | 2.20E-05 | 0.00556 |

Cluster analysis was applied to clusterize the samples based on their AEF results (Figure 3-3). As illustrated in Figure 3-3, the two clusters level divided samples into OSPW (samples OSPW-1, OSPW-2 and OSPW-3) and groundwater (rest of the samples) clusters. The four-level clustering

divided the groundwater cluster into two more clusters, samples GW-4, GW-5, GW-9 & GW-10 and GW-6, GW-7 & GW-8, respectively.

Cluster analysis results were similar to the pre-mentioned pairwise test results represented in Table 3-2 except that the OSPW water samples were divided into two groups as well as the groundwater samples were grouped into another two groups. Although the two statistical tests have different procedures, the cluster analysis uses the distance matrix between the actual data results while the pairwise test uses the hypothesis test on the medians of the ranked dataset, two of the tests yielded similar results.

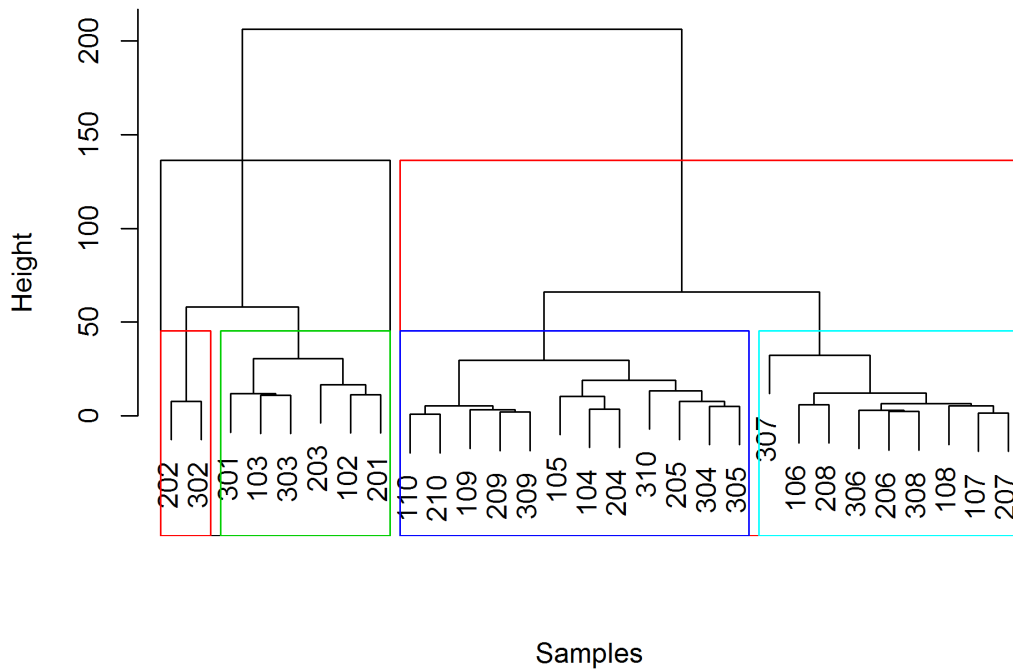


Figure 3-3 Cluster analysis results with two and four level clustering first number refers to the replicate while the second and third number refer to the sample number for example 204 represents the second replicate for sample number 4.

Figure 3-4 illustrates the boxplot of the AEF results grouped by the sample source type, OSPW and groundwater samples. OSPW consists of samples number 1 through 3, while 4 through 10 are groundwater samples. OSPW samples yielded higher AEF values and variance. Statistically, the OSPW and groundwater samples are significantly different (Chi-squared = 70.1, p-value < 0.05). It is found that the water source (OSPW vs groundwater) is the main factor that explains the variability between the samples. These findings explain results of the pairwise and cluster analysis (at two clusters level) tests.

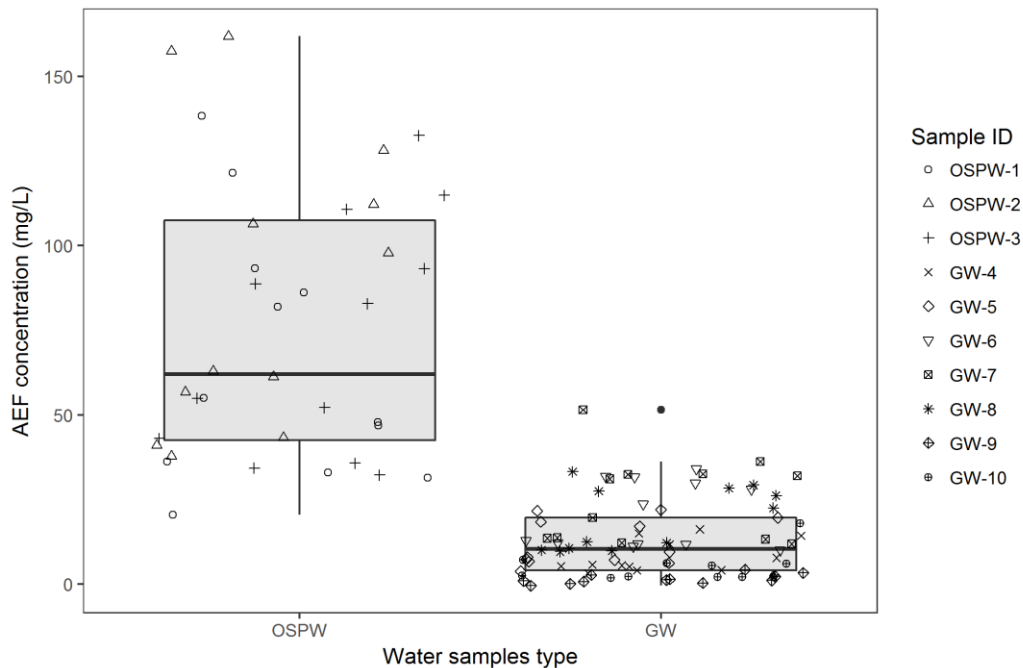


Figure 3-4 Boxplot of AEF results of the OSPW and groundwater (GW) samples. Horizontal lines represent first quartile, median, and third quartiles define the boxes, while the bottom and top tails represent the 5th and 95th percentiles.

For better understanding the difference between the samples, AEF results grouped by sampling sites is illustrated using boxplots in Figure 3-5. As seen in Figure 3-5, the OSPW results (samples 1, 2, and 3) show the highest median and variance values. The groundwater sites show

lower median and variance values. Among the groundwater sites, JPM Basal (samples 5, 6, and 7) revealed the highest median and variance values followed by MRM basal (sample 8). The lowest median and variance values were at sampling sites Mid McMarry (sample 4), and JPM PC (samples 9 and 10). These results fully explain the cluster (at 4 clusters level) and pairwise test results. Therefore, the sampling sites have the highest effect on the samples median values.

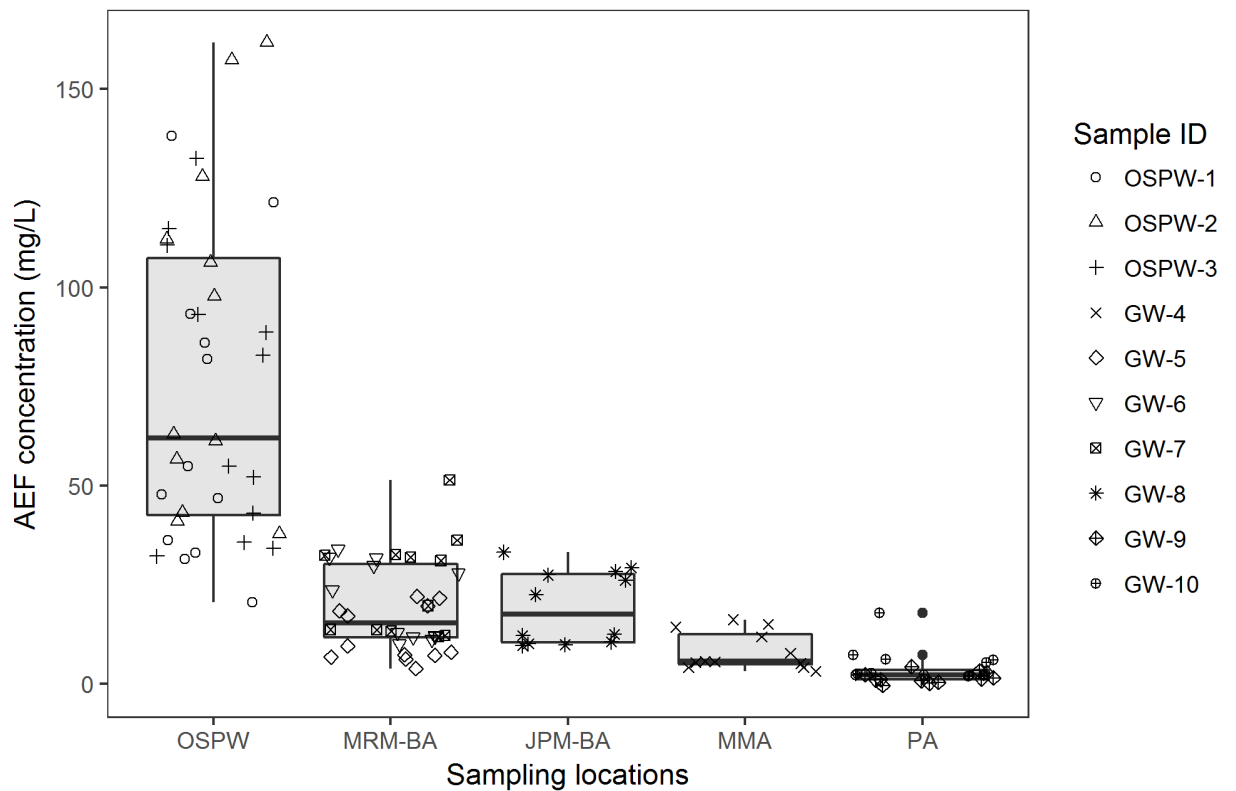


Figure 3-5 Boxplot shows the FTIR results grouped by the sampling location. Horizontal lines represent first quartile, median, and third quartiles define the boxes, while the bottom and top tails represent the 5th and 95th percentiles.

These results show that using FTIR results, AEFs, along with the statistical analysis can be used as a screening technique in a monitoring program for the environment/reclamation purposes in the oil sands area. In recent study, synchronous fluorescence spectroscopy (SFS) method, which is used to estimate the aromatic content of OSPW sample, was not able to differentiate between OSPW samples (Frank et al., 2016). To differentiate between samples, the high resolution methods

(GC× GC-ToF/MS and LC/GC-QToF/MS) were used along with principal component analysis (PCA) (Frank et al., 2016; Frank et al., 2014b).

3.4.2. Differences between measurement methods

As seen in Figure 3-6, for any given sample, the highest AEF value was obtained by using the OSPW extract calibration with the SPE preparation method. On the other hand, the lowest was measured by the Fluka calibration and LLE preparation method. Statistically, using Kruskal-Wallis Test, results from the four measurements were significantly different (Chi-squared = 12.7, and p-value <0.05). To understand why the four groups are different, pairwise test was implemented (Table 3-3).

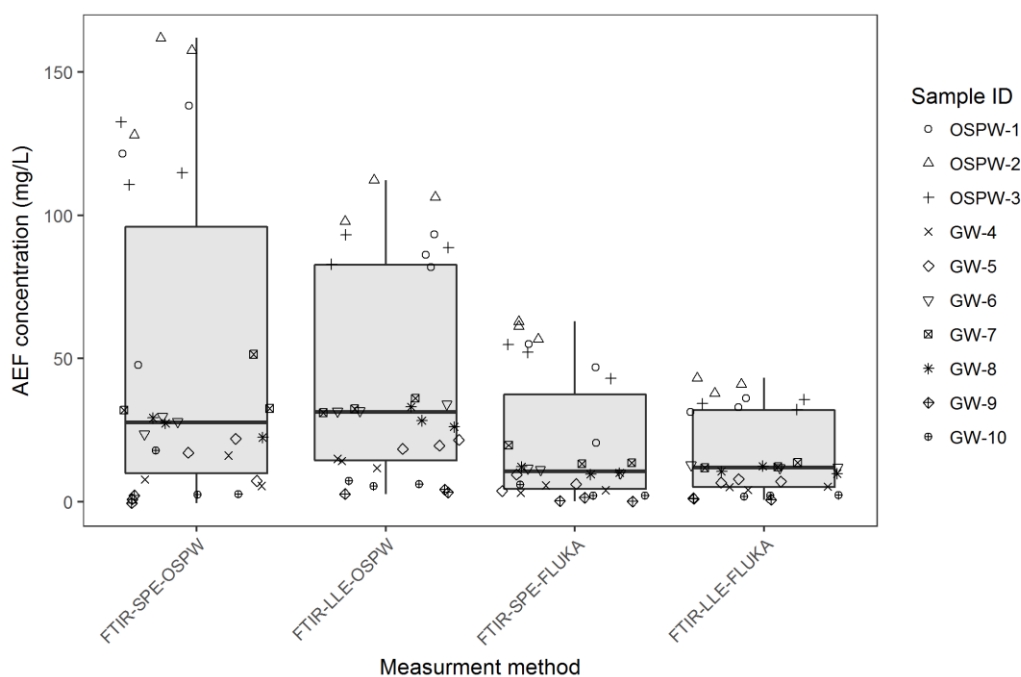


Figure 3-6 Boxplot elucidating the analysis results for the samples (1 to 10) using FTIR Fluka and OSPW standards as well as the two extraction methods LLE and SPE. Horizontal lines represent first quartile, median, and third quartiles define the boxes, while the bottom and top tails represent the 5th and 95th percentiles.

As seen in the Table 3-3, the difference did not exist between the LLE and SPE results within the same calibration method (p-value > 0.05 for the krusal walistest between FTIR FLUKA

LLE & FTIR FLUKA SPE and FTIR OSPW Ext. LLE & FTIR OSPW.Ext.SPE respectively. However, when comparing the two calibration methods, i.e. FLUKA and OSPW Ext. that extracted by the same technique for example LLE, the P-value < 0.05. This finding is in accordance with literature (Headley and McMartin, 2004). For further investigation, the difference between the two calibration methods as well as the separation method is studied in the following two sections.

Table 3-3 pairwise test result p-value matrix

| | FTIR-LLE-FLUKA | FTIR-SPE-FLUKA | FTIR-LLE-OSPW |
|----------------|----------------|----------------|---------------|
| FTIR-SPE-FLUKA | 0.7524 | - | - |
| FTIR-LLE-OSPW | 0.0043 | 0.0055 | - |
| FTIR-SPE-OSPW | 0.0225 | 0.0345 | 0.9941 |

3.4.3. Differences between calibration methods

Samples AEF value varies based on the used calibration method. Herein, two calibration methods were used the Fluka and OSPW extract methods. AEF results boxplot grouped by the calibration methods are shown in Figure 3-7. For any given sample, OSPW extract yields higher value than the Fluka standard method.

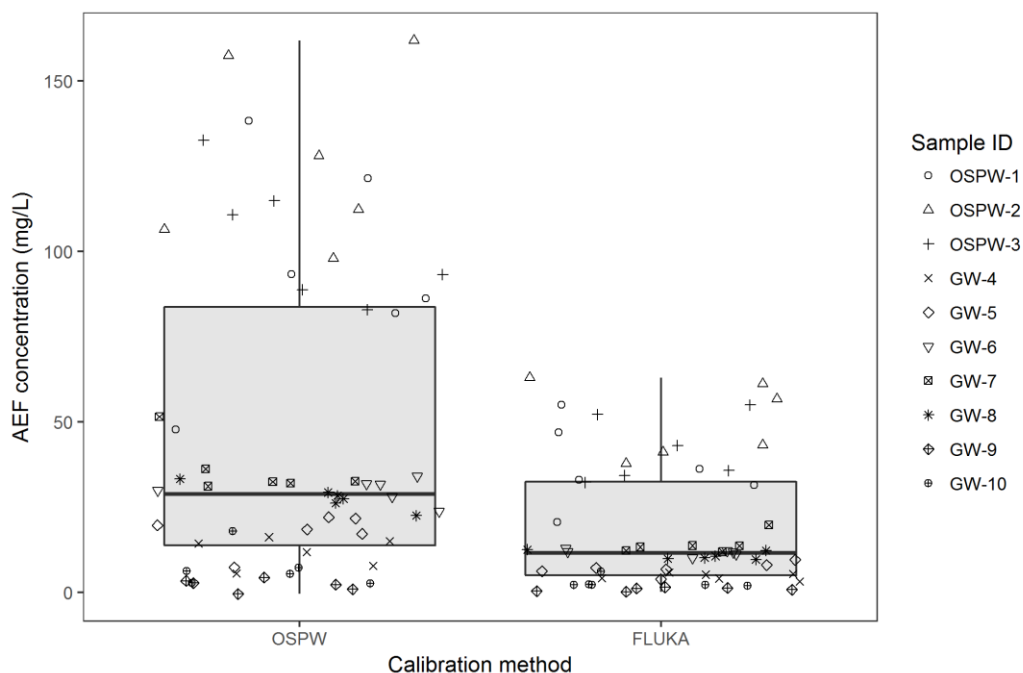


Figure 3-7 Boxplot of the samples AEF concentrations grouped by the calibration method. Horizontal lines represent first quartile, median, and third quartiles define the boxes, while the bottom and top tails represent the 5th and 95th percentiles.

Statistically, according to Mann Whitney test, there is a significant difference between the two calibration methods ($W = 1126$, and $p\text{-value} < 0.05$). The difference between the two calibration methods can be attributed to the organic compounds that are being detected at the FTIR frequencies 1704 and 1743 cm^{-1} . In case of the OSPW extract, the compounds detected, beside NAs, are fatty acids, acyclic and cyclic ketones in addition to aldehydes and amides. While in case of Fluka, NAs that follow the classical NAs formula are the compounds being detected (Dean, 1995). Also, it was previously reported that the AEF found in the natural oil sands water samples are more complex than commercial NA mixtures (Headley and McMartin, 2004). To roughly estimate the relationship between the OSPW extract and Fluka standards results, in the current study, a linear model was developed between the two sets of data. Model equation is $Y = 2.50X + 0.6$, where Y

is the AEF results quantified using the OSPW extract standard method, and X is the AEF quantified using Fluka commercial NAs standard method. Model coefficient of determination (R^2) is 0.99 with p-value < 0.05 . The linear model suggested that the OSPW extract standards results is about 2.5 times those of the Fluka standard. Findings of this study was in accordance with reported results from Martin et al (2008) who reported that the OSPW extract yield higher AEF concentration than the commercial mixtures (Martin et al., 2008; Sun et al., 2014b)

3.4.4. Differences between separation methods

Figure 3-8 shows boxplot of the AEF results grouped by the separation method. For any given sample, the SPE method yields AEF slight higher than the LLE method (16.74 mg L⁻¹ for LLE 17.55 mg L⁻¹ for the SPE). By applying Mann-Whitney-Wilcoxon test to statistically differentiate between the two groups, the test statistic shows that there is no significant statistical difference between the two groups ($W = 1811$ with p-value = > 0.05). A linear model between the SPE and LLE sets of data suggested that, for the current study, the SPE separation method yields 1.37 times higher AEF than the LLE method. The model is $Y = 1.37X - 4.7$ where Y is the AEF results measured using SPE method, and X in the AEF measured using the LLE method. Although there is no statistical difference, the SPE separate 1.37 times AEF more than the LLE separation method. These results align with the findings of Headley et al, (2013a) and Juhascik and Jenkins (2009), who reported that the SPE method is less selective compared to the LLE method, allowing more compounds to be extracted from the water samples (Headley et al., 2013a; Juhascik and Jenkins, 2009).

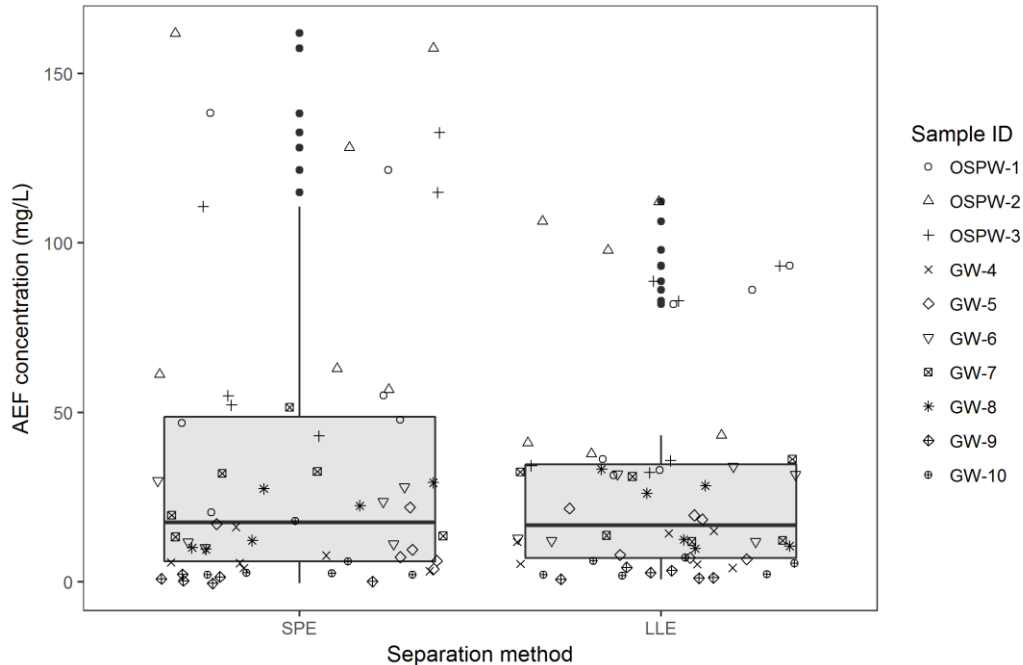


Figure 3-8 boxplot illustrating the AEF results grouped by the separation method (LLE and SPE). Horizontal lines represent first quartile, median, and third quartiles define the boxes, while the bottom and top tails represent the 5th and 95th percentiles. Black dots indicated points that are more than 3 standard deviation away from the mean.

3.4.5. Differences between replicates

The statistical differences between the three batches were studied (Figure 3-9). The results of Kruskal-Wallis test revealed that there is no significant statistical difference between the three replicates (Chi-squared = 0.93, p-value >0.05). These results confirm that there is no significant difference between the three replicates and the high quality of measurements conducted in this study. The nonsignificant difference between batches can be explained that the time between sampling campaigns is not enough to detect a change of the AEF. These results confirm that the difference between samples drawn from the same site in short period of time (weeks to few months) is not significant, as found by Farnk et al (Frank et al., 2016).

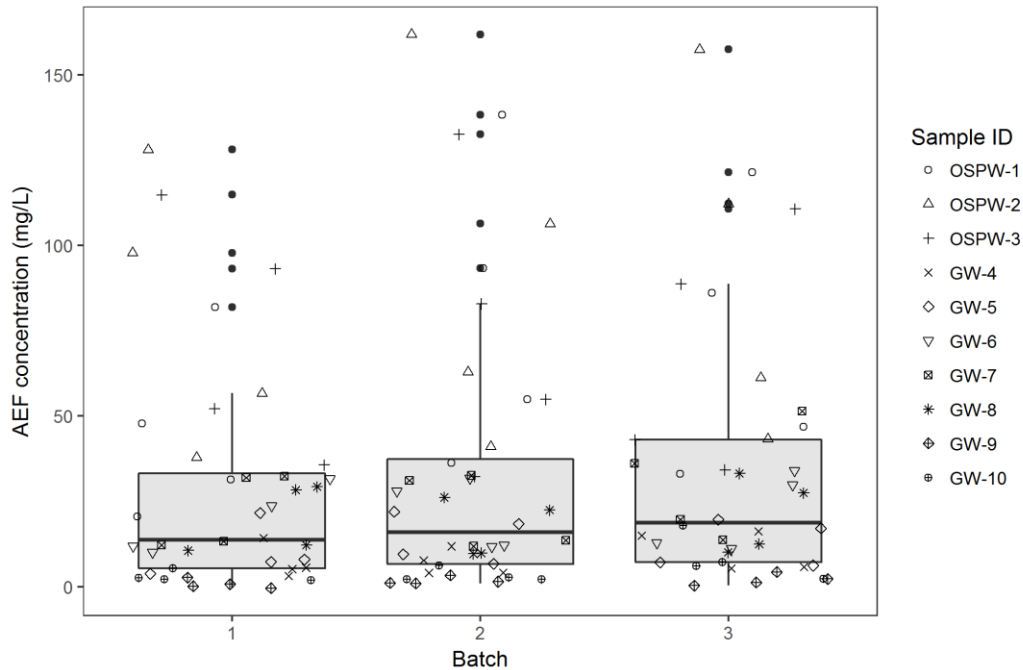


Figure 3-9 Boxplot illustrating the AEF results grouped by the batch number. Horizontal lines represent first quartile, median, and third quartiles define the boxes, while the bottom and top tails represent the 5th and 95th percentiles. Black dots indicated points that are more than 3 standard deviation away from the mean.

3.4. Conclusion and Recommendations

This study used non-parametric statistical tools to investigate the differences between the AEF results for 10 samples locations (with 3 replicates). AEF was quantified using FTIR method with two standard methods and two separation methods. The primary factor differentiating samples median AEF concentration was not surprising the sampling location and sample water type (i.e., OSPW and groundwater). The main cause for the variance within each of the samples is the measurement method. FTIR results with SPE separation and OSPW extract calibration method yielded the highest AEF values. On the other hand, FTIR results obtained from the LLE separation and Fluka calibration method show the lowest AEF values. Also, it is worthy to note that for samples under study, the AEF results based on OSPW extract calibration method were about 2.5

times higher than the AEF results obtained using the Fluka calibration method. Moreover, the AEF results based on SPE separation method were approximately 1.37 times higher than those samples extracted using the LLE separation method. The novelty of this work is to use a non-parametric statistical method to understand the effect of standards, pre-treatment and sampling location on quantification of AEF using the FTIR method. The findings of this study could be utilized when comparing various studies using different calibration standard or sample preparation method, to achieve explicit understanding of AEF measurements using FTIR method and to help in developing a standard method in the future.

The results of this study could help in environmental monitoring programs for areas that might be affected by NAs due to natural exposure or due to industrial activities. In particular, it may help in evaluating the OSPW treatment and restoration efforts in the oil sands area.

Chapter 4 : Adsorption Isotherm, Kinetic Modeling and Thermodynamics of Trans-4-Pentylcyclohexanecarboxylic Acid on Mesoporous Carbon Xerogel³

4.1. Introduction

Alberta's oil sands (tar sands) mines ranked as the world's third largest proven resource of oil with proven reserves of 168 billion barrels (Alberta-Government, 2014). Bitumen is extracted using either in-situ mining or surface mining approaches. The surface mineable area accounts for about 3 percent of the oil sands reserves area, while the rest of the recoverable bitumen is too deep to be extracted by surface mining approaches. In the deep oil sands mines, the bitumen can be extracted using in-situ extraction technologies (Alberta-Government, 2014). The steam assisted gravity drainage (SAGD) process is used in the extraction of the bitumen from the oil sands deep mines. The recovery rate of the bitumen in the in-situ method is projected to be in the range of 40 to 70 % (ACR-Alberta, 2004). In the surface mineable portion of the oil sands, Clark's hot water extraction process is used to extract the bitumen from the ore with recovery rate about 90% (ACR-Alberta, 2004). Surface mining tailings consists of a mixture of water, sand, fine silts, clay, residual bitumen and lighter hydrocarbons, inorganic salts and water soluble organic compounds (GC, 2015). Tailings are transported and stored in basins that known as tailings bonds. Tailing bonds surface area was reported as 180 square kilometers in 2013 (Government, 2013). In the tailing ponds, the solids are allowed to settle, the heavier solids, such as sands, are settle quickly, while the lighter solids, such as silt and clay, take years to settle forming what is known as mature fine

³ A version of this chapter will be submitted to Chemosphere journal as "Ibrahim M. D., Messele, S.A., and Gamal El-Din, M.: "Adsorption Isotherm, Kinetic Modeling and Thermodynamics of Trans-4-Pentylcyclohexanecarboxylic acid on Mesoporous Carbon Xerogel".

tailings (MFT) (GC, 2015). According to the agreements between the oil sands companies and the government of Alberta, it is required that the tailing ponds be reduced and reclaimed no later than five years after the tailing ponds are no longer in the service (GC, 2015).

For each cubic meter of synthetic crude oil produced using the hot water extraction method, about nine cubic meters of raw tailings are produced. The tailings produced are a mix of sand, fine tailings and Oil sands process-affected waters (OSPW) (Brown and Ulrich, 2015).

Toxicity of OSPW to the aquatic and terrestrial biota has been reported (He et al., 2012b; Klamerth et al., 2015; Meshref et al., 2017; Perez-Estrada et al., 2011; Scott et al., 2008c). OSPW toxicity was attributed to a group of organic acids called naphthenic acids (NAs) (Anderson et al., 2012a; Klamerth et al., 2015; Marentette et al., 2015b). NAs are a complex mixture of organic acids such as alicyclic and aliphatic carboxylic acids that are naturally existing in the petroleum products (Clemente and Fedorak, 2005; El-Din et al., 2011; Scott et al., 2005b). Classical NAs follow the general formula $C_nH_{2n+z}O_x$, where n represents the carbon number and (8 to 30), Z identifies the hydrogen deficiency (0 to -12), and X represent the number of oxygen (2 to 6) (Clemente and Fedorak, 2005; Grewer et al., 2010a). Up to date, the structure of individual components of the NAs has not be accomplished yet because of its high complexity. Instead, the identification and quantification of NAs is accomplished based on the carbon and hydrogen deficiency numbers. Currently, most popular method used in quantification and identification of NAs are Fourier Transform Infrared (FT-IR) spectroscopy, Gas Chromatography Mass Spectrometry (GC-MS), and High-Performance Liquid Chromatography mass spectrometry (HPLC-MS) (Clemente and Fedorak, 2005). NAs concentration varied from 110 mg L⁻¹ in the fresh OSPW to 50 mg L⁻¹ in some of the tailing ponds according to the OSPW source and age (Allen, 2008a; Brown and Ulrich, 2015).The treatment of OSPW were studied using biological

(Islam et al., 2014c; Xue et al., 2016b; Zhang et al., 2016), physical (Gamal El-Din et al., 2011b; Moustafa et al., 2015; Moustafa et al., 2014c; Zubot et al., 2012b), and chemical treatment methods (Afzal et al., 2012; Meshref et al., 2017; Pérez-Estrada et al., 2011; Wang et al., 2013b).

Adsorption is one of the techniques used to remove the NAs from OSPW. Adsorbents used in previous studies were granular activated carbon (GAC), powder activated carbon (PAC), raw and activated petroleum coke (PC), silica alumina, zeolite, and Organic rich soil (Azad et al., 2013; El-Din et al., 2011; Iranmanesh et al., 2014; Janfada et al., 2006; Mohamed et al., 2015a; Small, 2011; Zubot, 2011). High removal of NAs was attributed to the mesoporosity, surface activation and the surface area of the adsorbent (Iranmanesh et al., 2014). Carbon Xerogel (CX) is a synthesized polymer-based adsorbent that can be tailored to meet specific needs. CX has low density, high porosity, high surface area and tailorable pore size and surface chemistry (Mahata et al., 2007). CX characteristics can be controlled by changing the synthesis parameters such as drying conditions, pH, type and amount of solvent, concentration of reactants, temperature and time of the synthesis process and the carbonization process, whereas the pH and concentration of reagents are the most two important factors that affect the final characteristics of the CX (Bermudez et al., 2015; Job et al., 2005; Rey-Raap et al., 2016).

CX were successfully used as adsorbents in air and water purification applications such as CO₂ capturing, VOC removal and removal of oil and toxic organic compounds from wastewater (Moreno-Castilla and Maldonado-Hodar, 2005; Rey-Raap et al., 2014). In this study, CX was synthesized, characterized and its performance was tested in removing NA model compound Trans-4-pentylcyclohexanecarboxylic (TPCA) from aqueous solutions. The effect of temperature, pH and ion strength was studied. For the sake of comparison between the performances of the

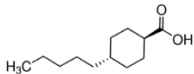
synthesized CX with other adsorbent, a commercial granular activated carbon was used in this study. Adsorption isotherm, kinetics and thermodynamics of the process were also investigated.

4.2. Materials and methods

4.2.1. Material

Trans-4-Pentylcyclohexanecarboxylic acid (TPCA) of 97% and 50–52% sodium hydroxide were purchased from Sigma-Aldrich (ON, Canada). The 99.9% sulfuric acid (H₂SO₄), and sodium chloride (NaCl) were purchased from Fisher Scientific (AB, Canada). 99% Acetonitrile, 98% ammonium acetate, 99% acetic acid, 99% resorcinol, 99% formaldehyde (37 wt. % in H₂O, contains 10-15% Methanol as stabilizer), 99% potassium phosphate monobasic (KH₂PO₄) and 99% potassium phosphate dibasic (K₂HPO₄) were purchased from Fisher Scientific (AB, Canada). Ultrapure water was obtained from a Millipore and Elga system (Synergy UV instrument, Millipore, Molsheim, France). Commercial granular activated carbon (GAC) was obtained from Cleartech, (AB, Canada). The main physico-chemical properties of the TPCA are presented in Table 4-1. All chemicals were used as received without further purification.

Table 4-1 Physico-chemical properties of TPCA model NA compounds used.

| Model Compounds | Formula | Structure | Molecular Weight (g/mol) | Log K _{OW} | Solubility at 25°C (mg/L) |
|-----------------|--|---|--------------------------|---------------------|---------------------------|
| TPCA | C ₁₂ H ₂₂ O ₂ |  | 198.30 | 1.62 | 75.5 |

4.2.2. Carbon xerogel preparation

A 25 g of resorcinol was dissolved in 40 mL of Milli-Q water and 34 mL of formaldehyde was added to it and the pH was adjusted to 5.5 using 2 M NaOH (Mahata et al. 2007). The solution was then stirred for 90 minutes to ensure complete dissolution and left in an oven at 60°C for 3 days to allow for gelation (Mahata et al. 2007). Curing of the gelled solution was done in the same oven for a week at the following temperatures; first day 60°C, second day 80°C, third day 100°C, and 120°C for the fourth day, and finally maintained at 105°C for the last three days. The dry gels went through carbonization in a furnace under a nitrogen flow of 1 L/min. The CX gel was heated in the furnace by first being heated from room temperature and held at 200°C for an hour, then heated up to 700°C and maintained for three hours before being cooled down to room temperature over the duration of an hour. Finally, the carbonized gel was crushed and sieved to the desired size of 0.6 to 1.4 mm (CX). The commercial GAC was sieved to obtain a particle size from 0.6 to 1.4 mm (GAC).

4.2.3. TPCA preparation and analysis

TPCA stock solution (75 mg/L) was prepared in 0.05 M phosphate buffer solution (~ pH 8) in volumetric flask and was stirred for at least 12 hours, to make sure that the TPCA was dissolved. TPCA samples were analysed using liquid chromatogram mass spectrometer (LC-MS) (Waters instruments, Toronto, Canada), equipped with column C18, 1.7µm, 50 mm x 2.1 mm with temperature= 40 °C. Solvent A: 4 mM ammonium acetate with 0.1% acetic acid, and B, 100% acetonitrile. Flow rate and, injection volume was 0.4 mL.min⁻¹ and 2µL, respectively.

4.2.4. Adsorbents characterization

The adsorbent's surface morphology was characterized using scanning electron microscope (SEM), VEGA3, Tescan Inc., Cranberry, PA, USA. The SEM was operated at an

accelerated voltage of 20 kV. Adsorbent's surface area was measured using nitrogen adsorption/desorption isotherm performed at 77 °K (IQ2MP, Quantachrome, FL, USA). Samples were degassed at 120 °C before analyses to ensure the dryness of adsorbents samples. Brunauer–Emmett–Teller (BET) equation at the relative pressure range of 0.01–0.07 was used in determining the specific surface area of the adsorbents. Pore volume was determined using V-t model.

A Bio-rad diffuse reflectance FT-IR spectrophotometer (FTS 6000, Philadelphia, PA, USA) was used to identify the functional groups on the surface of the adsorbents. The adsorbents were dried at 110 °C overnight in the oven, mixed with potassium bromide (KBr) (FT-IR grade, Sigma-Aldrich, ON, Canada) at a 5 % by weight ratio, and grounded to result in a fine powder. Pure KBr was used to collect the background spectra. The spectra were recorded with 128 scans and 4 cm⁻¹.

Thermogravimetric analysis (TGA) was performed using a Pyris 1 TGA made by Perkin Elmer (Norwalk, CT, USA). The temperature program was 30-900°C at 10 °C.min⁻¹ (the instrument went to about (940 °C) with isothermal holds at 120°C and 400°C for 60 minutes each.

To characterize the elemental composition and surface functional groups, X-ray photoelectron spectroscopy (XPS) analysis was performed using AXIS 165 spectrometer (Kratos Analytical, Japan). The depth of analysis was 2-5 nm and area of 400 x 700 µm under pressure of 3x10⁻⁸ Pa and monochromatic Al Ka source ($h\nu = 1486.6$ eV) at power 210 W. Instrument resolution was 0.55 eV for Ag 3d and 0.7 eV for Au 4f peaks. Vision-2 instrument software was used in data processing while the compositions were calculated using the elemental peaks provided by NIST database.

Determination of point of zero charge pH_{PZC} was carried out using solid addition method (Pourrezaei et al., 2014a). Experiment was done using adsorbent (CX and GAC) load of 0.5 g.L^{-1} in a total volume of 50 mL of 0.1 M NaCl. The pH was adjusted using 0.1 M H_2SO_4 and 0.1 M NaOH resulting in a series of solutions with initial pHs of 4, 5, 6, 7, 8.5, and 10. After 24 hours of solution agitation using mechanical shaker (New Brunswick Scientific, CT, USA) at 210 rpm, all final pHs (pH_f) were measured. Then a chart between $\Delta \text{pH} = (pH_f - pH_0)$ and pH_0 was drawn. pH_{PZC} is the pH that corresponding to $\Delta \text{pH} = 0$.

4.2.5. Equilibrium time experiment

The Equilibrium time experiment was performed to determine the contact time needed to reach the equilibrium state between the adsorbent and the adsorbate (TPCA). In this experiment, the adsorbent load was 0.5 g.L^{-1} and the adsorbate concentrations was 60 mg L^{-1} . The total volume of the solution (50 mL) was placed on a mechanical shaker with 210 rpm at temperature of $20 \pm 1 \text{ }^\circ\text{C}$. Samples were taken at time intervals of 1, 2, 4, 6, 12, 20, 24, and 48 hours. The samples were collected and filtered through nylon syringe $0.2 \text{ }\mu\text{m}$ filters. The equilibrium time was obtained when the removal of the adsorbate reaches plateau with time (Pourrezaei et al., 2014b).

4.2.6. Isotherm experiments

Batch isotherm experiments were carried out by adding a fixed amount of adsorbents, CX and GAC, (0.025 g) into 125-mL Erlenmeyer flasks containing 50 mL of different initial concentrations (15, 30, 45, 60 and 75 mg L^{-1}) of TPCA solution at a temperature of $20 \pm 1 \text{ }^\circ\text{C}$. The flasks were agitated in a mechanical shaker at 210 rpm for 24 hours. The initial and equilibrium TPCA concentrations were determined by LC_MS. All experiments were carried out in duplicates. The amount of adsorption at equilibrium, q_e (mg/g), was calculated by:

$$q_e = \frac{(C_0 - C_e)V}{W} \quad \text{Equation 1}$$

where C_0 and C_e (mg L^{-1}) are the liquid –phase concentrations of TPCA at initial and equilibrium, respectively. V (L) is the volume of the solution and W (g) is the mass of dry adsorbent used.

Langmuir, Freundlich, and Dubinin-Radushkevitch (D-R) models were used in modeling the isotherm data, Equations 2 to 4 show linear form of Langmuir, Freundlich and D-R models.

$$\frac{1}{q_e} = \frac{1}{q_m} + \frac{1}{q_m K_L} \frac{1}{C_e} \quad \text{Equation 2}$$

where, q_m are the maximum mass sorbed at equilibrium (mg g^{-1}). K_L is Langmuir adsorption constant.

$$\ln(q_e) = \ln k_F + \frac{1}{n} \ln(C_e) \quad \text{Equation 3}$$

where, K_F , and n are Freundlich adsorption constants.

$$\ln(q_e) = \ln(q_m) - K_{DR} \varepsilon_{DR}^2 \quad \text{Equation 4}$$

where, K_{DR} , is Dubinin-Radushkevitch adsorption constant. ε is Polanyi potential which is defined as:

$$\varepsilon = RT \ln \left[1 + \frac{1}{C_e} \right] \quad \text{Equation 5}$$

4.2.7. Kinetic experiments

For kinetics studies, 0.025 g of CX and GAC were contacted with 50 mL of TPCA (60 mg/L) using mechanical shaker at 210 rpm. At predetermined intervals of time, solutions were analyzed for the final concentration of TPCA. The amount of adsorption q_t (mg g^{-1}), at time t (h), was calculated by:

$$qt = \frac{(C_0 - C_t)V}{W} \quad \text{Equation 6}$$

where C_t (mg L^{-1}) is concentrations of TPCA at time t .

Pseudo-first, and pseudo-second order models were used to identify the TPCA adsorption rate on both CX and GAC adsorbents. Bangham, and Webber-Morris intraparticle diffusion models were used to identify the rate limiting step in the adsorption process. Equations for first, second pseudo order, Bangham and Webber-Morris kinetic models' were presented from Eq 7-10, respectively.

$$\frac{dq_t}{dt} = k_1(q_e - q_t) \quad \text{Equation 7}$$

where k_1 is the rate constant of pseudo first order (hour^{-1})

$$\frac{dq_t}{dt} = K_2(q_e - q_t)^2 \quad \text{Equation 8}$$

where K_2 is the rate constant of pseudo second order ($\text{g.mg}^{-1}.\text{hr}^{-1}$)

$$q_t = K_{int}t^{0.5} + C \quad \text{Equation 9}$$

where K_{int} is the intra-particle diffusion rate constant ($\text{mg g}^{-1}.\text{min}^{-1/2}$)

$$q_t = K_B t^\vartheta \quad \text{Equation 10}$$

where K_B is Bangham interparticle diffusion rate constant ($\text{mg g}^{-1}.\text{min}^\vartheta$)

4.2.8. Effect of solution pH, temperature and ion strength

The effects of solution pH, temperature and ion strength were studied by agitating 0.025 g of carbon material (CX and GAC) and 50 mL of 60 mg L^{-1} TPCA concentration at different initial solution pH (5, 6.5, 8, and 10), temperature (4, 10, and 20) and concentration of NaCl (0, 0.1, 0.2, 0.3, 0.4 and 0.5 M). Agitation was provided for 24 hours at a constant agitation speed of 210 rpm. The pH was adjusted by adding a few drops of diluted NaOH or H_2SO_4 .

4.2.9. Statistical analysis

All models (equilibrium and kinetics) parameters were determined using linear fitting. Determination coefficients (R^2), residual root-mean-square error (RMSE), and sum of square of the errors (ERRSQ) were used as a measure of goodness of fit according to the following equations (Lu et al., 2015).

$$R^2 = \frac{(Q_{meas} - \bar{Q}_{calc})^2}{\sum_{i=1}^n (Q_{meas} - \bar{Q}_{calc})^2 + (Q_{meas} - Q_{calc})^2} \quad \text{Equation 11}$$

$$RMSE = \sqrt{\frac{1}{n-2} \sum_{i=1}^n (Q_{meas} - Q_{calc})^2} \quad \text{Equation 12}$$

$$ERRSQ = \sum_{i=1}^n (Q_{meas} - Q_{calc})^2 \quad \text{Equation 13}$$

Where Q_{meas} = the measured experiment data, Q_{calc} = the calculated data with isotherm or kinetic model, \bar{Q}_{calc} = the average of Q_{calc} , and n = the number of data points.

4.3. Results and discussion

4.3.1. Textural property characterization

The textural property of CX and GAC is presented in Table 4-2. The GAC shows higher surface area ($976 \text{ m}^2 \text{ g}^{-1}$) while the CX surface area was found to be $573 \text{ m}^2 \text{ g}^{-1}$. In terms of the total pore volume, results show that the CX has a total of pore volumes of $1.54 \text{ cm}^3 \text{ g}^{-1}$ and the GAC has only $0.599 \text{ cm}^3 \text{ g}^{-1}$. This shows the high porosity of the CX compared to the GAC. The mesoporous volume (V_{meso}) of CX is $1.340 \text{ cm}^3 \text{ g}^{-1}$, i.e., mesoporous volume corresponds to 87 % of the total pore volume which confirms that the CX is a mesoporous adsorbent while the GAC is mostly microporous adsorbent (i.e., 60 % of the total pore volume is associated to

micropores). This is confirmed by the average pore diameter which found to be 11 nm for the CX and 2 nm for the GAC. Therefore, the CX is a mesoporous and the GAC is a microporous adsorbent.

Table 4-2 BET surface area, micro (pores with diameter less than 2 μm), meso (pores with diameter less from 2 to 50 μm)porous area for CX, and GAC.

| Sample | S_{BET} ($\text{m}^2 \text{g}^{-1}$) | S_{micro} ($\text{m}^2 \text{g}^{-1}$) | V_{micro} ($\text{cm}^3 \text{g}^{-1}$) | V_{meso} ($\text{cm}^3 \text{g}^{-1}$) | V_{total} ($\text{cm}^3 \text{g}^{-1}$) | D_p (nm) |
|--------|--|--|---|--|---|---------------|
| CX | 573 | 438 | 0.205 | 1.340 | 1.545 | 11 |
| GAC | 976 | 839 | 0.386 | 0.213 | 0.599 | 2 |

4.3.2. Surface morphology and functional groups (SEM, FT-IR and XPS)

The surface morphologies of CX and GAC were investigated using the SEM imaging. Figure 4-1 shows the SEM images of the CX and the GAC. The results show that the CX has a rough surface with pores which indicates the porous structure of the CX and the GAC shows some roughness and flak.

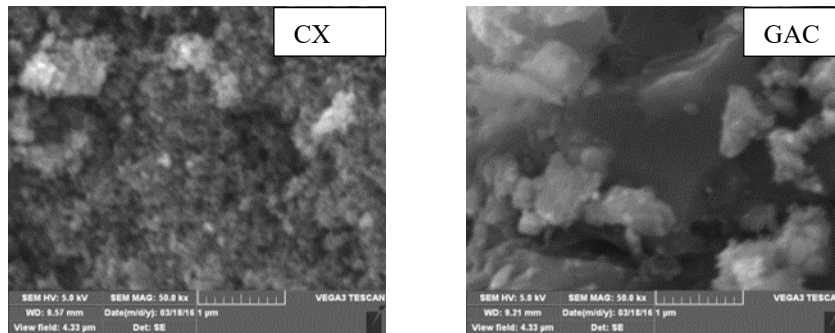


Figure 4-1 SEM imaging for CX, and GAC at 50 k times

Figure 4-2 shows the FT-IR analysis of the CX and GAC. Results revealed the presence of carbonyl groups ($\text{C}=\text{O}$ stretch at 1400 cm^{-1}), and carboxyl groups ($\text{C}-\text{O}$ bond at 1650 cm^{-1}) on CX surface. For GAC, carboxyl groups ($\text{C}-\text{O}$ stretch at 1650 cm^{-1}), hydroxyl groups ($-\text{OH}$ bond 3500

cm^{-1}), and carbonyl ($\text{C}=\text{O}$ stretch at 1400 cm^{-1}), were found (Hadizade et al., 2017; Inyinbor et al., 2016; Pourrezaei et al., 2011; Tan et al., 2007).

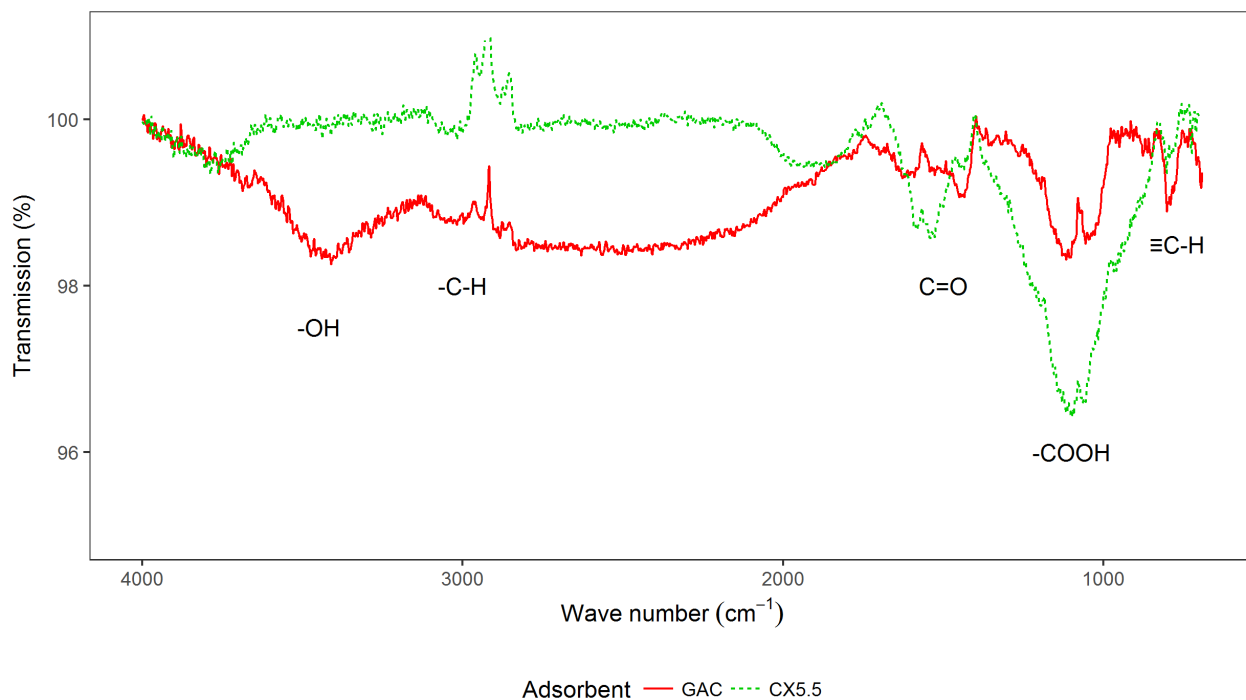


Figure 4-2 FT-IR spectrum of CX and GAC.

XPS results, presented in Figure 4-3 and Figure 4-4, confirm the presence of carbonyl, alkyne and carboxyl functional groups on the surface of CX and GAC. Percentage of oxygen containing functional groups are presented in

Table 4-3. These results affirm that the surface functional groups that present on the GAC surface are more abundant when compared to those groups on the CX surface.

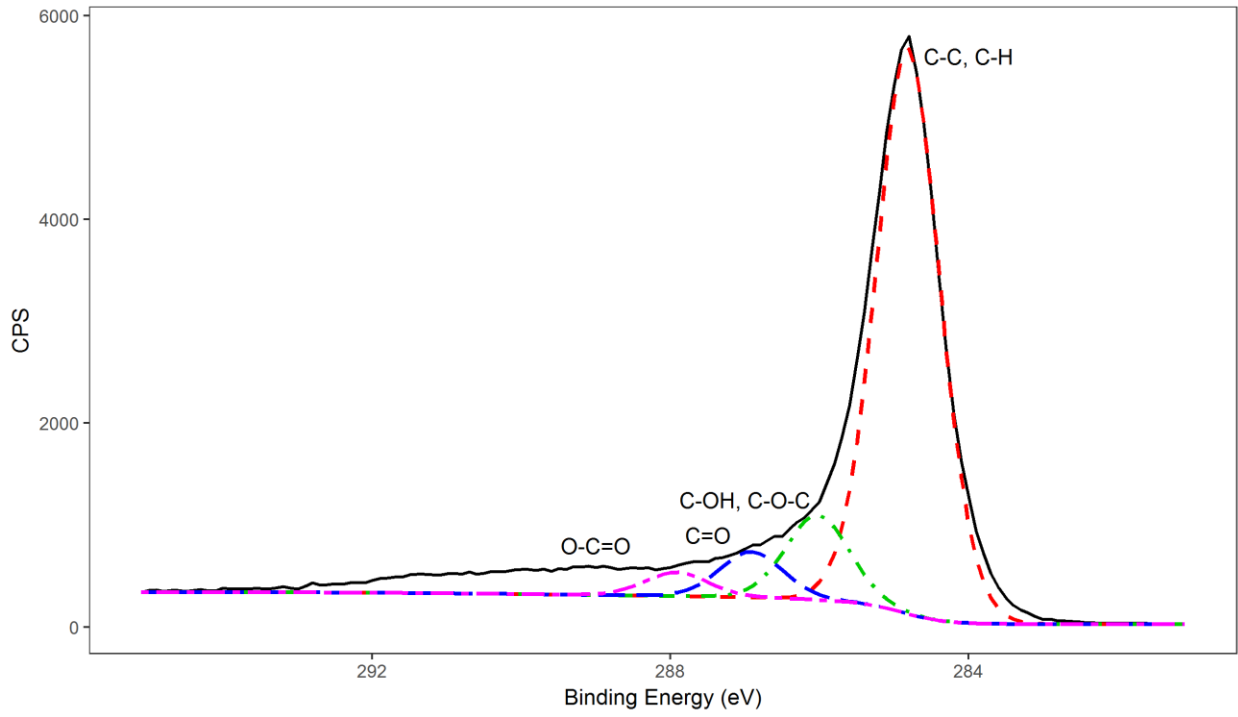


Figure 4-3 CX XPS C1s peak deconvolution

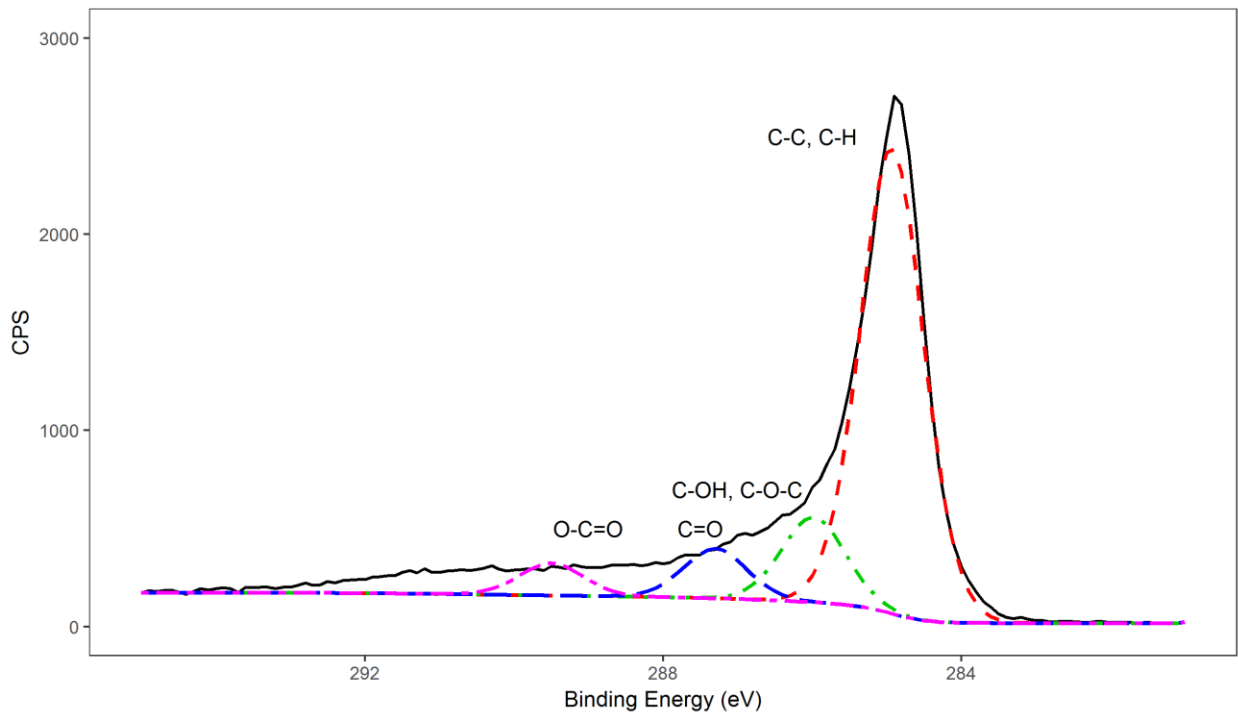


Figure 4-4 GAC XPS C1s peak deconvolution

Table 4-3 Concentration of oxygen-containing functional groups as determined by XPS analysis

| Functional group | Oxygen functional groups (%) | |
|------------------|------------------------------|------|
| | CX | GAC |
| C-OH (%) | 10 | 13.5 |
| C=O (%) | 8.13 | 13 |

4.3.3. Thermal gravimetric analysis (TGA)

TGA analysis was performed on raw and saturated adsorbents (CX and GAC) to investigate the thermal stability and the mechanism of the adsorption. Results (Figure 4-5) show a loss of weight at 120 and 400 °C, which is related to the desorption of water and carboxylic acids from the surface of the adsorbents (Pourrezaei et al., 2014b). Similar trends were shown in the thermal desorption profile, which suggest Phys sorption of the adsorbate on the surface of the adsorbent (Pourrezaei et al., 2014b).

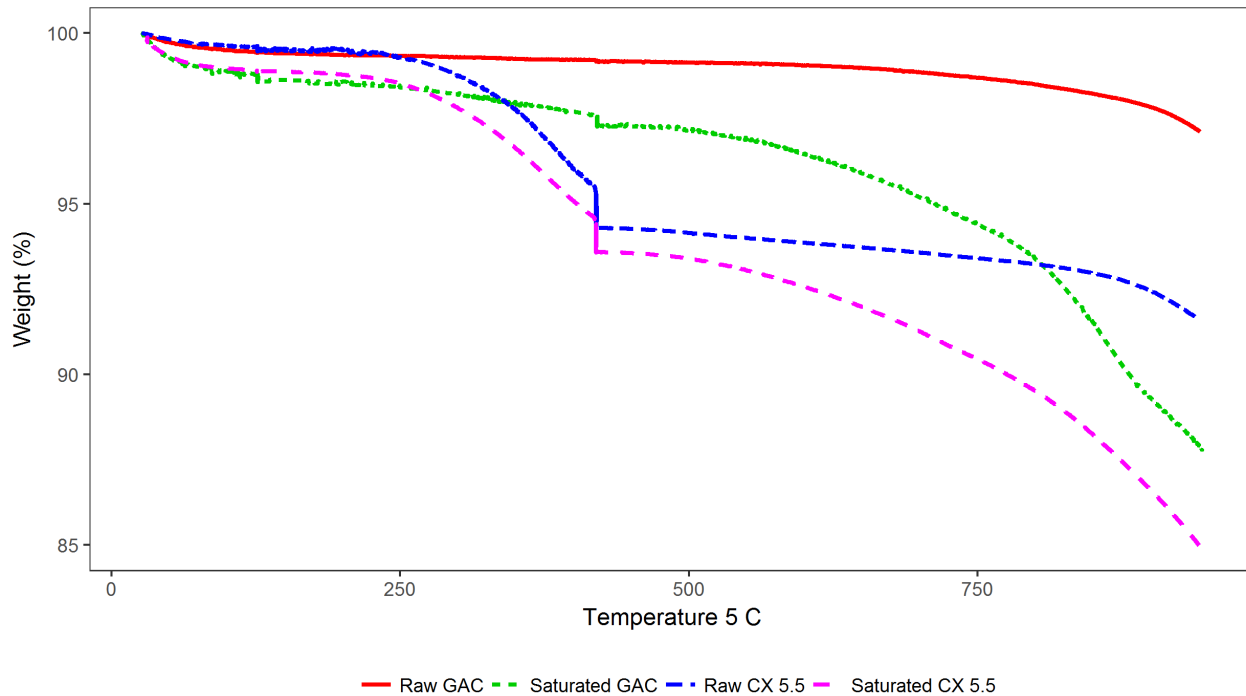


Figure 4-5 TGA analysis for raw and saturated adsorbents

4.3.4. pH_{PZC}

Carbon based adsorbents have amphoteric characteristics; hence, based on the solution pH, the surface of the adsorbent can be either positively or negatively charged (Faria et al., 2004; Silva et al., 1996). To determine the surface charge of the adsorbent, pH_{PZC} must be known. pH_{PZC} is corresponding to the pH where there is no charge at the adsorbent surface. By knowing the solution pH and the pH_{PZC} , the charge of the adsorbent surface can be determined. At solution pH greater than the pH_{PZC} , the adsorbent surface has a negative charge. In contrast, if the pH of the solution is less than the pH_{PZC} , the surface of the adsorbent becomes a positively charged (Faria et al., 2004). Results of the experiment, shown in Figure 4-6, revealed that the pH_{PZC} of the CX, and GAC were 6.7 and 6.9. Based on these results and knowing that the pH of the solution is 8.0, the surface of adsorbents in this study is negatively charged. The

negativity of the adsorbent surface can be explained by the presence of carboxylic, and phenolic groups on the adsorbents surface. These functional groups are ionized (deprotonated) at the pH of 8.0 (Moustafa et al., 2014b).

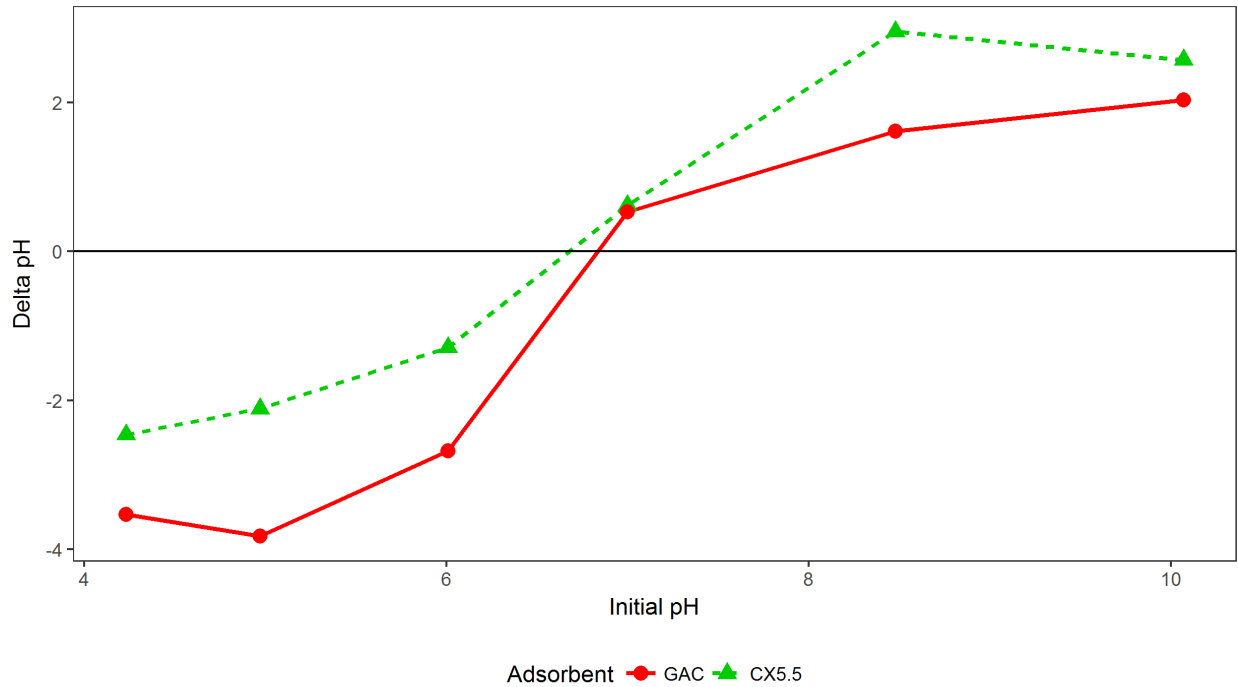


Figure 4-6 pH_{pzc} experimental results. Horizontal line represents the $\Delta pH=0$.

4.3.5. Equilibrium time experiments

The remaining of TPCA concentration versus time is shown in **Error! Reference source not found**. It is notable that the removal rate is fast (linear trend) for the first 4 hours. After 12 hours, about 80 % of the TPCA removal took place for GAC and 60 % for CX. After 24 hours, more than 90% and 70 % of the removal was achieved for GAC and CX, respectively and the removal follows a plateau. After 48 hours, the maximum amount of removal (about 70 % and 98 % for CX and GAC respectively) was achieved. The linear portion of the curve represents

the diffusion of the adsorbate to the surface layer of the adsorbent, and the plateau part represents the diffusion of the adsorbate to the internal pores of the adsorbate (Goel et al., 2005; Pourrezaei et al., 2014b). The fast rate of adsorption in the linear portion may be explained by the plenty of readily accessible sites. Later, the concentration of the adsorbed TPCA increased which decrease the adsorption driving force. Therefore, rate of adsorption becomes slower till reaching the plateau (Ahmad and Kumar, 2010; Farsad et al., 2017; Inyinbor et al., 2016; Saha et al., 2010).

For the linear portion of the curve, it is noticed that the adsorption rate of the TPCA to the CX surface is higher than the GAC rate, this can be attributed to the mesoporous structure and the high pore volume of the CX. For the plateau part, the GAC has higher adsorption which may be explained by the presence of oxygen functional groups on the GAC surface as illustrated in Table 4-3. The equilibrium time for NAs related adsorption experiment was reported between 16 and 24 hours (Iranmanesh et al., 2014; Moustafa et al., 2015; Pourrezaei et al., 2014b; Sarkar, 2014; Small et al., 2012a). Based on the results and previous literature, 24 hours was chosen as the equilibrium time for the following experiments.

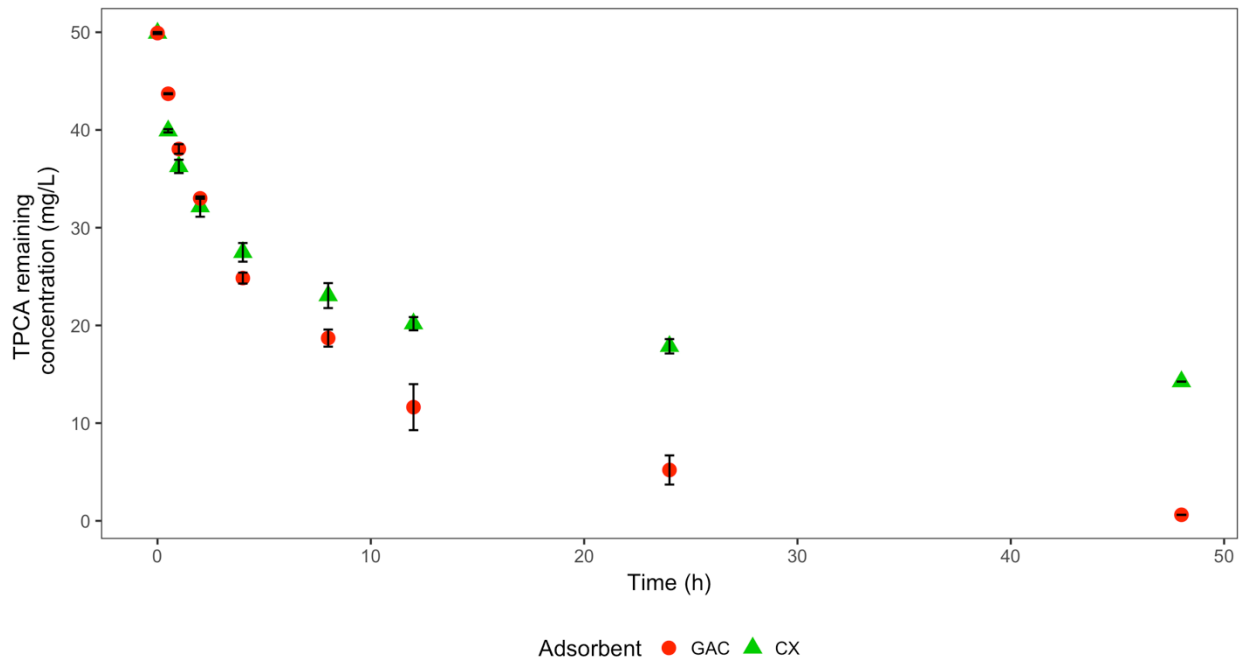


Figure 4-7 TPCA remaining concentration using CX 5.5 and GAC. Experiment conditions- total solution volume: 50 mL, shaking Speed: 210 rpm, initial concentration: 50 mg L⁻¹, adsorbents concentration: 0.5 g.L⁻¹.

4.3.6. Adsorption isotherm modeling

Three isotherms were tested for their ability to describe the experimental results, namely the Langmuir isotherm, the Freundlich isotherm, and the Dubinin-Radushkevitch (D-R) isotherm. The different isotherms of CX and GAC are presented in Figure 4-8, Figure 4-9, and Figure 4-10 respectively. Isotherms constants are shown in Table 4-4. Results show that Langmuir isotherm described the TPCA adsorption process on CX and GAC indicated by coefficient of determination (R^2) of 0.97 and 0.96 respectively. The maximum capacity of the CX and GAC based on Langmuir isotherm was calculated as 69.9 and 102 mg g⁻¹ respectively, these values are higher than the capacity of many of the adsorbents used in NAs removal from water that were reported in the literature such as raw petroleum coke (1.0 mg g⁻¹) (Pourrezaei

et al., 2014b; Zubot, 2010), exfoliated graphite (11.2 , 5.13, and 2.4 mg g⁻¹) (Moustafa et al., 2014c), activated carbon based on sawdust precursor (33 mg g⁻¹) (Iranmanesh et al., 2014), and organic rich soil (0.25 mg g⁻¹) (Janfada et al., 2006).

Table 4-4 Langmuir, Freundlich, and D-R isotherms parameters

| Isotherm model | Parameter | CX | GAC |
|----------------|---|--------------------------------------|--------|
| Langmuir | q _m (mg g ⁻¹) | 69.9 | 102 |
| | K _L (g.mg ⁻¹) | 1.08 | 0.54 |
| | r ² | 0.97 | 0.96 |
| | ERRSQ | 0.0007 | 0.0013 |
| | RMSE | 0.0129 | 0.0178 |
| | Freundlich | 1/n | 0.24 |
| Freundlich | K _F (g.mg ⁻¹) | 34.42 | 33.95 |
| | r ² | 0.82 | 0.88 |
| | ERRSQ | 0.0018 | 0.0010 |
| | RMSE | 0.0212 | 0.0162 |
| | D-R | q _m (g.mg ⁻¹) | 64.8 |
| D-R | K _{DR} (M ² .kJ ⁻²) | -0.015 | -0.227 |
| | E (kJ.M ⁻¹) | 5.8 | 1.5 |
| | r ² | 0.87 | 0.81 |
| | ERRSQ | 0.0011 | 0.0043 |
| | RMSE | 0.0166 | 0.0326 |

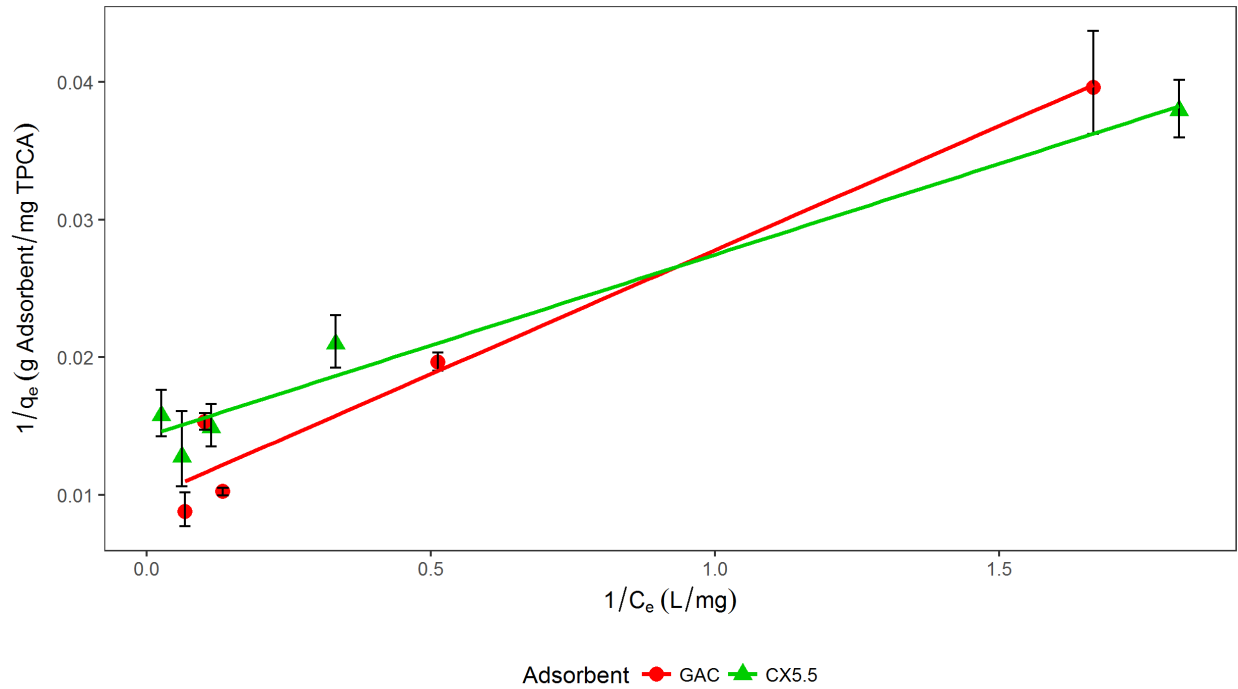


Figure 4-8 TPCA Langmuir isotherm for CX and GAC Experiment conditions- total solution volume: 50 mL, shaking Speed: 210 rpm, initial concentration: 60 mg L^{-1} , adsorbents concentration: 0.5 g.L^{-1} . All measurement were taken in duplicates

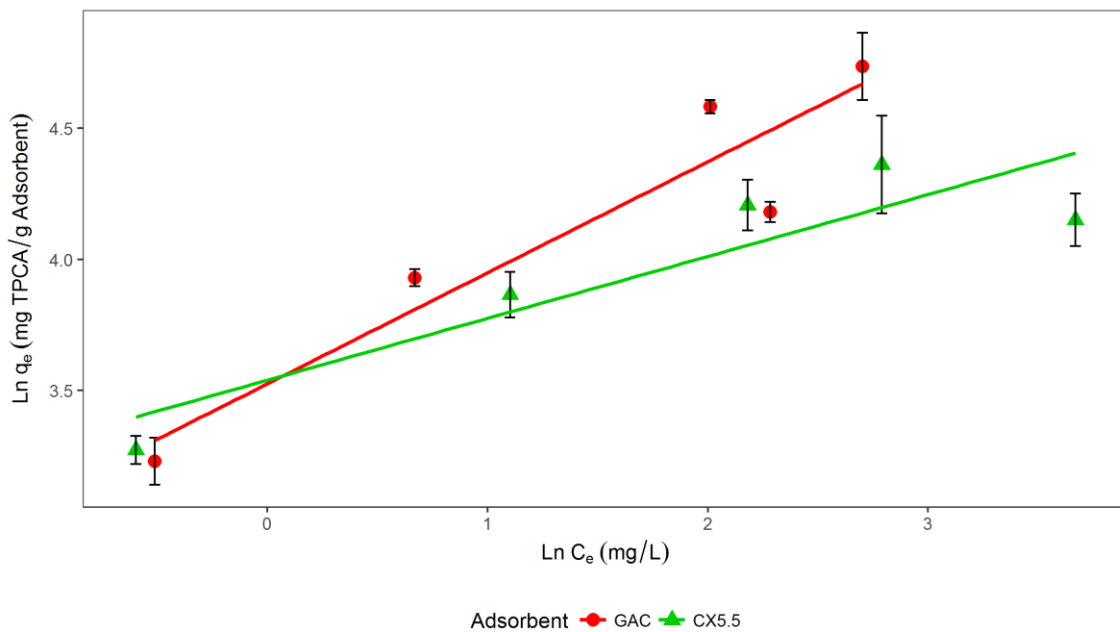


Figure 4-9 TPCA Freundlich isotherm for CX and AC. Experiment conditions- total solution volume: 50 mL, shaking Speed: 210 rpm, initial concentration: 60 mg L^{-1} , adsorbents concentration: 0.5 g.L^{-1} . All measurement were taken in duplicates

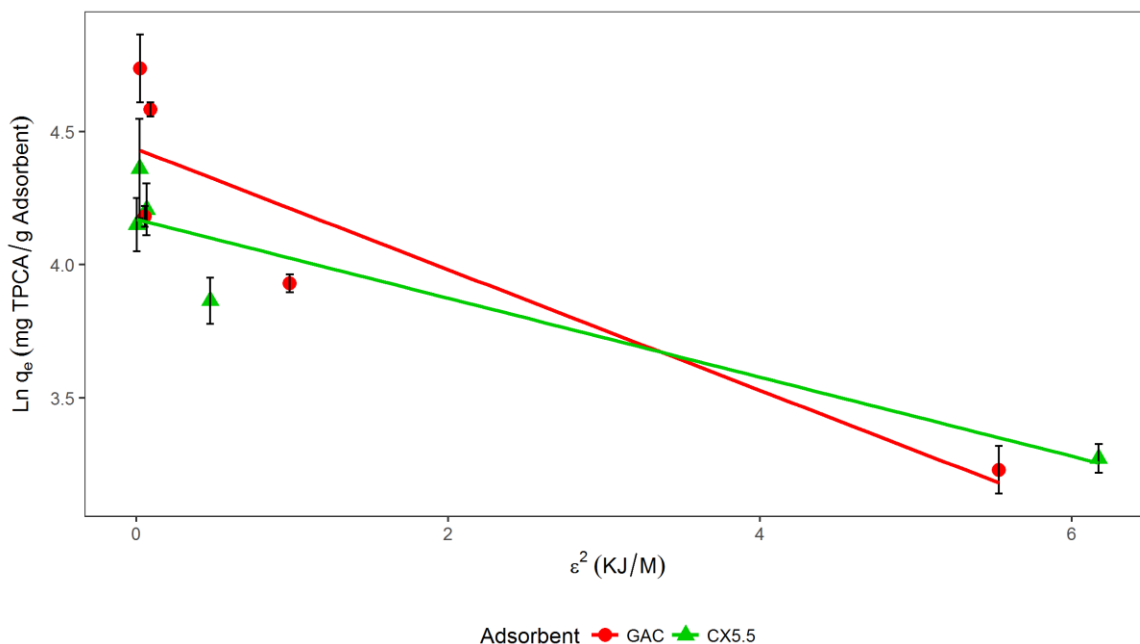


Figure 4-10 TPCA D-R isotherm for CX and GAC. Experiment conditions- total solution volume: 50 mL, shaking Speed: 210 rpm, initial concentration: 60 mg L⁻¹, adsorbents concentration: 0.5 g.L⁻¹. . All measurement were taken in duplicates

The Freundlich isotherms' R^2 were 0.82, and 0.88 for CX and GAC respectively. Values of $(1/n)$ are less than 1 for both adsorbents indicating the high affinity between the CX and GAC (adsorbents) and TPCA (the adsorbate) (Boparai et al., 2011). The D-R isotherms' R^2 were 0.87 and 0.82 for CX and GAC respectively. The activation energy was calculated for the CX and GAC and it was found to be less than 8 kJ.mol⁻¹ indicating the physio nature of the adsorption process (Lu et al., 2015; Pourrezaei et al., 2014b). Based on results, the TPCA adsorption on CX and GAC is physical monolayer adsorption, and adsorbent surface is homogenous without any interaction between adsorption sites (Sawyer et al., 2003). The maximum capacity of the CX and GAC based on Langmuir isotherm was calculated as 69.9 and 102 mg g⁻¹ respectively. Therefore, Langmuir fits best for the TPCA adsorption to the CX surface ($R^2 = 0.97$ and 0.96 for CX and GAC respectively). These results confirm the characterization data that found that the CX and GAC surface are not heteroatomic surfaces

and previous findings that studied the adsorption of NAs model compounds on the surface of activated carbons.

4.3.7. Adsorption Kinetics

To determine the adsorption kinetics, pseudo first order, and pseudo second order models were used to fit the experimental results, see equations 7 and 8. By integrating equation 7 and 8 using the limit conditions ($t = 0$ to $t=t$ and $q=0$ to $q=q_e$), linear forms can be obtained as equation 14 and 15 respectively (Zhu et al., 2011).

$$\ln(q_n - q_t) = \ln q_n - k_1 t \quad \text{Equation 14}$$

$$\frac{t}{q_t} = \frac{1}{k_2 q_n^2} + \frac{1}{q_n} t \quad \text{Equation 15}$$

where q_n is the amount of the adsorbate removed by one square meters of the adsorbent (mg TPCA removed/ m^2 of adsorbent). K_1 and q_n can be obtained from the slope and the intercept of the straight line between time and $\ln(q_n - q_t)$ as shown in Figure 4-11. For second order model (Figure 4-12), K_2 and q_n can be calculated from the slope and the intercept of the straight line between time and (t/q_t) . K_1 , K_2 , q_n from both pseudo-first order and pseudo-second order models for TPCA adsorption process on CX and GAC are shown in Table 4-5. All the results were calculated based on the normalized q (q_n). This way of calculating the q will eliminate the effect of the surface area when comparing the two adsorbents performance. As shown in Table 4-5, K_1 , the pseudo first order rate, is 0.204 and 0.142 (hr^{-1}) for CX and GAC, with R^2 of 0.98 and 0.99 respectively. These values illustrate the rate of TPCA adsorption to the CX surface is about 1.5 times faster than the adsorption to the GAC surface. For Pseudo-second order model, the rate constant (K_2) was found to be 4.146 and 1.65 ($g\ mg^{-1}hr^{-1}$) for CX and GAC, with R^2 of 0.99 and 0.96 respectively. The pseudo-second order model rate values show that the adsorption rate of TPCA on CX surface is more than 2 times faster than the rate

on GAC surface. Based on the values of experimental and modeled data, pseudo first order models fit the CX and GAC data well (ERRSQ = $1 * 10^{-4}$ and $2 * 10^{-5}$ for CX and GAC respectively and RMSE = 0.0037 and 0.00175 for CX and GAC respectively) Figure 4-13 and Figure 4-14. The difference in performance between the CX and the GAC at pseudo first and second order models can be attributed to the high mesoporosity and high pore volume of the CX compared to the GAC.

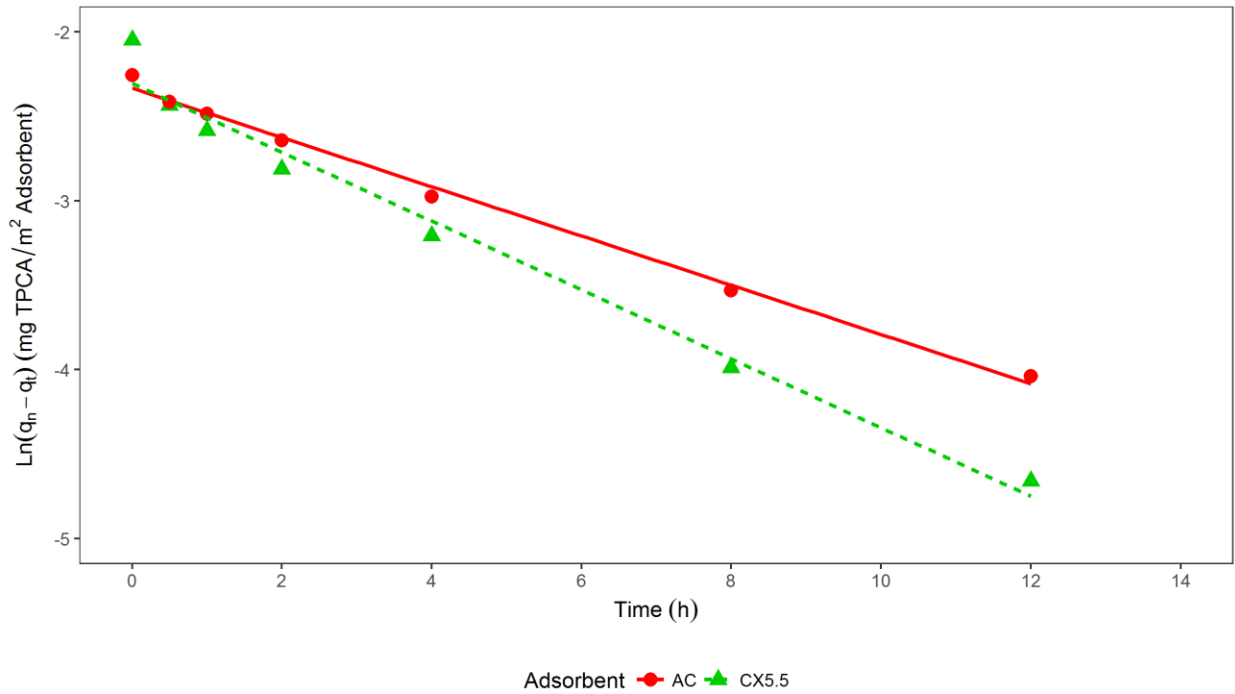


Figure 4-11 Pseudo-first-order models for CX and GAC

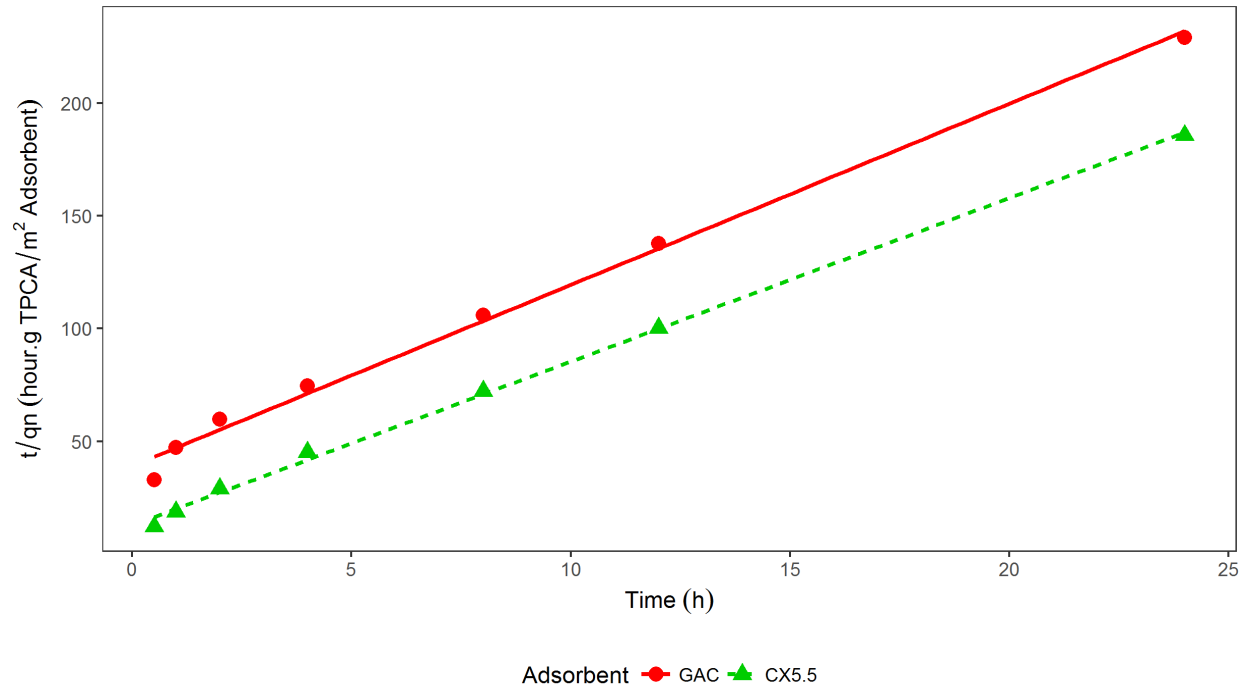


Figure 4-12 Pseudo second order model for TPCA removal using GAC and CX. Experiment conditions- total solution volume: 50 mL, shaking Speed: 210 rpm, initial concentration: 60 mg L⁻¹, adsorbents concentration: 0.5 g.L⁻¹

Table 4-5 Kinteric parametrs from first, second, bagham, and Weber-Morris models that describes the TPCA adsorption on CX and GAC

| Model | Parameter | CX | GAC |
|-------------------------------------|---|---------|---------|
| Pseudo -first-order | K_1 (hr ⁻¹) | 0.204 | 0.142 |
| | q_n calc. (mg m ⁻²) | 0.100 | 0.094 |
| | q_n (mg m ⁻²) | 0.120 | 0.100 |
| | r^2 | 0.980 | 0.990 |
| | ERRSQ | 0.00010 | 0.00002 |
| | RMSE | 0.00375 | 0.00175 |
| Pseudo -second-order | K_2 (g mg ⁻¹ hr ⁻¹) | 4.146 | 1.650 |
| | q_n calc (mg m ⁻²) | 0.138 | 0.120 |
| | q_n (mg m ⁻²) | 0.120 | 0.100 |
| | r^2 | 0.990 | 0.960 |
| | ERRSQ | 0.00021 | 0.00003 |
| | RMSE | 0.00541 | 0.00222 |
| Intraparticle Model (bangham) | K_B (mg m ⁻²) | 0.054 | 0.023 |
| | V | 0.310 | 0.530 |
| | q_n calc (mg m ⁻²) | 0.144 | 0.122 |
| | q_n (mg m ⁻²) | 0.120 | 0.100 |
| | r^2 | 0.980 | 0.980 |
| | ERRSQ | 0.00034 | 0.00040 |
| Intraparticle Model (Webber-Morris) | RMSE | 0.00697 | 0.00754 |
| | K_{int} (mg g ⁻¹ h ^{-1/2}) | 0.022 | 0.023 |
| | q_n calc (mg m ⁻²) | 0.130 | 0.113 |
| | q_n (mg m ⁻²) | 0.120 | 0.100 |
| | C [intercept] | 0.024 | 0.002 |
| | r^2 | 0.910 | 0.960 |
| Webber-Morris model-film diffusion | ERRSQ | 0.00183 | 0.00026 |
| | RMSE | 0.01615 | 0.00611 |
| | K_{id1} (mg g ⁻¹ h ^{-1/2}) | 0.043 | 0.026 |
| Webber-Morris model-pore diffusion | C [intercept] | 0.005 | -0.002 |
| | r^2 | 0.978 | 0.983 |
| | K_{id2} (mg g ⁻¹ h ^{-1/2}) | 0.013 | 0.017 |
| Webber-Morris model-pore diffusion | C [intercept] | 0.068 | 0.024 |
| | r^2 | 0.880 | 0.960 |

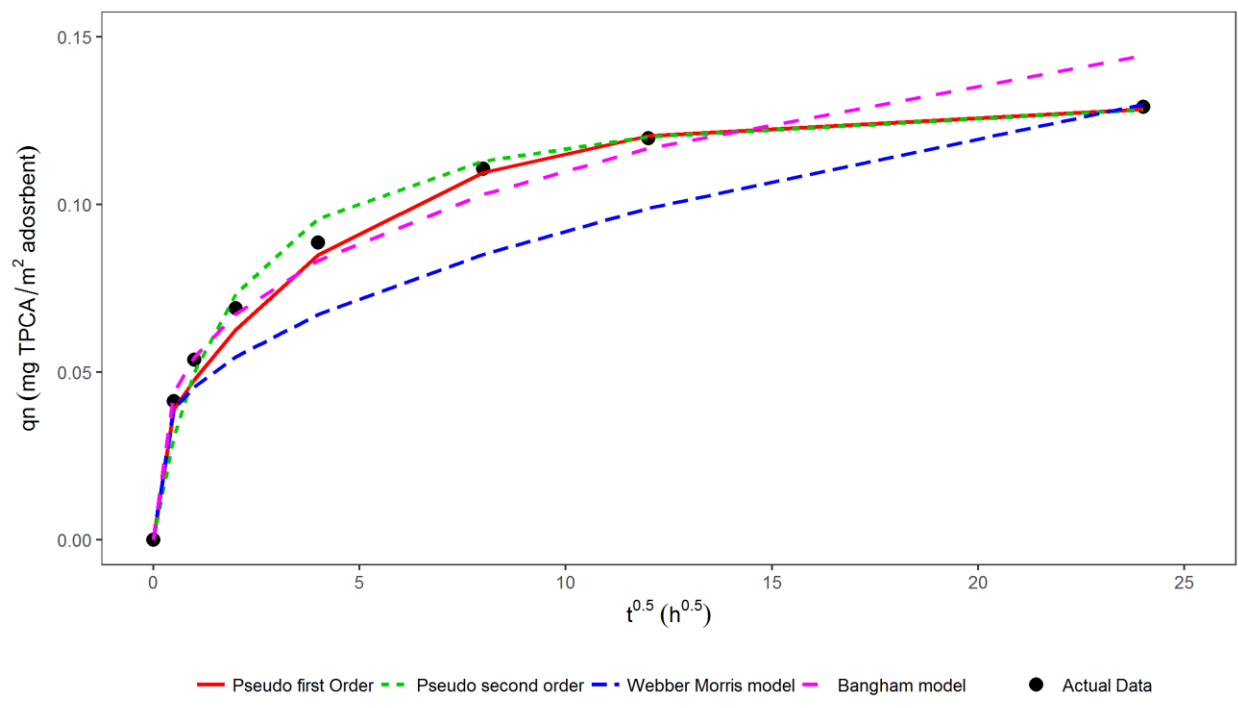


Figure 4-13 All kinetic models with the actual data for CX

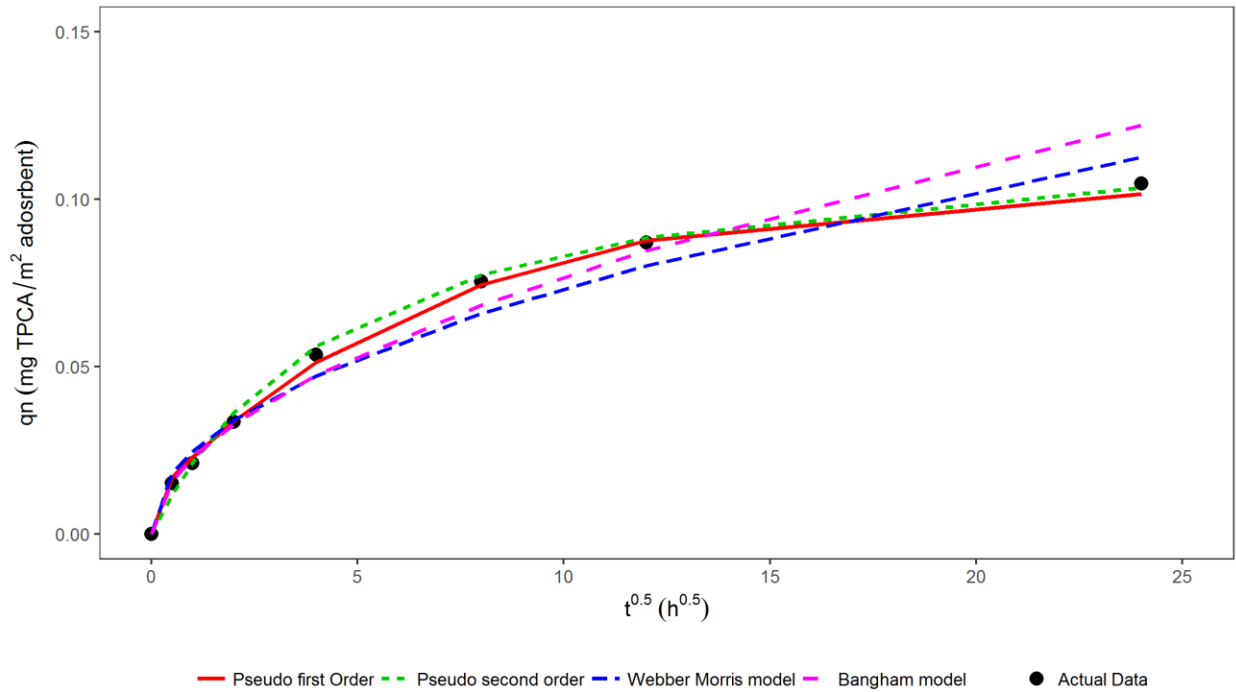


Figure 4-14 All kinetic models with the actual data for GAC

4.3.8. Intra-particle diffusion model

Four major steps are involved in the adsorption process: a) film diffusion, b) intraparticle diffusion, c) interior surface diffusion and d) adsorption to the surface. For investigating the rate limiting step for the adsorption process, two intraparticle diffusion kinetic models were fitted to the experimental data: Weber-Morris and Bingham models intra particle diffusion models. Linear form of both models is in Equation 9 and 16 respectively.

$$\ln q_t = \ln k + \vartheta \ln(t) \quad \text{Equation 16}$$

Bangham model assumes that the rate limiting step is the diffusion step (Srivastava et al., 2006). Results show that experimental data for CX and GAC fits this model with $R^2 = 0.976$ and 0.983 respectively, see Figure 4-15. Therefore, the TPCA adsorption process limiting step is the pore diffusion step (Inyinbor et al., 2016; Srivastava et al., 2006).

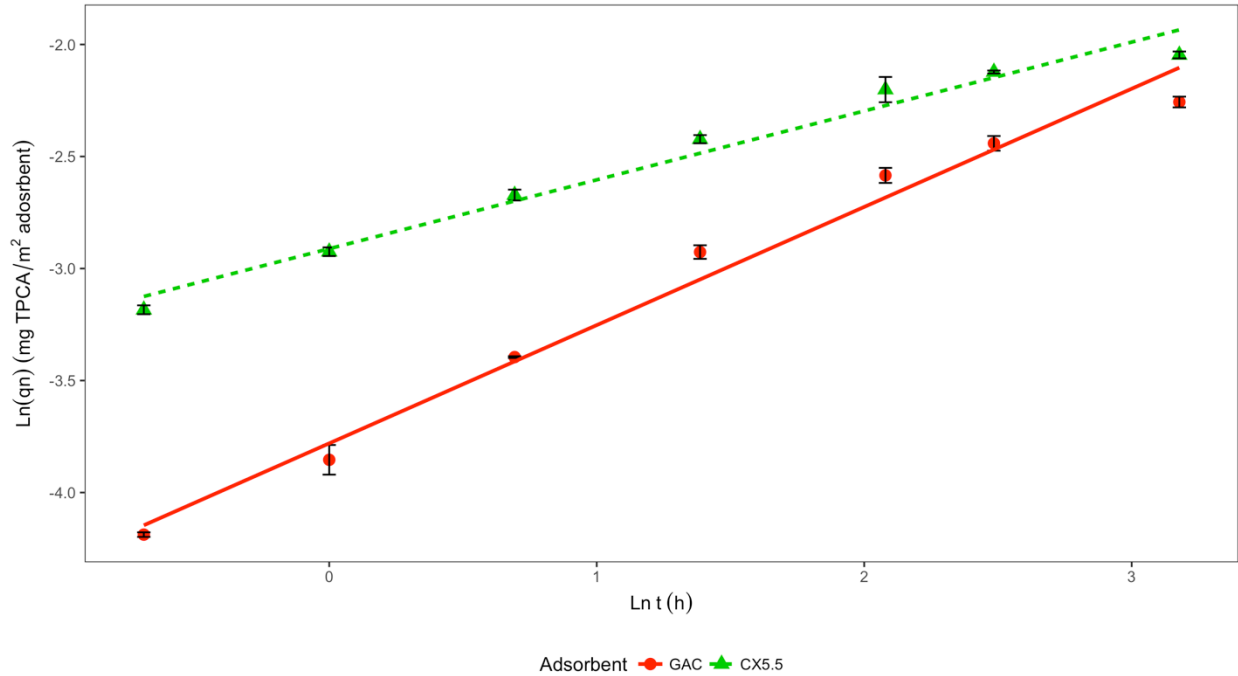


Figure 4-15 Bangham model for TPCA removal using GAC and CX. Experiment conditions- total solution volume: 50 mL, shaking Speed: 210 rpm, initial concentration: 60 mg L⁻¹, adsorbents concentration: 0.5 g L⁻¹

For better understanding the pore diffusion process, Weber-Morris model was applied on the experimental data. According to Weber-Morris model, if the intraparticle diffusion is the sole rate-limiting step, one straight line between the q_n and $t^{1/2}$ should go through the origin (Lu et al., 2015; Qiu et al., 2009). If the model's straight line didn't go through the origin, then, the diffusion of adsorbate into the pores of the adsorbent is not the only limiting step (Chowdhury et al., 2011; Onal, 2006; Srivastava et al., 2006). In case of multi-linear plot, two or more steps are significantly influencing the diffusion process (Srivastava et al., 2006). Constant C, the intercept in Equation 9, is related to the boundary layer thickness, i.e. the greater C value the greater boundary thickness (Mall et al., 2005; Onal, 2006; Srivastava et al., 2006). Results in Table 4-5 shows that the C values for CX and GAC are 0.024 and 0.002, this implies that the boundary in case of CX is greater than the GAC boundary. Therefore, the

adsorption process may be controlled by film diffusion and intra-particle diffusion synchronously. By dividing the Weber-Morris model into two separate lines, see Figure 4-16

The deviation of the line from the origin is attributed to the difference between the rate of mass transfer in the initial, which is the diffusion through the boundary layer/external film diffusion, and the final stages of the adsorption process (Srivastava et al., 2006).

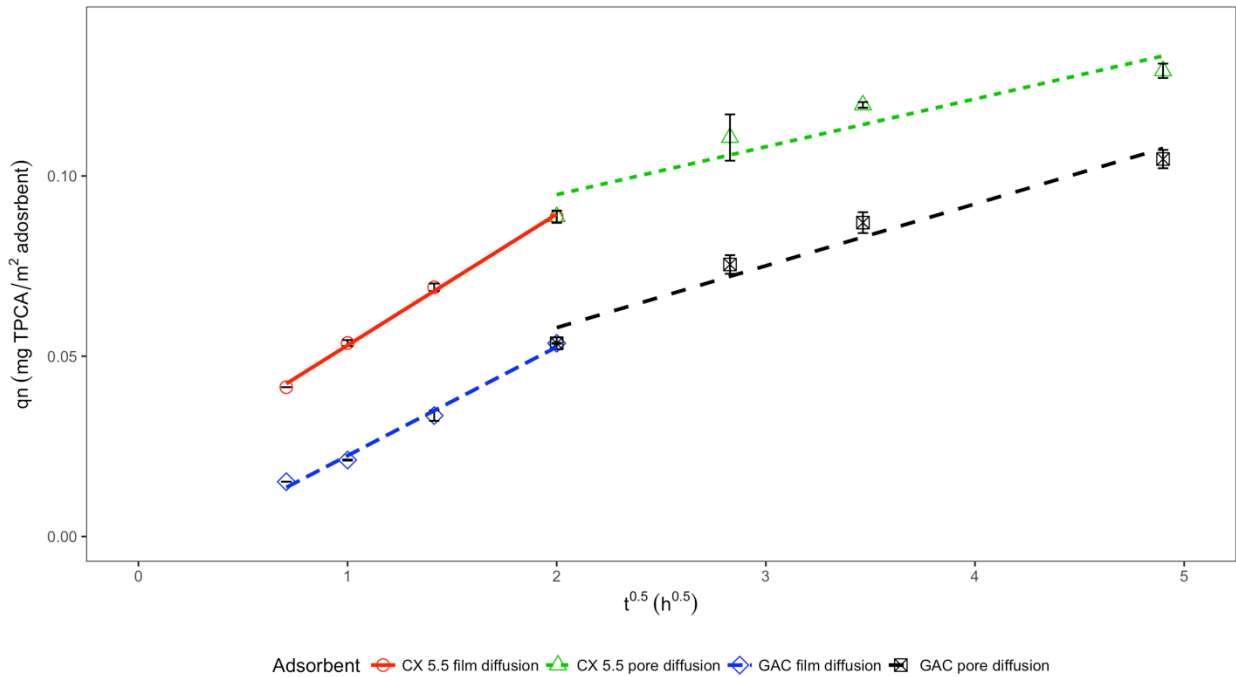


Figure 4-16 Weber-Morris model for TPCA removal using GAC and CX. Experiment conditions- total solution volume: 50 mL, shaking Speed: 210 rpm, initial concentration: 60 mg L⁻¹, adsorbents concentration: 0.5 g.L⁻¹. All measurement were taken in duplicates

The first straight line is showing the diffusion through the macropores, while the second straight line illustrates the micropores diffusion (Inyinbor et al., 2016; Srivastava et al., 2006). The film diffusion rate of the, 0.043 and 0.026 mg g⁻¹ h^{-1/2} for CX and GAC respectively, is greater than the rate of diffusion in the pores, 0.013 and 0.017 mg g⁻¹ h^{-1/2} for CX and GAC respectively as illustrated in Table 4-5. Hence, the rate limiting step is the diffusion of the

TPCA into the pores (Lu et al., 2015). The rate of film and pore diffusion on CX are faster than the GAC due to the high pore volume and mesoporosity nature of the CX.

4.3.9. Temperature effect

Temperature is a key factor that govern the adsorption process. The effect of temperature on TPCA adsorption on CX, and GAC was investigated from 4°C to 20°C. Results, Figure 4-17, show that an increase in the temperature results in an increase in the TPCA amount adsorbed to CX and GAC, which implies that the TPCA adsorption process is an endothermic process. Similar behaviour was reported with removing model naphthenic acid using activated carbon (Sarkar, 2014).

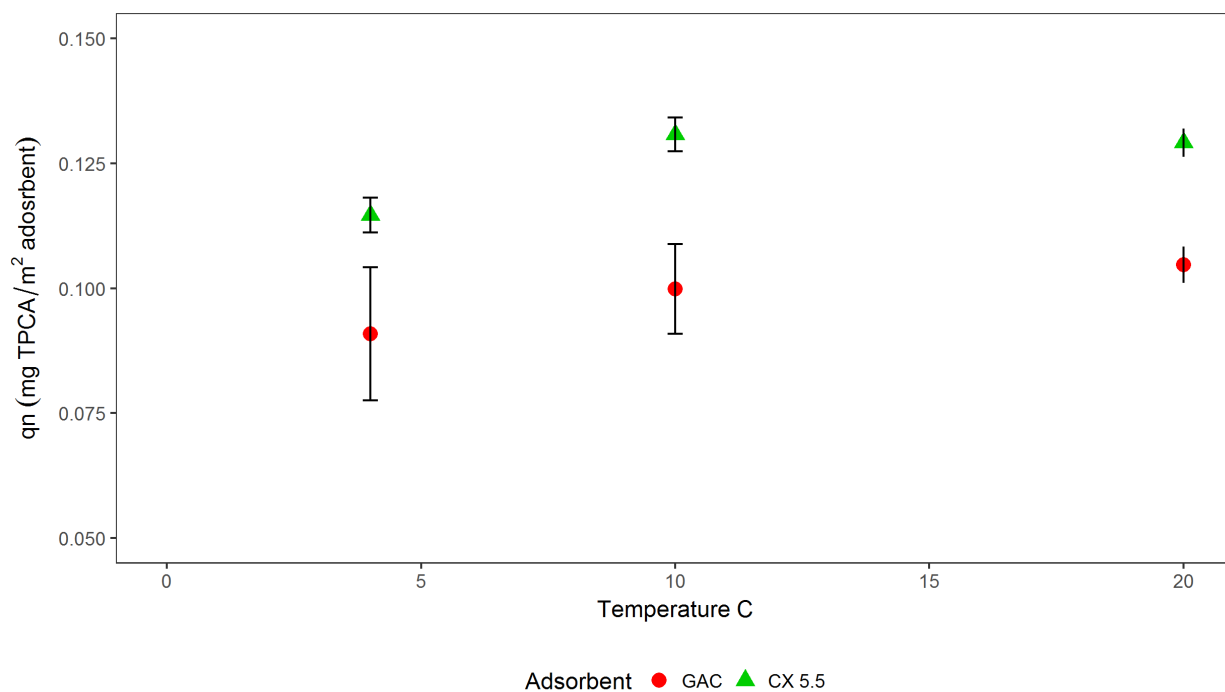


Figure 4-17 Temperature effect on q (q normalized by the adsorbent surface area) of TPCA using CX and GAC. Experiment conditions- total solution volume: 50 mL, shaking Speed: 210 rpm, initial concentration: 60 mg L⁻¹, adsorbents concentration: 0.5 g.L⁻¹. All measurement were taken in duplicates

4.3.10. Ionic strength effect

To simulate the OSPW conditions, the adsorption of TPCA was carried out in different ion strengths ranging from 0 to 0.5 M NaCl, see Figure 4-18. Results show an increase in the removal percentage with the increase of the ion strength for CX. For GAC, almost no change in the removal percentage with the increase of the ion strength. Results implies the negligible effect of the ion strength on the TPCA adsorption process on CX and GAC. The results can be explained that the adsorption is a surface phenomenon that is not affected by the ionic strength (Ipek, 2014). Similar results were shown by other studies of ionized weak acid adsorption up to 0.3 M CaCl₂, which show that the adsorption mechanism is not influenced by the ionic exchange and the adsorption process is solely accomplished using the weak Van der Waal's forces (Li et al., 2013).

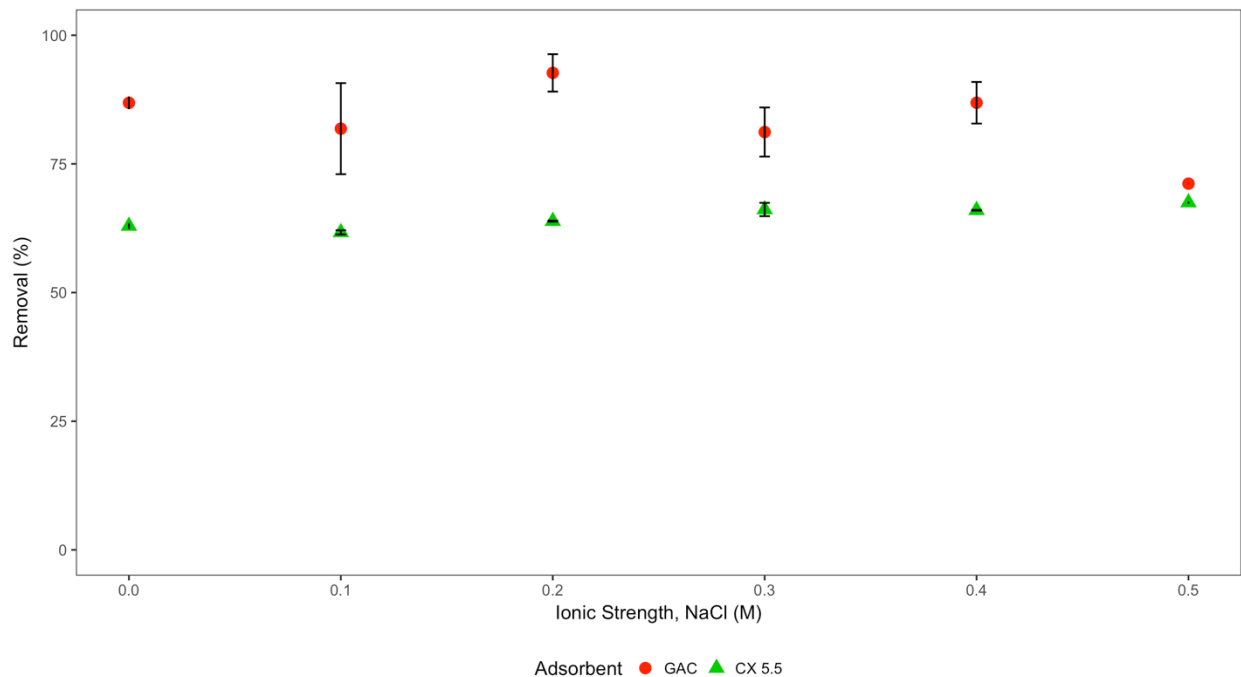


Figure 4-18 effect of ionic strength on TPCA adsorption after 24 hours using CX, and GAC. Experiment conditions- total solution volume: 50 mL, shaking Speed: 210 rpm, initial concentration: 60 mg L⁻¹, adsorbents concentration: 0.5 g.L⁻¹. All measurement were taken in duplicates

4.3.11. pH effect

Figure 4-19 shows the removal percentage of the TPCA onto CX and GAC surfaces at 3 pHs (6.5, 8, and 10). The removal percentage is higher for pH 6.5 and is about the same value for pHs 8 and 10. This may be attributed to the adsorbent surface charge. As amphoteric materials, CX and GAC surface charges are affected by the pH of the solution (Faria et al., 2004; Silva et al., 1996). Below the pH_{PZC} , the adsorbent surface charge is positive, and at pH greater than the pH_{PZC} , the adsorbent surface charge is negative, pH_{PZC} for CX and GAC are 6.7 and 6.9 respectively. On the other hand, the NA pK_a is in the range of 5-6 (Perez-Estrada et al., 2011), thus charge is negative for pH greater than the pK_a .

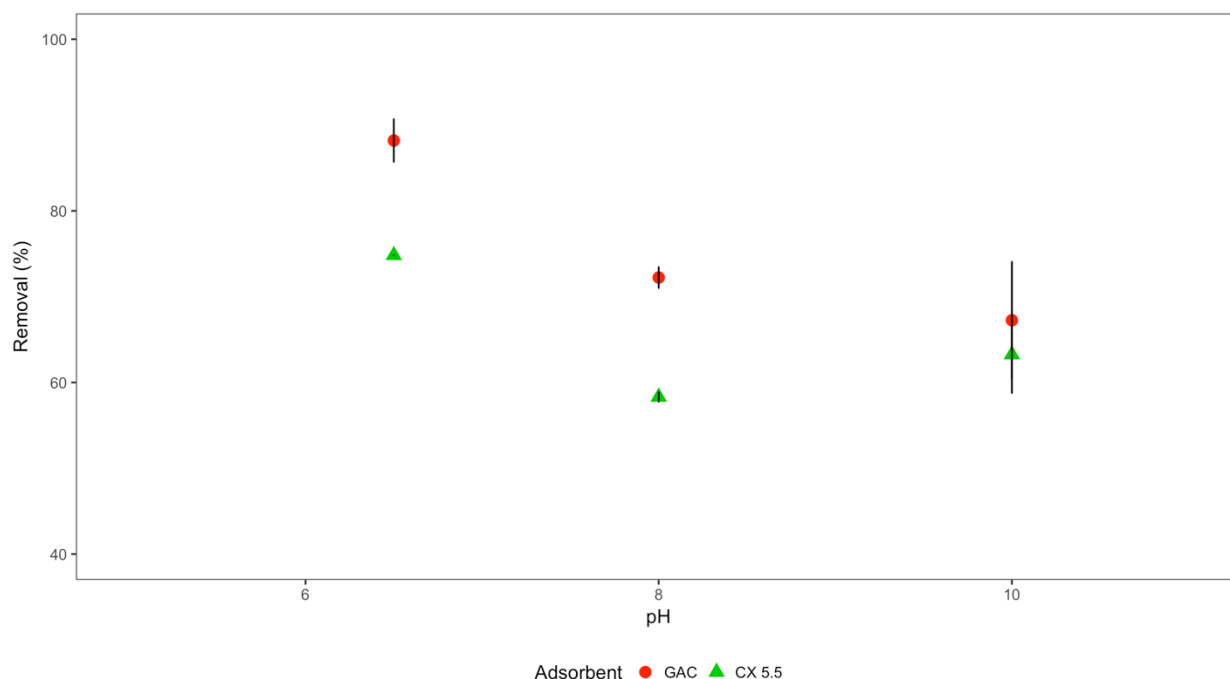


Figure 4-19 Effect of pH on TPCA adsorption after 24 hours using CX, and GAC. Experiment conditions- total solution volume: 50 mL, shaking Speed: 210 rpm, initial concentration: 60 mg L⁻¹, adsorbents concentration: 0.5 g.L⁻¹, pH =8.0. All measurement were taken in duplicates

4.3.12. Activation energy

Using the rate constant derived from pseudo second order model (K_2), activation energy can be calculated using Arrhenius equation, see Equation 11

$$K_2 = Ae^{-\frac{E_a}{RT}} \quad \text{Equation 17}$$

where K_2 is pseudo second order rate constant (g.mg⁻¹.hr⁻¹), A is the frequency factor g.mg⁻¹.hr⁻¹, E_a = Arrhenius activation energy (J.mol⁻¹), R is the universal gas constant = 8.314 J.mole⁻¹ K⁻¹, and T is the temperature in K. Linear version of this equation is shown in Equation 13.

$$\ln K_2 = \ln A - \frac{E_a}{RT} \quad \text{Equation 18}$$

Ea and A values can be obtained from the slope and the intercept of the linear relationship between $\ln K_2$ and $1/T$, see Figure 4-20. The activation energy was found to be 9.75 KJ.mol^{-1} and 1.2 KJ.mol^{-1} for CX and GAC respectively. The values of activation energy lie in the physical range ($< 40 \text{ KJ.mol}^{-1}$) (Boparai et al., 2011; Lu et al., 2015), this confirms the finding from D-R isotherm that the TPCA adsorption on the CX and GAC is a physical adsorption process. These values also imply that the adsorption process is a diffusion controlled process as the diffusion controlled processes typically have relatively small activation energy in contrast to the surface adsorption controlled processes that usually have a high value of activation energy (Chowdhury et al., 2011; Saha and Chowdhury, 2011).

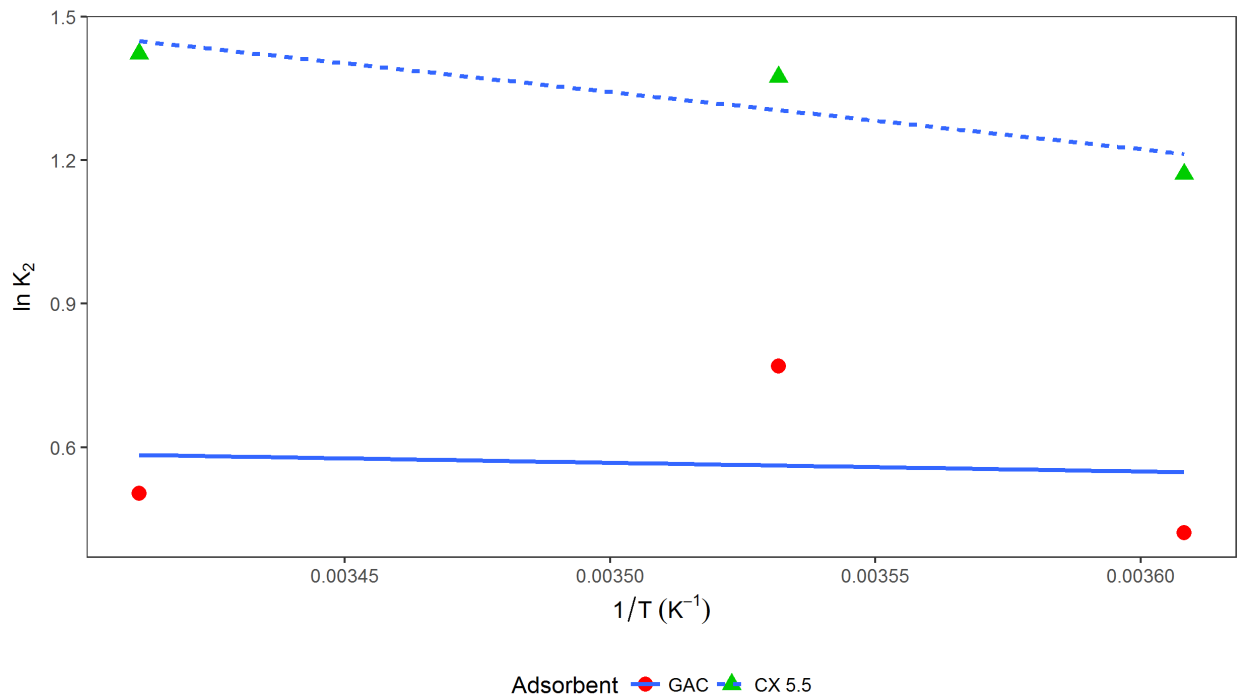


Figure 4-20 Linear Arrhenius equation $\ln K_2$ vs $1/T$

4.3.13. Thermodynamic calculations

Thermodynamic parameters such as Gibbs free energy change (ΔG^0), enthalpy change (ΔH^0), and entropy change (ΔS^0) that describes the TPCA adsorption on the CX and GAC surface can be estimated by considering the equilibrium constants. For the adsorption between TPCA and CX and GAC, the equilibrium constant (K_C) can be defined as following (Zhu et al., 2011).

$$K_C = \frac{C_{AE}}{C_e} = \frac{C_0 - C_e}{C_e} \quad \text{Equation 19}$$

Where C_{AE} = the adsorbed amount at equilibrium, C_0 = initial concentration of the adsorbate (mgL^{-1}), and C_e = the equilibrium concentration of the adsorbate (mg L^{-1}). Gibbs free energy change can be determined using the following equation:

$$\Delta G^0 = -RT \ln K_C \quad \text{Equation 20}$$

Where R is the universal gas constant $\text{Jmol}^{-1}\text{k}^{-1}$, and T is the temperature (K). Using the relationship $\Delta G^0 = \Delta H^0 - T\Delta S^0$ and equation 20, the following relationship can be determined:

$$\ln K_C = \frac{\Delta S^0}{R} - \frac{\Delta H^0}{R} * \frac{1}{T} \quad \text{Equation 21}$$

By plotting a straight line between $\ln K_C$ and $(1/T)$, see Figure 4-21 , both ΔH^0 and ΔS^0 can be calculated from the slope and the intercept respectively. ΔH^0 values were 11.1 and 31.511 KJ.mol^{-1} for CX and GAC, respectively. ΔS^0 were found to be 0.043 and 0.124 KJ.mol^{-1} for CX and GAC, respectively, Results are shown in

Table 4-6. The positive ΔH^0 values indicated the endothermic nature of the adsorption reaction of TPCA both adsorbents, and the increasing of the adsorption capacity temperature increase. The positive ΔS^0 implied the increase of the disorder at the interface between the

aqueous and solid surfaces (Boparai et al., 2011; Lu et al., 2015). For ΔG^0 , the negative values illustrate that the TPCA adsorption is a spontaneous process and the high affinity between the TPCA and both CX and GAC (Boparai et al., 2011; Lu et al., 2015; Onal, 2006; Zhu et al., 2011).

Table 4-6 Thermodynamic parameters results

| Adsorbent | 1/t (K ⁻¹) | ΔH^0 (KJ.mol ⁻¹) | ΔS^0 (KJ.mol ⁻¹) | ΔG^0 (KJ.mol ⁻¹) |
|-----------|------------------------|--------------------------------------|--------------------------------------|--------------------------------------|
| CX | 277 | 11.102 | 0.043 | -0.738 |
| | 283 | | | -0.994 |
| | 293 | | | -1.421 |
| GAC | 277 | 31.511 | 0.124 | -2.726 |
| | 283 | | | -3.467 |
| | 293 | | | -4.702 |

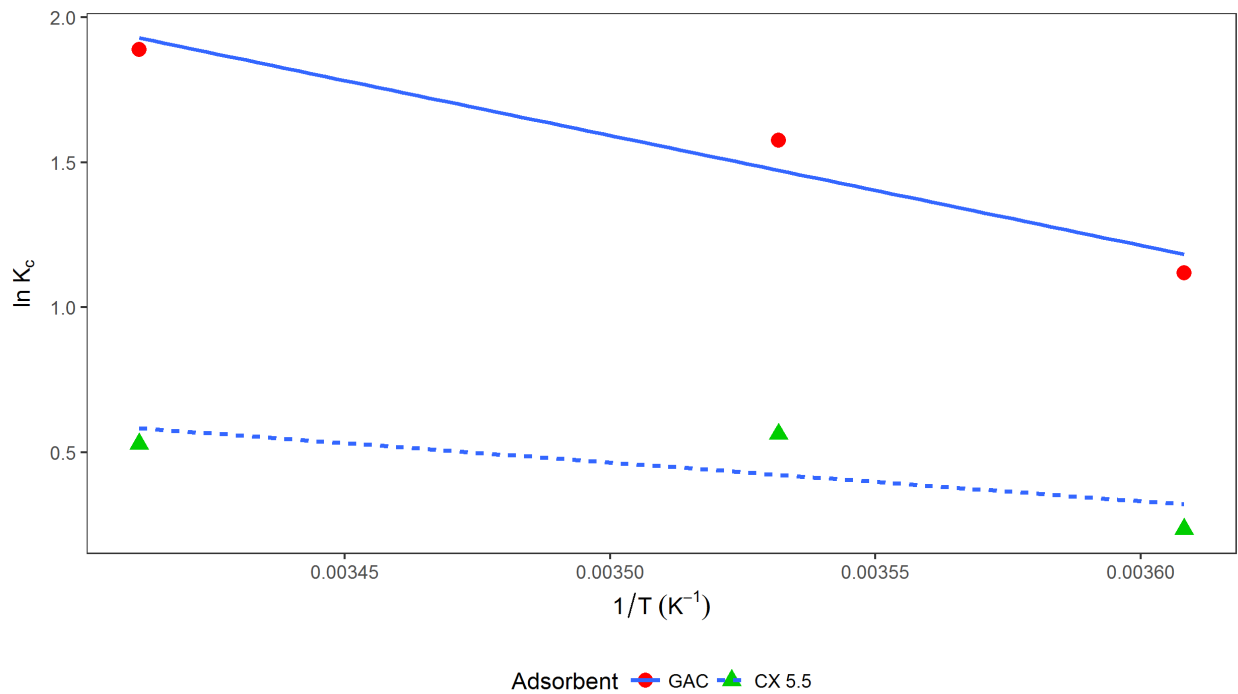


Figure 4-21 Ln Kc vs 1/T

4.3.14. Adsorption mechanism

It is hard to attribute the adsorption of organic compound from aqueous solution to simple and coherent mechanism (Bansal and Goyal, 2005a). Many factors affect the adsorption mechanism of the organic compounds from solution. For example, the hydrophobicity of the compound, the dispersive interaction between the solution and the compound, the size of the organic molecule, the porous structure of the adsorbent, the adsorbent surface charge, which is highly related to the pH_{PZC} , the hydrogen bonding between the organic molecules and the adsorbent surface (Bansal and Goyal, 2005a). Therefore, the adsorption of the organic compounds may be attributed to one or more of the following mechanisms. A) Simple electrostatic interaction, B) Dispersive interactions between the organic molecule and the π electrons of the adsorbent, C) Hydrophobic interactions and D) Hydrogen bond (Bansal and Goyal, 2005a; Moreno-Castilla, 2004; Pan and Xing, 2008; Sawyer et al., 2003). In this study, given the negative charge of both the TPCA and the surface of the two-adsorbents used herein at $pH \sim 8.0$, and the aliphatic nature of the TPCA, the first two mechanisms (electrostatic interaction and π - π bond) are excluded (Hunter and Sanders, 1990; Moreno-Castilla, 2004). In hydrophobic interaction, usually the change in the entropy (ΔS^0) is bigger than the change in the enthalpy (ΔH^0), with a total of negative change in the free Gibbs energy (ΔG^0) (Atkins and De Paula, 2006). This is not the case in this study as explained in the thermodynamic calculations section (4.3.13), the change in entropy (0.043, and 0.124 $KJ.mol^{-1}$ for CX and GAC respectively) is less than the change in enthalpy (11.1, and 31.51 $KJ.mol^{-1}$ for CX and GAC respectively) with negative change in the free Gibbs energy as illustrated in Table 4-6, . Hence, it is likely that the adsorption mechanism is the hydrogen bond.

The negative charged assisted hydrogen bond (-CAHB) was studied by Li et al. (2013) and Moustafa et al. (2014b) as a possible adsorption mechanism for removing the protonated organic acids using carbon-based adsorbent. It was concluded that the main factor that affects the adsorption of the protonated NA, such as TPCA, on the adsorbent surface is the octanol-water partitioning coefficient (K_{ow}) of both the neutral and ionized forms of the acid (Moustafa et al., 2014b). Therefore, the most possible mechanism of TPCA adsorption on the surface of CX and the GAC is the (-CAHB). Consequently, the most likely mechanisms that contribute to the adsorption of the TPCA to the surface of the CX and GAC are the hydrogen bond specially the negative assisted hydrogen bond.

4.4. Conclusion

Removal of model NAs (TPCA) from alkaline aqueous solution is quite a challenge due to the negative charge of the ionized acid as well as the negativity of the adsorbent surface. Carbon xerogel total pores volume was greater than the commercial GAC used in this experiment. Using mesoporous carbon-based xerogel, a significant removal of TPCA was achieved. The adsorption was found to be physical process with calculated Arrhenius activation energy of 10 KJ.mole^{-1} . Process kinetics follow the pseudo first order kinetics. Langmuir is the best isotherm to describe the adsorption. Webber-Morris kinetic model show that the rate limiting step is the pores diffusion step. Thermodynamic calculations affirm that the TPCA adsorption on CX and GAC surfaces is spontaneous process, with positive enthalpy and entropy and negative free Gibbs energy. The effect of the temperature (in the range of 4 to $20 \text{ }^{\circ}\text{C}$) was marginal.

The ion strength of the solution (between 0 and 0.5 M NaCl) has a minimal effect on the adsorption process. Solution pH affects the adsorbent's surface charge ($\text{pH}_{\text{PZC}} \cong 7$) and the

charge of the solute ($pK_a \cong 5$). The adsorption of ionized NAs acid on carbon-based adsorbents is affected by the K_{ow} . The findings of this research will contribute to the understanding of the adsorption process mechanism of the naphthenic acids onto carbon-based adsorbents for better developing a treatment process/train that removes such compounds, hence, reducing the OSPW toxicity and safely release to the surrounding environment.

Chapter 5 : Final Conclusions and Recommendations

5.1. Thesis summary

Releasing the OSPW to the environment in an environmentally safely manner is one of the main challenges that face the oil sands industry in northern Alberta, Canada. For long time, the toxicity of OSPW was mainly attributed to NAs. Till today, there is no standard method in place which universally used to identify and quantify the NAs in environmental samples. However, many methods are used to estimate the NAs in environmental samples such as FTIR, UPLC-TOFMS. Sample preparation, chemical standard, as well as the sample type are affecting the results of both methods. On preparation for developing a standard method that may universally use in identifying and quantifying the NAs, a comparison between the two methods and the impact of previously mentioned factors on the NAs quantification is studied in chapter 2. Results show that the FTIR (using LLE and Fluka NA standard) can be used as a surrogate and/or screening parameter for the UPLC-TOFMS, and it was suggested for routine monitoring of the OSPW in the field as well as evaluation method for treatment of the OSPW. In chapter 3, more deep research was conducted using statistical methods on the effect of the sample type, chemical standard and preparation method on the FTIR results. Chapter 3 aimed at developing statistically significant relationship between different FTIR results so the results that was published using different preparation method or/and chemical standard can be related to each other and compiled in one database for comparison. Chapter 4 focused on removing NAs model compound (TPCA) from form alkaline solution (pH ~ 8) using adsorption on the surface of CX. The isotherm, kinetics and thermodynamics of the process were studied. Also, the effect of pH, temperature, and ion strength was investigated.

5.2. Conclusions Summary

Based on the results, it can be concluded that using the SPE method in the OSPW sample pre-treatment yielded higher concentrations compared to LLE regardless of the water sample type (GW and OSPW) and quantification method (FTIR and TPLC-TOFMS). This conclusion is supported by the findings that the SPE concentrations were found to be 1.0 to 1.4 folds higher than the LLE results. On the other hand, LLE results yielded O₂ species concentrations in the extracted NAs higher than those of the SPE results. The difference in the O₂ species concentration can be attributed to the hydrophobicity that leads to higher concentration of O₂ to move from the water phase to the organic phase (DCM). The difference between the concentrations of Fluka and OSPW extract NAs standards is a direct result of the difference in NAs species distribution between the Fluka and the OSPW NAs standards. Apart from the differences between the concentrations of the Fluka and the OSPW NAs standards, a strong correlation between the NAs results measured using FTIR and UPLC-TOFMS calibrated with Fluka NAs and OSPW extracted standards. The strong correlation shows the possibility of using the FTIR results as a surrogate for UPLC-TOFMS results calibrated using the Fluka and OSPW extracted standard.

Focusing more on the FTIR method as suggested surrogate method for the UPLC-TOFMS, the non-parametric statistical analysis shows that the primary factor differentiating between the samples is the sampling location and sample water type (GW and OSPW). The highest concentration of all samples was found to be the result with SPE separation and calibrated using the OSPW extract NAs standard. The lowest results were obtained using the LLE separation and Fluka standard NAs. Results measured using the OSPW extract standard NAs

were found about 2.5 times higher than those of the Fluka NAs standards. For the difference between the SPE and LLE separation method, the SPE results were about 1.37 times higher in magnitude than the LLE results.

SPE method of separation, which is based on the adsorption process, was found to be effective in separating the NAs from the OSPW samples. Therefore, the adsorption process was selected for removing the NAs from the OSPW samples. NAs model compound (TPCA) removal from alkaline solution using the CX was found to be a spontaneous physical process as evident by the activation energy ($9.75 \text{ KJ.mole}^{-1}$), and thermodynamic calculations. Langmuir is the best isotherm to describe the TPCA removal process using the CX. The adsorption is a pseudo second order process and the rate limiting step is the diffusion. The effect of temperature and ion strength on the adsorption process is not significant while the pH effect is significant. These conclusions will enhance our understanding to the NAs removal process using the adsorption process and may contribute to the effort of developing treatment train for the OSPW which will be an important step towards the safely and environmentally friendly release of the OSPW to the environment.

5.3. Recommendations and future work

For quantifying the NAs in OSPW sample, it is recommended to use the SPE as a pre-treatment method for all environmental samples as SPE results are repeatable and it has maximum recovery when it is compared with the LLE method. Moreover, it is recommended to use the FTIR as standard as surrogate parameter for screening purposes and/or as evaluation parameter for routine monitoring programs. Also, FTIR method can be used in evaluating the efficiency of water treatment methods and reclamation for environmental samples that may have NAs present in it.

Based on the statistical analysis performed in chapter 3, it is recommended to take into consideration the difference between the pre-treatment methods as well as the standards used in calibration when comparing two sets of results from the literature. Also, it is highly advisable that one database should be developed to compile all NAs results taking into consideration the difference due to pre-treatment, chemical standards, and water sample type. These comparisons can be considered as one step towards establishing a universal standard method for identifying and quantifying the NAs in the environmental samples.

The findings of this work are a step that may help in developing a universal method for identifying and quantifying the NAs that can be used as standard in environmental and industrial water quality monitoring programs as well as for evaluating the wastewater treatment that may contain NAs as a pollutant.

CX as an adsorbent material is a good alternative to treat any processed water as it has a higher mesoporous volume and wide pore diameter. It is recommended to functionalize the CX surface to evaluate the effect of introducing more functional groups to the CX surface (surface chemistry) in removing the NAs from the alkaline water samples. Also, it is recommended to evaluate the CX

potential in removing the NAs from a complex water matrix, such as Fluka commercial NAs and the real processed water samples.

References

- ACR-Alberta. Oil sands Technology Roadmap: Unlocking the potential. Alberta Chamber of Resources, 2004.
- Afzal A, Drzewicz P, Martin JW, El-Din MG. Decomposition of cyclohexanoic acid by the UV/H₂O₂ process under various conditions. *Science of the Total Environment* 2012; 426: 387-392.
- Ahmad R, Kumar R. Adsorption studies of hazardous malachite green onto treated ginger waste. *Journal of Environmental Management* 2010; 91: 1032-1038.
- Alberta, School of Energy and the Environment, Edmonton, Alberta, 2012, pp. 65.
- Alberta-Government. Alberta oil sands Fact sheet Alberta Government, 2014.
- Alberta-Government. Fact sheet- Talk about oil Sands, 2013.
- Allen EW. Process water treatment in Canada's oil sands industry: I. Target pollutants and treatment objectives. *Journal of Environmental Engineering and Science* 2008a; 7: 123-138.
- Allen EW. Process water treatment in Canada's oil sands industry: II. A review of emerging technologies. *Journal of Environmental Engineering and Science* 2008b; 7: 499-524.
- Alpatova A, Kim ES, Sun XH, Hwang G, Liu Y, El-Din MG. Fabrication of porous polymeric nanocomposite membranes with enhanced anti-fouling properties: Effect of casting composition. *Journal of Membrane Science* 2013; 444: 449-460.
- Anderson J, Wiseman SB, Moustafa A, El-Din MG, Liber K, Giesy JP. Effects of exposure to oil sands process-affected water from experimental reclamation ponds on *Chironomus dilutus*. *Water Research* 2012a; 46: 1662-1672.

- Anderson JC, Wiseman SB, Wang N, Moustafa A, Perez-Estrada L, El-Din MC, et al. Effectiveness of Ozonation Treatment in Eliminating Toxicity of Oil Sands Process-Affected Water to *Chironomus dilutus*. *Environmental Science & Technology* 2012b; 46: 486-493.
- Armstrong SA, Headley JV, Peru KM, Germida JJ. Phytotoxicity of oil sands naphthenic acids and dissipation from systems planted with emergent aquatic macrophytes. *Journal of Environmental Science and Health Part a-Toxic/Hazardous Substances & Environmental Engineering* 2008; 43: 36-42.
- Atkins PW, De Paula J. *Physical chemistry for the life sciences*. Oxford, U New York: Oxford University Press ; W.H. Freeman, 2006.
- Azad FS, Abedi J, Iranmanesh S. Removal of naphthenic acids using adsorption process and the effect of the addition of salt. *Journal of Environmental Science and Health Part a-Toxic/Hazardous Substances & Environmental Engineering* 2013; 48: 1649-1654.
- Bansal RC, Goyal G. *Activated Carbon Adsorption and Environment*. *Activated Carbon Adsorption*. CRC Press, 2005a, pp. 297-371.
- Bansal RC, Goyal G. *Activated Carbon and Its Surface Structure*. *Activated Carbon Adsorption*. CRC Press, 2005a, pp. 1-65.
- Bansal RC, Goyal G. *Adsorption Energetics, Models, and Isotherm Equations*. *Activated Carbon Adsorption*. CRC Press, 2005c, pp. 67-143.
- Bansal RC, Goyal M. *Activated carbon adsorption / Roop Chand Bansal, Meenakshi Goyal: Boca Raton : Taylor & Francis, 2005., 2005c.*

- Barrow MP, Headley JV, Peru KM, Derrick PJ. Fourier transform ion cyclotron resonance mass spectrometry of principal components in oilsands naphthenic acids. *Journal of Chromatography A* 2004; 1058: 51-59.
- Barrow MP, Peru KM, Fahlman B, Hewitt LM, Frank RA, Headley JV. Beyond Naphthenic Acids: Environmental Screening of Water from Natural Sources and the Athabasca Oil Sands Industry Using Atmospheric Pressure Photoionization Fourier Transform Ion Cyclotron Resonance Mass Spectrometry. *Journal of The American Society for Mass Spectrometry* 2015; 26: 1508-1521.
- Barrow MP, Witt M, Headley JV, Peru KM. Athabasca Oil Sands Process Water: Characterization by Atmospheric Pressure Photoionization and Electrospray Ionization Fourier Transform Ion Cyclotron Resonance Mass Spectrometry. *Analytical Chemistry* 2010; 82: 3727-3735.
- Bataineh M, Scott AC, Fedorak PM, Martin JW. Capillary HPLC/QTOF-MS for characterizing complex naphthenic acid mixtures and their microbial transformation. *Analytical Chemistry* 2006; 78: 8354-8361.
- Benjamin MM. *Water Chemistry* / Mark M. Benjamin: Long Grove, IL : Waveland Press, 2010., 2010.
- Bermudez JM, Beneroso D, Rey-Raap N, Arenillas A, Menendez JA. Energy consumption estimation in the scaling-up of microwave heating processes. *Chemical Engineering and Processing* 2015; 95: 1-8.
- Board ERC. Energy Resources Conservation Board Tailings Management Assessment Report:Oil

- Bonnefous JL, Boulieu R. Comparison of Solid-Phase Extraction and Liquid-Liquid Extraction Methods for Liquid Chromatographic Determination of Diltiazem and its Metabolites in Plasma. *Journal of Liquid Chromatography* 1990; 13: 3799-3807.
- Boparai HK, Joseph M, O'Carroll DM. Kinetics and thermodynamics of cadmium ion removal by adsorption onto nano zerovalent iron particles. *Journal of Hazardous Materials* 2011; 186: 458-465.
- Bowman DT, Slater GF, Warren LA, McCarry BE. Identification of individual thiophene-, indane-, tetralin-, cyclohexane-, and adamantane-type carboxylic acids in composite tailings pore water from Alberta oil sands. *Rapid Communications in Mass Spectrometry* 2014; 28: 2075-2083.
- Brown LD, Perez-Estrada L, Wang N, El-Din MG, Martin JW, Fedorak PM, et al. Indigenous microbes survive in situ ozonation improving biodegradation of dissolved organic matter in aged oil sands process-affected waters. *Chemosphere* 2013; 93: 2748-2755.
- Brown LD, Ulrich AC. Oil sands naphthenic acids: A review of properties, measurement, and treatment. *Chemosphere* 2015; 127: 276-290.
- CAPP. The fact on oil sands, 2015.
- Chowdhury S, Mishra R, Saha P, Kushwaha P. Adsorption thermodynamics, kinetics and isosteric heat of adsorption of malachite green onto chemically modified rice husk. *Desalination* 2011; 265: 159-168.
- Clemente JS, Fedorak PM. A review of the occurrence, analyses, toxicity, and biodegradation of naphthenic acids. *Chemosphere* 2005: 585.
- Dean JA. *Analytical Chemistry Handbook*: McGraw-Hill, 1995.

- Edzwald J. *Water Quality & Treatment: A Handbook on Drinking Water*: mcgraw-Hill Education, 2010.
- El-Din MG, Fu HJ, Wang N, Chelme-Ayala P, Perez-Estrada L, Drzewicz P, et al. Naphthenic acids speciation and removal during petroleum-coke adsorption and ozonation of oil sands process-affected water. *Science of the Total Environment* 2011; 409: 5119-5125.
- Energy Resources Conservation Board (2012) Energy Resources Conservation Board Tailings Management Assessment Report: Oil Sands Mining Industry , (posted date: June 12, 2013), from Alberta Energy Regulator, Accessed online April 2017: <http://osipfiles.alberta.ca/datasets/158/TailingsManagementAssessmentReport2011-2012.pdf>.
- Faria PCC, Orfao JJM, Pereira MFR. Adsorption of anionic and cationic dyes on activated carbons with different surface chemistries. *Water Research* 2004; 38: 2043-2052.
- Farsad A, Ahmadpour A, Bastami TR, Yaqubzadeh A. Synthesis of strong silica aerogel by PEDS at ambient conditions for adsorptive removal of para-dichlorobenzene from water. *Journal of Sol-Gel Science and Technology* 2017; 84: 246-257.
- Frank RA, Milestone CB, Rowland SJ, Headley JV, Kavanagh RJ, Lengger SK, et al. Assessing spatial and temporal variability of acid-extractable organics in oil sands process-affected waters. *Chemosphere* 2016; 160: 303-313.
- Frank RA, Roy JW, Bickerton G, Rowland SJ, Headley JV, Scarlett AG, et al. Profiling Oil Sands Mixtures from Industrial Developments and Natural Groundwaters for Source Identification. *Environmental Science & Technology* 2014; 48: 2660-2670.

- Gamal El-Din M, Fu HJ, Wang N, Chelme-Ayala P, Perez-Estrada L, Drzewicz P, et al. Naphthenic acids speciation and removal during petroleum-coke adsorption and ozonation of oil sands process-affected water. *Sci. Total Environ.* 2011a; 409: 5119-5125.
- Garcia-Garcia E, Ge JQ, Oladiran A, Montgomery B, El-Din MG, Perez-Estrada LC, et al. Ozone treatment ameliorates oil sands process water toxicity to the mammalian immune system. *WATER RESEARCH* 2011; 45: 5849-5857.
- Garcia-Garcia E, Pun J, Hodgkinson J, Perez-Estrada LA, El-Din MG, Smith DW, et al. Commercial naphthenic acids and the organic fraction of oil sands process water induce different effects on pro-inflammatory gene expression and macrophage phagocytosis in mice. *Journal of Applied Toxicology* 2012; 32: 968-979.
- GC. Oil Sands: A strategic resources for Canada, north America and global markets. Tailing management, Government of Canada website, 2015.
- Goel J, Kadirvelu K, Rajagopal C, Garg VK. Investigation of adsorption of lead, mercury and nickel from aqueous solutions onto carbon aerogel. *Journal of Chemical Technology and Biotechnology* 2005; 80: 469-476.
- Grewer DM, Young RF, Whittal RM, Fedorak PM. Naphthenic acids and other acid-extractables in water samples from Alberta: What is being measured? *Sci. Total Environ.* 2010b; 408: 5997-6010.
- Hadizade G, Binaeian E, Emami MRS. Preparation and characterization of hexagonal mesoporous silica/polyacrylamide nanocomposite capsule (PAM-HMS) for dye removal from aqueous solutions. *Journal of Molecular Liquids* 2017; 238: 499-507.

- Hagen MO, Katzenback BA, Islam MDS, El-Din MG, Belosevic M. The Analysis of Goldfish (*Carassius auratus* L.) Innate Immune Responses After Acute and Subchronic Exposures to Oil Sands Process-Affected Water. *Toxicological Sciences* 2014a; 138: 59-68.
- Han XM, MacKinnon MD, Martin JW. Estimating the in situ biodegradation of naphthenic acids in oil sands process waters by HPLC/HRMS. *Chemosphere* 2009; 76: 63-70.
- Han XM, Scott AC, Fedorak PM, Bataineh M, Martin JW. Influence of molecular structure on the biodegradability of naphthenic acids. *Environmental Science & Technology* 2008; 42: 1290-1295.
- He Y, Patterson S, Wang N, Hecker M, Martin JW, El-Din MG, et al. Toxicity of untreated and ozone-treated oil sands process-affected water (OSPW) to early life stages of the fathead minnow (*Pimephales promelas*). *Water Research* 2012; 46: 6359-6368.
- Headley JV, Du JL, Peru KM, McMartin DW. Electrospray ionization mass spectrometry of the photodegradation of naphthenic acids mixtures irradiated with titanium dioxide. *J. of Environ.l Sci. and Health Part A* 2009; 44: 591-597.
- Headley JV, Kumar P, Dalai A, Peru KM, Bailey J, McMartin DW, et al. Fourier Transform Ion Cyclotron Resonance Mass Spectrometry Characterization of Treated Athabasca Oil Sands Processed Waters. *Energy & Fuels* 2015; 29: 2768-2773.
- Headley JV, mcmartin DW. A Review of the Occurrence and Fate of Naphthenic Acids in Aquatic Environments. *Journal of Environmental Science & Health, Part A: Toxic/Hazardous Substances & Environmental Engineering* 2004; 39: 1989-2010.
- Headley JV, Peru KM, Adenugba AA, Du J-L, McMartin DW. Dissipation of naphthenic acids mixtures by lake biofilms. *J. of Environ. Sci.and Health, Part AJ. of Environ. Sci.and Health, Part A* 2010a; 45: 1027-1036.

- Headley JV, Peru KM, Fahlman B, Colodey A, McMartin DW. Selective solvent extraction and characterization of the acid extractable fraction of Athabasca oils sands process waters by Orbitrap mass spectrometry. *International Journal of Mass Spectrometry* 2013b; 345–347: 104-108.
- Headley JV, Peru KM, Mishra S, Meda V, Dalai AK, McMartin DW, et al. Characterization of oil sands naphthenic acids treated with ultraviolet and microwave radiation by negative ion electrospray Fourier transform ion cyclotron resonance mass spectrometry. *Rapid Commun. Mass Spectrom.* 2010c; 24: 3121-3126.
- Headley JV, Peru KM, Mohamed MH, Frank RA, Martin JW, Hazewinkel RRO, et al. Chemical fingerprinting of naphthenic acids and oil sands process waters A review of analytical methods for environmental samples. *Journal of Environmental Science and Health Part a-Toxic/Hazardous Substances & Environmental Engineering* 2013b; 48: 1145-1163.
- Hindle R, Noestheden M, Peru K, Headley J. Quantitative analysis of naphthenic acids in water by liquid chromatography-accurate mass time-of-flight mass spectrometry. *J. Chroma. A* 2013; 1286: 166-174.
- Huang R, McPhedran KN, Gamal El-Din M. Ultra Performance Liquid Chromatography Ion Mobility Time-of-Flight Mass Spectrometry Characterization of Naphthenic Acids Species from Oil Sands Process-Affected Water. *Environ. Sci. Technol.* 2015a.
- Huang R, Sun N, Chelme-Ayala P, McPhedran KN, Changelov M, Gamal El-Din M. Fractionation of oil sands-process affected water using pH-dependent extractions: A study of dissociation constants for naphthenic acids species. *Chemosphere* 2015b; 127: 291-296.

- Hughes SA, Mahaffey A, Shore B, Baker J, Kilgour B, Brown C, et al. Using Ultrahigh-Resolution Mass Spectrometry and Toxicity Identification Techniques to Characterize the Toxicity of Oil Sands Process-Affected Water: the Case for Classical Naphthenic Acids. *Environmental Toxicology and Chemistry* 2017; n/a-n/a.
- Hunter CA, Sanders jkm. The nature of pi-pi interactions. *Journal of the American Chemical Society* 1990; 112: 5525-5534.
- Hwang G, Dong T, Islam MS, Sheng ZY, Perez-Estrada LA, Liu Y, et al. The impacts of ozonation on oil sands process-affected water biodegradability and biofilm formation characteristics in bioreactors. *Bioresource Technology* 2013; 130: 269-277.
- Inyinbor AA, Adekola FA, Olatunji GA. Kinetics, isotherms and thermodynamic modeling of liquid phase adsorption of Rhodamine B dye onto *Raphia hookerie* fruit epicarp. *Water Resources and Industry* 2016; 15: 14-27.
- Ipek IY. Application of Kinetic, Isotherm, and Thermodynamic Models for Atrazine Adsorption on Nanoporous Polymeric Adsorbents. *Separation Science and Technology* 2014; 49: 2358-2365.
- Iranmanesh S, Harding T, Abedi J, Seyedeyn-Azad F, Layzell DB. Adsorption of naphthenic acids on high surface area activated carbons. *Journal of Environmental Science and Health Part a-Toxic/Hazardous Substances & Environmental Engineering* 2014; 49: 913-922.
- Islam MS, Moreira J, Chelme-Ayala P, Gamal El-Din M. Prediction of naphthenic acid species degradation by kinetic and surrogate models during the ozonation of oil sands process-affected water. *Science of the Total Environment* 2014; 493: 282-290.

- Islam S, Tumpa F, Xue JK, Huang CK, Sharma K, Shi YJ, et al. Biological Fixed Film. *Water Environment Research* 2014b; 86: 1070-1100.
- Janfada A, Hheadley J, Peru K, Barbour S. A Laboratory Evaluation of the Sorption of Oil Sands Naphthenic Acids on Organic Rich Soils. *Journal of Environmental Science & Health, Part A: Toxic/Hazardous Substances & Environmental Engineering* 2006; 41: 985-997.
- Jensen-Fontaine M. Vanadium Speciation In Samples Relevant To The Athabasca Oil Sands Region. In: Jensen-Fontaine M, Alberta U, editors. 52, 2012.
- Jivraj MN, MacKinnon M, Fung B. Naphthenic acids extraction and quantitative analyses with FT-IR spectroscopy. *Syncrude Analytical Methods Manual*, fourth ed. Syncrude Canada Ltd. Research Department, Edmonton, AB. 1995.
- Job N, They A, Pirard R, Marien J, Kocon L, Rouzaud JN, et al. Carbon aerogels, cryogels and xerogels: Influence of the drying method on the textural properties of porous carbon materials. *Carbon* 2005; 43: 2481-2494.
- Jones D, West CE, Scarlett AG, Frank RA, Rowland SJ. Isolation and estimation of the 'aromatic' naphthenic acid content of an oil sands process-affected water extract. *Journal of Chromatography A* 2012; 1247: 171-175.
- Juhascik MP, Jenkins AJ. Comparison of Liquid/Liquid and Solid-Phase Extraction for Alkaline Drugs. *Journal of Chromatographic Science* 2009; 47: 553-557.
- Kannel PR, Gan TY. Naphthenic acids degradation and toxicity mitigation in tailings wastewater systems and aquatic environments: A review. *Journal of environmental*

science and health part a-toxic/hazardous substances & environmental engineering 2012; 47: 1-21.

Kim ES, Liu Y, El-Din MG Evaluation of Membrane Fouling for In-Line Filtration of Oil Sands Process-Affected Water: The Effects of Pretreatment Conditions. Environmental Science & Technology 2012; 46: 2877-2884.

Kim ES, Liu Y, El-Din MG The effects of pretreatment on nanofiltration and reverse osmosis membrane filtration for desalination of oil sands process-affected water. Separation and Purification Technology 2011; 81: 418-428.

Klamerth N, Moreira J, Li C, Singh A, McPhedran KN, Chelme-Ayala P, et al. Effect of ozonation on the naphthenic acids' speciation and toxicity of pH-dependent organic extracts of oil sands process-affected water. Science of the Total Environment 2015; 506: 66-75.

Li XY, Pignatello JJ, Wang YQ, Xing BS. New Insight into Adsorption Mechanism of Ionizable Compounds on Carbon Nanotubes. Environmental Science & Technology 2013; 47: 8334-8341.

Liang XM, Zhu XD, Butler EC. Comparison of four advanced oxidation processes for the removal of naphthenic acids from model oil sands process water. Journal of Hazardous Materials 2011; 190: 168-176.

Lowell S. Characterization of porous solids and powders : surface area, pore size, and density / by S. Lowell ... [et al.]: Dordrecht ; Boston : Springer, c2006., 2006.

Lu X, Caps R, Fricke J, Alviso CT, Pekala RW. Correlation Between Structure And Thermal-Conductivity Of Organic Aerogels. Journal of Non-Crystalline Solids 1995; 188: 226-234.

- Lu X, Shao YS, Gao NY, Ding L. Equilibrium, Thermodynamic, and Kinetic Studies of the Adsorption of 2,4-Dichlorophenoxyacetic Acid from Aqueous Solution by MIEX Resin. *Journal of Chemical and Engineering Data* 2015; 60: 1259-1269.
- Mahaffey A, Dubé M. Review of the composition and toxicity of oil sands process-affected water. *Environmental Reviews* 2016; 25: 97-114.
- Mahata N, Silva AR, Pereira MFR, Freire C, de Castro B, Figueiredo JL. Anchoring of a Mn(salen)Cl complex onto mesoporous carbon xerogels. *Journal of Colloid and Interface Science* 2007; 311: 152-158.
- Mall ID, Srivastava VC, Agarwal NK, Mishra IM. Adsorptive removal of malachite green dye from aqueous solution by bagasse fly ash and activated carbon-kinetic study and equilibrium isotherm analyses. *Colloids and Surfaces a-Physicochemical and Engineering Aspects* 2005; 264: 17-28.
- Marentette JR, Frank RA, Bartlett AJ, Gillis PL, Hewitt LM, Peru KM, et al. Toxicity of naphthenic acid fraction components extracted from fresh and aged oil sands process-affected waters, and commercial naphthenic acid mixtures, to fathead minnow (*Pimephales promelas*) embryos. *Aquatic Toxicology* 2015a; 164: 108-117.
- Martin JW, Barri T, Han XM, Fedorak PM, El-Din MG, Perez L, et al. Ozonation of Oil Sands Process-Affected Water Accelerates Microbial Bioremediation. *Environ. Sci. Technol.* 2010; 44: 8350-8356.
- Martin JW, Han XM, Peru KM, Headley JV. Comparison of high- and low-resolution electrospray ionization mass spectrometry for the analysis of naphthenic acid mixtures in oil sands process water. *Rapid Communications in Mass Spectrometry* 2008; 22: 1919-1924.

- Martin JW. The Challenge: Safe release and reintegration of oil sands process-affected water. *Environmental Toxicology and Chemistry* 2015; 34: 2682-2682.
- Mattson JS, Mark HB. *Activated Carbon: Surface Chemistry and Adsorption from Solution*: M. Dekker, 1971.
- McMartin DW, Headley JV, Friesen DA, Peru KM, Gillies JA. Photolysis of naphthenic acids in natural surface water. *J. of Environ.l Sci. and Health Part A* 2004; 39: 1361-1383.
- McQueen AD, Kinley CM, Hendrikse M, Gaspari DP, Calomeni AJ, Iwinski KJ, et al. A risk-based approach for identifying constituents of concern in oil sands process-affected water from the Athabasca Oil Sands region. *Chemosphere* 2017; 173: 340-350.
- Menéndez JA, Martín-Gullón I. *Types of carbon adsorbents and their production*. Teresa J. Badosz, 2006., 2006.
- Merlin M, Guigard SE, Fedorak PM. Detecting naphthenic acids in waters by gas chromatography-mass spectrometry. *Journal of Chromatography A* 2007; 1140: 225-229.
- Meshref MNA, Klammerth N, Islam MS, McPhedran KN, Gamal El-Din M. Understanding the similarities and differences between ozone and peroxone in the degradation of naphthenic acids: Comparative performance for potential treatment. *Chemosphere* 2017; 180: 149-159.
- Mohamed MH, Udoetok IA, Wilson LD, Headley JV. Fractionation of carboxylate anions from aqueous solution using chitosan cross-linked sorbent materials. *Rsc Advances* 2015a; 5: 82065-82077.
- Mohamed MH, Wilson LD, Shah JR, Bailey J, Peru KM, Headley JV. A novel solid-state fractionation of naphthenic acid fraction components from oil sands process-affected water. *Chemosphere* 2015b; 136: 252-258.

- Morandi GD, Wiseman SB, Pereira A, Mankidy R, Gault IGM, Martin JW, et al. Effects-Directed Analysis of Dissolved Organic Compounds in Oil Sands Process-Affected Water. *Environ. Sci. Technol.* 2015b; 49: 12395-12404.
- Morandi GD, Zhang K, Wiseman SB, Pereira AdS, Martin JW, Giesy JP. Effect of Lipid Partitioning on Predictions of Acute Toxicity of Oil Sands Process Affected Water to Embryos of Fathead Minnow (*Pimephales promelas*). *Environ. Sci. & Technol.* 2016.
- Moreno-Castilla C, Maldonado-Hodar FJ. Carbon aerogels for catalysis applications: An overview. *Carbon* 2005; 43: 455-465.
- Moreno-Castilla C. Adsorption of organic molecules from aqueous solutions on carbon materials. *Carbon* 2004; 42: 83-94.
- Moustafa AMA, Huang J, McPhedran KN, Zeng HB, El-Din MG Probing the Adsorption of Weak Acids on Graphite Using Amplitude Modulation-Frequency Modulation Atomic Force Microscopy. *Langmuir* 2015; 31: 3069-3075.
- Moustafa AMA, Kim ES, Alpatova A, Sun N, Smith S, Kang S, et al. Impact of polymeric membrane filtration of oil sands process water on organic compounds quantification. *Water Science and Technology* 2014a; 70: 771-779.
- Moustafa AMA, McPhedran KN, Moreira J, El-Din MG Investigation of Mono/Competitive Adsorption of Environmentally Relevant Ionized Weak Acids on Graphite: Impact of Molecular Properties and Thermodynamics. *Environmental Science & Technology* 2014b; 48: 14472-14480.
- Noestheden MR, Headley JV, Peru KM, Barrow MP, Burton LL, Sakuma T, et al. Rapid Characterization of Naphthenic Acids Using Differential Mobility Spectrometry and Mass Spectrometry. *Environ. Sci. & Technol.* 2014; 48: 10264-10272.

- Nyakas A, Han J, Peru KM, Headley JV, Borchers CH. Comprehensive analysis of oil sands processed water by direct-infusion fourier-transform ion cyclotron resonance mass spectrometry with and without offline UHPLC sample prefractionation. *Environ. Sci. Technol.* 2013; 47: 4471-4479.
- Oil Sands Performance Report 2015 (Dated April 22, 2016). Accessed online April 2017: http://www.shell.ca/en_ca/energy-and-innovation/oil-sands/oil-sands-performance-report/_jcr_content/par/textimage_78af.stream/1463441702776/00cfc57a8625b41538ec24a2fc9d2e7160147b85367300b8dd8b9cb735aa1736/she-2055-oil-sands-performance-report-2015-final1.pdf, Shell Canada Limited, (2016).
- Onal Y. Kinetics of adsorption of dyes from aqueous solution using activated carbon prepared from waste apricot. *Journal of Hazardous Materials* 2006; 137: 1719-1728.
- Pan B, Xing BS. Adsorption Mechanisms of Organic Chemicals on Carbon Nanotubes. *Environmental Science & Technology* 2008; 42: 9005-9013.
- Pekala RW. Organic Aerogels From The Polycondensation Of Resorcinol With Formaldehyde. *Journal of Materials Science* 1989; 24: 3221-3227.
- Pereira AS, Bhattacharjee S, Martin JW, Alberta U. Characterization Of Oil Sands Process-Affected Waters By Liquid Chromatography Orbitrap Mass Spectrometry. *Environmental Science & Technology* 2013; 47: 5504-5513.
- Pereira AS, Islam MDS, El-Din MG, Martin JW. Ozonation degrades all detectable organic compound classes in oil sands process-affected water; an application of high-performance liquid chromatography/orbitrap mass spectrometry. *Rapid Communications in Mass Spectrometry* 2013; 27: 2317-2326.

- Pérez-Estrada LA, Han X, Drzewicz P, Gamal El-Din M, Fedorak PM, Martin JW. Structure-reactivity of naphthenic acids in the ozonation process. *Environmental Science & Technology* 2011; 45: 7431-7437.
- Perez-Estrada LA, Han XM, Drzewicz P, El-Din MG, Fedorak PM, Martin JW. Structure-Reactivity of Naphthenic Acids in the Ozonation Process. *Environmental Science & Technology* 2011; 45: 7431-7437.
- Pourrezaei P, Alpatova A, Chelme-Ayala P, Perez-Estrada L, Jensen-Fontaine M, Le X, et al. Impact of petroleum coke characteristics on the adsorption of the organic fractions from oil sands process-affected water. *International Journal of Environmental Science & Technology (IJEST)* 2014; 11: 2037-2050.
- Pourrezaei P, Drzewicz P, Wang YN, El-Din MG, Perez-Estrada LA, Martin JW, et al. The Impact of Metallic Coagulants on the Removal of Organic Compounds from Oil Sands Process-Affected Water. *Environmental Science & Technology* 2011; 45: 8452-8459.
- Pourrezaei P. Physico-chemical processes for oil sands process-affected water treatment. [electronic resource]: Edmonton, Alta. : University of Alberta, 2013., 2013.
- Qiu H, Lv L, Pan BC, Zhang QJ, Zhang WM, Zhang QX. Critical review in adsorption kinetic models. *Journal of Zhejiang University-Science A* 2009; 10: 716-724.
- Quinlan PJ, Tam KC. Water treatment technologies for the remediation of naphthenic acids in oil sands process-affected water. *Chemical Engineering Journal* 2015; 279: 696-714.
- Ramirez-Montoya LA, Concheso A, Alonso-Buenaposada ID, Garcia H, Menendez JA, Arenillas A, et al. Protein adsorption and activity on carbon xerogels with narrow pore size distributions covering a wide mesoporous range. *Carbon* 2017; 118: 743-751.

- Reinardy HC, Scarlett AG, Henry TB, West CE, Hewitt LM, Frank RA, et al. Aromatic Naphthenic Acids In Oil Sands Process-Affected Water, Resolved By Gcxgc-Ms, Only Weakly Induce The Gene For Vitellogenin Production In Zebrafish (Danio Rerio) Larvae. *Environmental Science & Technology* 2013; 47: 6614-6620.
- Rey-Raap N, Arenillas A, Menendez JA. A visual validation of the combined effect of ph and dilution on the porosity of carbon xerogels. *Microporous and Mesoporous Materials* 2016; 223: 89-93.
- Rey-Raap N, Menendez JA, Arenillas A. RF xerogels with tailored porosity over the entire nanoscale. *Microporous and Mesoporous Materials* 2014; 195: 266-275.
- Rogers VV, Liber K, MacKinnon MD. Isolation and characterization of naphthenic acids from Athabasca oil sands tailings pond water. *Chemosphere* 2002; 48: 519-527.
- Ross MS, Pereira AD, Fennell J, Davies M, Johnson J, Sliva L, et al. Quantitative and Qualitative Analysis of Naphthenic Acids in Natural Waters Surrounding the Canadian Oil Sands Industry. *Environmental Science & Technology* 2012; 46: 12796-12805.
- Rouquerol F. Adsorption by powders and porous solids [electronic resource] : principles, methodology and applications / F. Rouquerol... [et al.]: Amsterdam ; Boston : Academic Press, c2014.2nd ed., 2014.
- Rowland SJ, West CE, Scarlett AG, Jones D, Frank RA. Identification of individual tetra- and pentacyclic naphthenic acids in oil sands process water by comprehensive two-dimensional gas chromatography/mass spectrometry. *Rapid Communications in Mass Spectrometry* 2011b; 25: 1198-1204.
- Rudzinski WE, Oehlers L, Zhang Y. Tandem mass spectrometric characterization of commercial naphthenic acids and a Maya crude oil. *Energy & Fuels* 2002; 16: 1178-1185.

- S. Mishra VM, A. Dalai, D. McMartin, J. Headley and K. Peru. Photocatalysis of Naphthenic Acids in Water. *Water Resource and Protection* 2010; 2: 644-650 doi: 10.4236/jwarp.2010.27074.
- Saha P, Chowdhury S, Gupta S, Kumar I. Insight into adsorption equilibrium, kinetics and thermodynamics of Malachite Green onto clayey soil of Indian origin. *Chemical Engineering Journal* 2010; 165: 874-882.
- Saha P, Chowdhury S. Insight Into Adsorption Thermodynamics. *Thermodynamics* 2011: 349-364.
- Sands Mining Industry , (posted date: June 12, 2013), from Alberta Energy Regulator, Accessed online April 2017: <http://osipfiles.alberta.ca/datasets/158/TailingsManagementAssessmentReport2011-2012.pdf>, 2012
- Sarkar B. Adsorption of single-ring model naphthenic acid from oil sands tailings pond water using petroleum coke-derived activated carbon. In: Sarkar B, Toronto U, editors. 52, 2014.
- Sawyer CN, mccarty PL, Parkin GF. *Chemistry for Environmental Engineering and Science: mcgraw-Hill higher education*, 2003.
- Scarlett AG, Reinardy HC, Henry TB, West CE, Frank RA, Hewitt LM, et al. Acute toxicity of aromatic and non-aromatic fractions of naphthenic acids extracted from oil sands process-affected water to larval zebrafish. *Chemosphere* 2013; 93: 415-420.
- Scott AC, Fedorak PM. *Petroleum coking : a review of coking processes and the characteristics, stability, and environmental aspects of coke produced by the oil sands companies / Angela C. Scott, Phillip M. Fedorak: [S.l. : s.n.], 2004., 2004.*

- Scott AC, MacKinnon MD, Fedorak PM. Naphthenic acids in athabasca oil sands tailings waters are less biodegradable than commercial naphthenic acids. *Environ. Sci. & Technol.* 2005a; 39: 8388-8394.
- Scott AC, Young RF, Fedorak PM. Comparison of GC–MS and FTIR methods for quantifying naphthenic acids in water samples. *Chemosphere* 2008b; 73: 1258-1264.
- Scott AC, Zubot W, MacKinnon MD, Smith DW, Fedorak PM. Ozonation of oil sands process water removes naphthenic acids and toxicity. *Chemosphere* 2008c; 71: 156-160.
- Shang D, Kim M, Haberl M, Legzdins A. Development of a rapid liquid chromatography tandem mass spectrometry method for screening of trace naphthenic acids in aqueous environments. *J Chromatogr A* 2013; 1278: 98-107.
- Silva IF, Ume JI, Scaroni AW, Radovic LR. Effects of surface chemistry of activated carbon on the adsorption of aromatics containing electron-withdrawing and electron-donating functional groups. *Abstracts of Papers of the American Chemical Society* 1996; 211: 129-FUEL.
- Small CC, Hashisho Z, Ulrich AC. Preparation and characterization of activated carbon from oil sands coke. *Fuel* 2012a; 92: 69-76.
- Small CC, Ulrich AC, Hashisho Z. Adsorption of Acid Extractable Oil Sands Tailings Organics onto Raw and Activated Oil Sands Coke. *Journal of Environmental Engineering-Asce* 2012b; 138: 833-840.
- Small CC. Activation of delayed and fluid petroleum coke for the adsorption and removal of naphthenic acids from oil sands tailings pond water [electronic resource] / by Christina Caroline Small: 2011., 2011.

- Shell Canada Limited, (2016) Oil Sands Performance Report 2015 (Dated April 22, 2016). Accessed online April 2017: http://www.shell.ca/en_ca/energy-and-innovation/oil-sands/oil-sands-performance-report/_jcr_content/par/textimage_78af.stream/1463441702776/00cfc57a8625b41538ec24a2fc9d2e7160147b85367300b8dd8b9cb735aa1736/she-2055-oil-sands-performance-report-2015-final1.pdf.
- Srivastava VC, Swamy MM, Mall ID, Prasad B, Mishra IM. Adsorptive removal of phenol by bagasse fly ash and activated carbon: Equilibrium, kinetics and thermodynamics. *Colloids and Surfaces a-Physicochemical and Engineering Aspects* 2006; 272: 89-104.
- Sun N, Chelme-Ayala P, Klammerth N, McPhedran KN, Islam MS, Perez-Estrada L, et al. Advanced Analytical Mass Spectrometric Techniques and Bioassays to Characterize Untreated and Ozonated Oil Sands Process-Affected Water. *Environ. Sci. Technol.* 2014a; 48: 11090-11099.
- Tan IAW, Hameed BH, Ahmad AL. Equilibrium and kinetic studies on basic dye adsorption by oil palm fibre activated carbon. *Chemical Engineering Journal* 2007; 127: 111-119.
- Turnbull A, Slavcheva E, Shone B. Factors controlling naphthenic acid corrosion. *Corrosion* 1998; 54: 922-930.
- van den Heuvel MR. In Response: An academic perspective on the release of oil sands process-affected water. *Environmental Toxicology and Chemistry* 2015; 34: 2682-2684.
- Verbeek AG, Mackay WC, Mackinnon MD. Proceedings of the Twentieth Annual Aquatic Toxicity Workshop. Vol 26, 1994.

- Wang J, Chen ZM, Chen BL. Adsorption of Polycyclic Aromatic Hydrocarbons by Graphene and Graphene Oxide Nanosheets. *Environmental Science & Technology* 2014; 48: 4817-4825.
- Wang N, Chelme-Ayala P, Perez-Estrada L, Garcia-Garcia E, Pun J, Martin JW, et al. Impact of Ozonation on Naphthenic Acids Speciation and Toxicity of Oil Sands Process-Affected Water to *Vibrio fischeri* and Mammalian Immune System. *Environ. Sci. Technol.* 2013a; 47: 6518-6526.
- Weber WJ. Adsorption processes. *Pure Appl. Chem.* 1974; 37: 375 – 392
- Wells MJM. Principles of Extraction and the Extraction of Semivolatile Organics from Liquids. *Sample Preparation Techniques in Analytical Chemistry*. John Wiley & Sons, Inc., 2003, pp. 37-138.
- West CE, Jones D, Scarlett AG, Rowland SJ. Compositional heterogeneity may limit the usefulness of some commercial naphthenic acids for toxicity assays. *Science of the Total Environment* 2011; 409: 4125-4131.
- West CE, Scarlett AG, Pureveen J, Tegelaar EW, Rowland SJ. Abundant naphthenic acids in oil sands process-affected water: studies by synthesis, derivatisation and two-dimensional gas chromatography/high-resolution mass spectrometry. *Rapid Communications In Mass Spectrometry* 2013; 27: 357-365.
- Woudneh MB, Coreen Hamilton M, Benskin JP, Wang G, McEachern P, Cosgrove JR. A novel derivatization-based liquid chromatography tandem mass spectrometry method for quantitative characterization of naphthenic acid isomer profiles in environmental waters. *J Chromatogr A* 2013; 1293: 36-43.

- Xue JK, Zhang YY, Liu Y, El-Din MG Effects of ozone pretreatment and operating conditions on membrane fouling behaviors of an anoxic-aerobic membrane bioreactor for oil sands process-affected water (OSPW) treatment. *Water Research* 2016a; 105: 444-455.
- Xue JK, Zhang YY, Liu Y, El-Din MG Treatment of oil sands process-affected water (OSPW) using a membrane bioreactor with a submerged flat-sheet ceramic microfiltration membrane. *Water Research* 2016b; 88: 1-11.
- Young RF, Orr EA, Goss GG, Fedorak PM. Detection of naphthenic acids in fish exposed to commercial naphthenic acids and oil sands process-affected water. *CHEMOSPHERE* 2007; 68: 518-527.
- Young RF, Wismer WV, Fedorak PM. Estimating naphthenic acids concentrations in laboratory-exposed fish and in fish from the wild. *Chemosphere* 2008; 73: 498-505.
- Yue S, Ramsay BA, Wang J, Ramsay J. Toxicity and composition profiles of solid phase extracts of oil sands process-affected water. *Sci. Total Environ.* 2015a; 538: 573-582.
- Yue SQ, Ramsay BA, Brown RS, Wang JX, Ramsay JA. Identification of Estrogenic Compounds in Oil Sands Process Waters by Effect Directed Analysis. *Environmental Science & Technology* 2015; 49: 570-577.
- Yue SQ, Ramsay BA, Brown RS, Wang JX, Ramsay JA. Identification of Estrogenic Compounds in Oil Sands Process Waters by Effect Directed Analysis. *Environmental Science & Technology* 2015b; 49: 570-577.
- Zhang K, Pereira AS, Martin JW. Estimates of Octanol–Water partitioning for thousands of dissolved organic species in oil sands process-affected water. *Environ. Sci. Technol.* 2015; 49: 8907-8913.

- Zhang YY, Xue JK, Liu Y, El-Din MG Treatment of oil sands process-affected water using membrane bioreactor coupled with ozonation: A comparative study. *Chemical Engineering Journal* 2016; 302: 485-497.
- Zhao B, Currie R, Mian H. Catalogue of analytical methods for naphthenic acids related to oil sands operations. 2012.
- Zhao B, R., Mian CaH. Catalogue of Analytical Methods for Naphthenic Acids Related to Oil Sands Operations. OSRIN Report No. TR-21. Oil Sands Research and Information Network, University of
- Zhu HS, Yang XJ, Mao YP, Chen Y, Long XL, Yuan WK. Adsorption of EDTA on activated carbon from aqueous solutions. *Journal of Hazardous Materials* 2011; 185: 951-957.
- Zubot W, MacKinnon MD, Chelme-Ayala P, Smith DW, El-Din MG Petroleum coke adsorption as a water management option for oil sands process-affected water. *Science of the Total Environment* 2012b; 427: 364-372.
- Zubot WA. Removal Of Naphthenic Acids From Oil Sands Process Water Using Petroleum Coke. In: Zubot WA, editor. 49, 2011, pp. 2652-2652.